An investigation of the coordination chemistry of N,N`-disubstituted sulfonylthiourea ligands with d^6 and d^8 transition metal centres.

A thesis
submitted in partial fulfilment
of the requirements for the degree
of
Master of Science (Research) In Chemistry
at
The University of Waikato
by

Matthew Christian Risi

THE UNIVERSITY OF
WAIKATO
Te Whare Wānanga o Waikato

2020

Abstract

The coordination chemistry of both square-planar and piano-stool metal complexes derived from an array of disubstituted sulfonylthiourea ligands with the d^8 and d^6 transition metal centres of nickel(II), palladium(II), platinum(II), gold(III) and ruthenium(II) was investigated. It was found that these ligands coordinate to the metal centre through both the S and N atoms of the thiourea moiety in a bidentate fashion, which is reminiscent of the coordination chemistry of traditional thiourea complexes. Square-planar d^8 metal complexes derived from sulfonylthioureas were characterised by both single crystal XRD and $^{31}P\{^1H\}$ NMR aided by ^{195}Pt coupling, to be in the *distal* isomer with no isomerisation detected. This is to say that the non-coordinated nitrogen atom of the core thiourea bears the sulfonyl group and is positioned away from the metal centre. This is in contrast to the coordination observed for the analogous acylthiourea complexes which tend to favour a bidentate S and O coordination mode through the acyl oxygen. This indicates the coordination mode observed for square-planar sulfonylthiourea complexes more closely resembles that of unsubstituted thioureas. Interestingly, single crystal XRD analysis of the piano-stool ruthenium complexes reveals the sulfonylthiourea ligand coordinated to the ruthenium metal centre in the unexpected *proximal* isomer. Comparison of this structure to some analogous piano-stool acylthiourea complexes show extremely similar structure and coordination and may indicate piano-stool structures derived from sulfonylthioureas resemble those of acylthioureas which in-turn is similar to the coordination mode adopted by simple thioureas. Moreover, through monitoring of the observed decomposition of Ni(II) and Pd(II) sulfonylthiourea complexes by ESI-MS and ^{31}P NMR and the attempted synthesis of monodentate Au(I) phosphine sulfonylthiourea complexes, it was discovered that these complexes have a tendency to form stable trinuclear aggregates of the formula $[M_3S_2L_3]^+$ (L = bidentate chelating ligand). The formation of these sulfide complexes is theorised to be a result of a hydroxide induced S-C bond cleavage promoted by the electron withdrawing sulfonyl subsistent. This observation matches closely to the well-known ability of thioureas to act as a source of sulfide upon reactions with metal ions.

Acknowledgements

Firstly, I must give special thanks to my supervisor, Professor Bill Henderson. You uphold the standard of what it means to be both a professor and supervisor. The guidance, knowledge, wisdom, and advice you have passed onto me will never be forgotten and I will be forever grateful for the opportunity to have been your student. Our weekly meetings of academic discussion and banter helped me keep some sense of sanity.

I must also thank Associate Professor Graham Saunders. The single crystal structures, discussion, guidance and your many visits to the graduate student room were invaluable to the completion of this thesis. Special mention must also be made for Associate Professor Michele Prinsep, without whom I may have never done a master's degree, your advice and confidence in me will not be forgotten. Many thanks also to Jenny Stockdill for continuous instrument support.

To the other graduate students of the C3.04 research laboratory, with particular mention to Sravan, Golf and Atiga. Thank you all for the continuous advice and friendship. I wish you all the best of luck in your studies and futures and look forward to hearing about your continued success.

To my parents, Robyn, and Walter Risi. Your continuous love, support and guidance throughout my entire life is to thank for all that I do. Everything good within me has started from the two of you and I hope that I continue to hold up the standards, wisdom, and guidance you have passed onto me.

To my good friends, Iain, and Joshua, our catch ups and backgammon games were a continuous highlight for the duration of my degree and much cheaper than therapy. Also, particular mention to Kirsty for our countless tearoom visits for banter and chemistry discussion.

Most importantly I wish to thank my amazing wife, Ashley. Your overwhelming love, encouragement, and support for the entire duration of my degree will never be forgotten. I only wish to one day be able to accurately show you my overwhelming thankfulness for everything you have done for me and to hopefully someday be able to repay you for your invaluable support, without which this thesis would not be possible. Thank you.

Table of contents

List of figures

List of tables

List of abbreviations

NMR - Nuclear Magnetic Resonance

d - doublet

t - triplet

m – multiplet (NMR)/medium (IR)

Hz - Hertz

J - Coupling Constant (in Hz)

ppm - parts-per-million

δ - chemical shift (in ppm)

MHz - Megahertz

br - broad (NMR, IR)

IR - Infra-Red

cm^{-1} - wavenumber

υ - frequency (IR) (in cm^{-1})

vs - very strong (IR)

s - singlet (NMR)/strong (IR)

ESI-MS - Electrospray Ionisation Mass Spectrometry

m/z - mass-to-charge ratio (ESI-MS)

XRD - x-ray diffraction

Å - Angstrom

mp - melting point

COD - 1,5-cyclooctadiene

Dppe - 1,2-bis(diphenylphosphino)ethane

Dppp - 1,3-bis(diphenylphosphino)propane

Bipy - 2,2'-bipyridine

tolyl - *p*-tolyl substituent

bp – 2-benzylpyridyl substituent

PPh_3 - triphenylphosphine

TCEP - tris(2-cyanoethyl)phosphine

en - ethylenediamine

DMF - dimethylformamide

$CDCl_3$ - deuterated chloroform

DMSO - dimethyl sulfoxide

1 Introduction

1.1 Thiourea

Thioureas, of the formula RNHC(S)NHR' shown in Figure 1.1, are a large range of organosulfur compounds closely related to urea (RNHC(O)NHR') with the exception of a sulfur on the primary carbon instead of an oxygen[1]. Thioureas are involved in the formation, or as a substituent of an array of organic and inorganic compounds[2, 3]. Literature regarding thiourea and thiourea derivatives are ubiquitous with extensive research being done within the area across many disciplines of chemistry. The reason for this high interest is due to the numerous applications[3] of thiourea, which include industrial uses as dyes[4], preparation of photography film[5] and plastics[6]. Thiourea derivatives have also been reported to have uses as insecticides[7], preservatives[8] and pharmaceutical precursors[9].

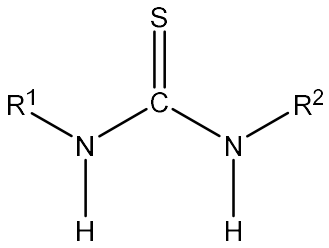

Figure 1.1: Structure of thiourea

Mono *N*-substituted thioureas are obtained from an equal molar reaction between an isothiocyanate (RNCS) and an ammonia (NH_3). Similarly, disubstituted thioureas are prepared by replacing an amine H to an R substituent (NHR)[3], shown in Figure 1.2.

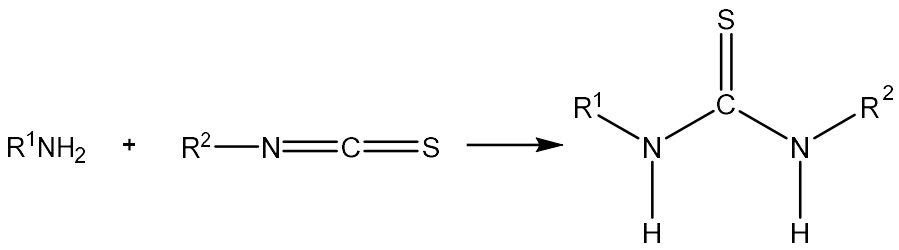

Figure 1.2: Synthetic route of disubstituted thiourea

Thioureas may also act as versatile ligands towards a large array of transition metal centres, able to coordinate to both hard and soft metals. Sulfur, the primary binding site, is a soft base therefore has an affinity for soft metal centres such as the platinum group or other late transition metals[10]. These metal complexes display two distinct coordination modes, monodentate[11-13] (*via* S) and bidentate[14, 15] (*via* S and N). This bidentate coordination mode results in a 4 membered ring structure, shown in Figure 1.3. This limited range of coordination modes is a result of the inability of a 6 membered chelating ring to be formed. Addition of third binding site may overcome this; such is seen with the closely related acylthioureas in Section 1.2.

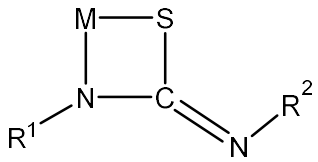

Figure 1.3: Bidentate coordination mode of thiourea

1.2 Acylthiourea

Addition of an acyl group (RC=O) onto the thiourea as a substituent results in a new class of compounds, acylthioureas, of the formula (RCONHC(S)NHR') shown in Figure 1.4. Acylthioureas are widely studied bidentate ligands showing coordination to a large array of metal centres[16]. The first example of this class of compounds was reported by Neucki *et al*[17] in 1873. It was also reported within this paper the first example of a platinum complex of an acylthiourea ligand. Extensive research has gone into studying acylthioureas as is evident by the 382 references given by Saeed *et al* in their review on the chemistry of acylthioureas[16] (after 2007).

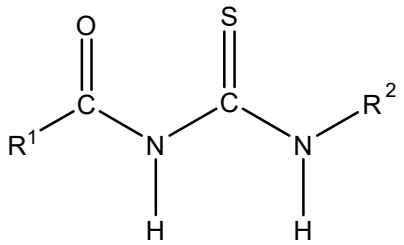

Figure 1.4: Structure of acylthiourea of the type H_2L

Recent increased interest in disubstituted acylthioureas has been noted[16, 18]. This increased interest is likely due to their numerous potential applications in platinum refining[18], solvent extraction[19] and HPLC determination[18] among many others. In many cases they offer a more environmentally friendly alternative to existing applications by following the green chemistry principles[20] which of late has been increasingly sought after.

Synthesis of acylthioureas was first reported by Douglas-Dains *et al*[21] whose method still remains the most common synthetic method for the preparation of acylthioureas, providing high yield and purity with the addition of inexpensive starting materials[18]. Synthesis involves the reaction of acyl isothiocyanates with a corresponding amino compound in acetone, shown in Figure 1.5.

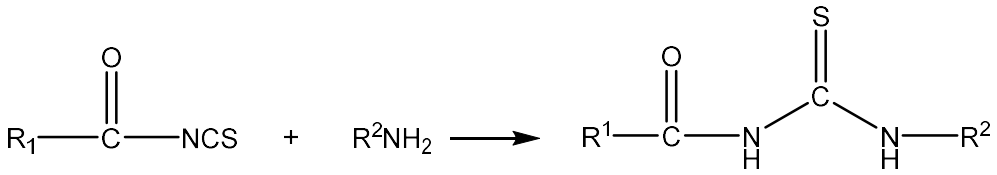

Figure 1.5: General synthesis of disubstituted acylthiourea.

Other synthetic methods for acylthioureas have been reported. One such example of an alternative synthetic methods is given as a treatment of aminothiocarbonylimidoyl chlorides with potassium thiocyanate followed by hydrolysis as reported by weber *et al*[22]. However, these methods are seldom used in comparison to Douglas-Dains *et al's* method.

Disubstituted acylthioureas contain both hard and soft binding sites giving similar bonding potential to thioureas[18]. However the addition of an acyl (R=O) binding site gives the possibility to form a 6 member chelating ring, adding a second bidentate coordination mode that is not seen in thioureas[16, 18]. Coordination of these ligands may be expected to resemble complexes of simple unsubstituted thioureas[23 18].

Examination of mononuclear transition metal complexes within the literature confirms these two bidentate coordination modes are possible[24, 25], a chelating coordination mode (*via* O and S) and the more traditional bidentate (*via* S and N). The coordination mode adopted by a structure is determined predominantly by stability, that is to say the coordination which produces the lower energy structures will be favoured. For this reason, it may be expected the 6 membered chelating mode would predominately form, shown in Figure 1.6.

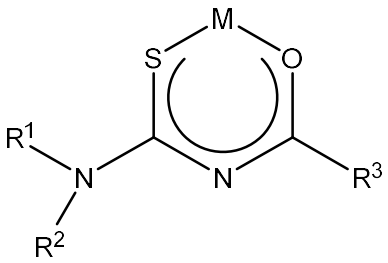

Figure 1.6: Chelating S-O coordination mode of acylthiourea

Coordination of trisubstituted acylthiourea ligands to an array of transition metals has been reviewed by Beyer *et al*[26], revealing that the favoured coordination mode for these metal complexes is the bidentate chelating coordination modes as discussed above. The lack of literature pertaining to the formation of disubstituted ligand metal complexes has been noted[18]. This may be due to the assumption of the coordination chemistry of both ligand types may be similar.

X-ray diffraction determined structures of acylthiourea ligands of the type H_2L and HL reveal a significant amount of intramolecular hydrogen bonding. This hydrogen bonding has been shown to influence the conformation of both the H_2L and HL type ligands. Regarding the H_2L ligand, this intramolecular hydrogen bonding has been shown to lock the ligand into a planar 6 member ring like structure with stabilisation from the thioamide (NH-C(S)) hydrogen bonding to the acyl oxygen atom[27, 28], shown in Figure 1.7. In contrast, the HL ligand within the solid state is shown to form a twisted formation with the sulfur and acyl oxygen pointing in opposite directions, as is to be expected from two electron rich atoms bonded closely[27, 29], also shown in Figure 1.7.

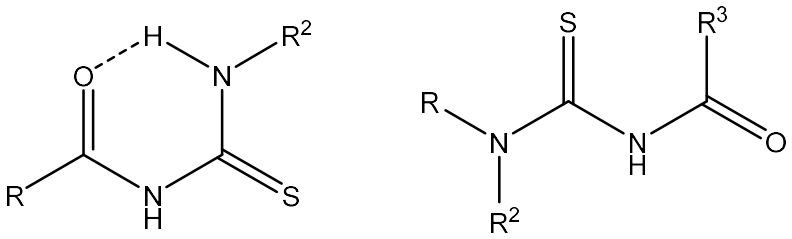

Figure 1.7: H_2L and HL acylthiourea ligand conformations

X-ray diffraction of the acylthiourea ligands also reveals the bond lengths of the amidic (O)C-NH (1.374 Å +/- 0.011 Å), thioamide NH-C(S) (1.409 Å +/- 0.016 Å) and (S)C-N(R/H) (1.327 Å +/- 0.006 Å) bonds[30, 31], shown in Figure 1.8, are shorter than a usual C-N single bond at 1.472 Å[26]. The (S)C-N(R/H) bond lengths are indicative of a partial double bond character; this observation is supported by the restricted rotation of this bond. Proton and carbon NMR of an HL ligand where R_1 and R_2 are equivalent (such as two CH_3 groups), two separate chemical resonances are observed, resolving the two methyl groups in $CDCl_3$ at room temperature[18]. As this observation of bonds is concerned with the (S)C-N(R/H) bond and is not influenced from the presence of the acyl group, it may be expected that this observation can also be made with simple unsubsidised thioureas and possibly sulfonylthioureas which would be of particular interest to this research.

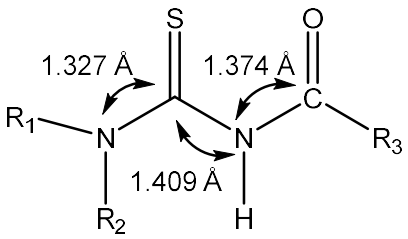

Figure 1.8: Acylthiourea bond lengths

It may be expected that acylthioureas and sulfonylthioureas might coordinate in similar modes, however due to the decreased electron donation from the sulfonyl group it may also be expected to prefer the bidentate S and N coordination. While an extensive amount of research has been done on acylthioureas and the corresponding metal complexes and coordination modes, very little coordination chemistry research has been done on sulfonylthioureas.

1.3 Sulfonylthiourea

Sulfonylthioureas of the formula ($RSO_2NHC(S)NHR'$), shown in Figure 1.9, can be considered closely related to acylthioureas differing by the presence of an organosulfonyl (RSO_2) substituent instead of an acyl (RCO). While closely related in structure, it can be expected that coordination of both ligands to metal centres can differ significantly. This predicted difference in coordination is a result of the sulfonyl group being much less likely to conjugate due to the much poorer election donation. It may be expected that instead, the sulfonylthiourea ligands would coordinate more traditionally in a bidentate S and N coordination mode.

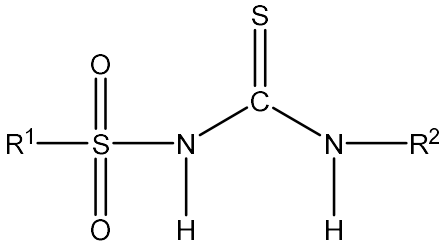

Figure 1.9: General structure of disubstituted sulfonylthiourea

The availability of the remaining substituents gives sulfonylthiourea ligands the ability to contain a large variety of alkyl and aryl substituents. This large array of variations gives the ability to refine the ligand's chemical and steric properties, giving rise to an array of applications. Such applications include antidiabetic potential[32], herbicides[7], plant growth regulators[7], thermosensitive recording material[33] and anion receptors[34]. Complexes with metal centres may also be formed. However, very little has been reported within the literature regarding sulfonylthioureas as ligands with the majority of reported research choosing to instead focus on the pharmaceutical properties.

1.4 Synthesis of sulfonylthioureas

An early recorded synthesis of a compound designated as a sulfonylthiourea is given by Arquet *et al* in the 1950's for the preparation of aryl sulfonylthioureas[35]. Synthesis is carried out by treatment of hydrogen sulfide with corresponding aryl sulfonyl cyanamides, shown in Figure 1.10.

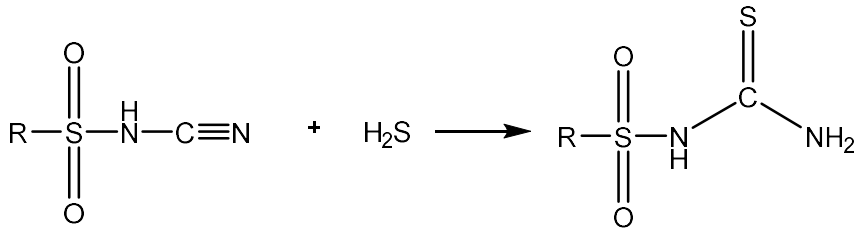

Figure 1.10: Reaction of an aryl sulfonyl cyanamide with hydrogen sulfide

This reaction gives the sulfonylthiourea product of the corresponding aryl sulfonyl cyanamide. Variability of products formed by this reaction is limited to compounds of the formula $RSO_2HNC(S)NH_2$. Sulfanilamides are a popular choice for the synthesis of sulfonylthioureas due to the ease in synthesis.

Another method for the synthesis of sulfonylthioureas as given by Shah *et al* who outline a method of a nucleophilic addition of sulfonamide and isothiocyanate[36]. The mixture is heated under reflux for 72 hours resulting in the $RSO_2HNC(S)NHR'$ product. This method of synthesis *via* the route RSO_2NH_2 + R'NCS, given below as Figure 1.11, overcomes the limited variability of the previous method by introducing a second variable substituent *via* the isothiocyanate. This was the method of choice for the sulfonylthiourea products created herein as will be discussed below.

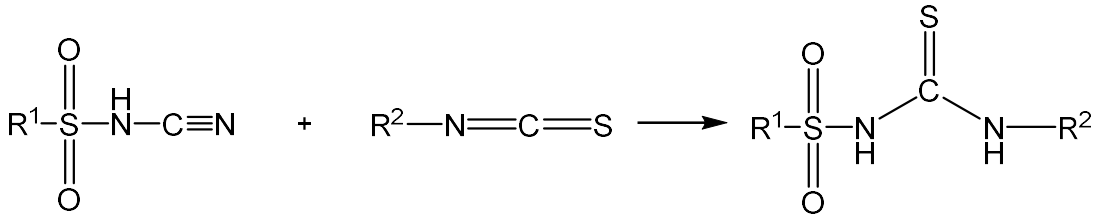

Figure 1.11: Reaction of an aryl sulfonyl cyanamide with an isothiocyanate

1.4.1 Alternative synthesis methods of sulfonylthioureas

Recent alternative methods for the synthesis of $RSO_2HNC(S)NHR'$, sulfonylthioureas have been proposed. One such alternative is given by Ding *et al* who proposed an aqueous phase reaction achieved in mild conditions and short reaction times[34]. The method involves an aqueous solution of RSO_2NHK added dropwise to a solution of dithiocarbonates, shown in Figure 1.12. While this method successfully reduces reaction time with milder conditions, the yields reported are similar to that of Shah *et al* while using the less common RSO_2NHK, which in most cases would require the conversion of the more common RSO_2NH_2, an extra added step.

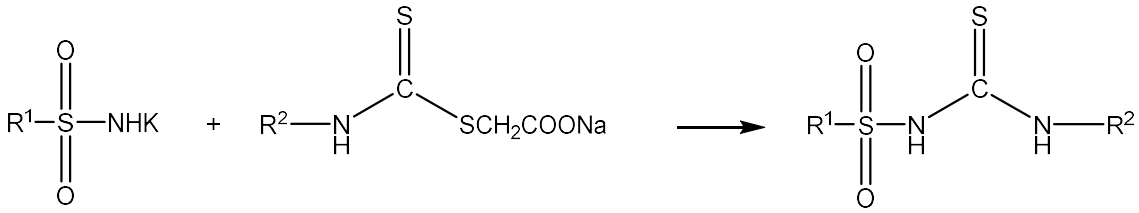

Figure 1.12: Aqueous phase synthesis of $RSO_2HNC(S)NHR'$

A second alternative method is given by Tan *et al* who demonstrated the first recorded application of mechanochemistry in the synthesis of sulfonylthioureas[37]. Mechanosynthesis provides a solvent free alternative for the synthesis of many organic and inorganic compounds such as metallodrugs and metal-organic frameworks. Base-assisted mechanosynthesis of the sulfonylthiourea with the formula ($TolSO_2NHC(S)NHPh$) was conducted on the gram scale with equal molar amounts of sulfonamide and K_2CO_3, milled for one hour followed by an equal molar amount of isothiocyanate and further milling for 2 hours. The reaction was worked up and acidified followed by filtration to isolate the product. The sulfonylthiourea $TolSO_2NHC(S)NHPh$ (Tol= *p*-tolyl, $CH_3C_6H_4$) compound produced was reported in high yield (91%) and high purity. Copper catalysed mechanosynthesis was also reported for other sulfonylthioureas in high yield (*ca*. 74%).

1.5 Coordination modes of sulfonylthiourea complexes

Examination of mononuclear transition metal complexes of sulfonylthioureas reveals two possible coordination modes, bidentate *via* O-S and also *via* S-N. The coordination mode adopted by a structure is determined predominantly by stability, that is to say the coordination which produces the lower energy structures will be favoured. For this reason, it can be expected that the chelating coordination mode would be favoured. However, due to the nature of the sulfonyl group being much less likely to participate in electron donation, it might be expected that a bidentate coordination mode through S and N might be favoured. Interestingly, monodentate coordination modes were not observed within the literature.

1.5.1 Chelating coordination mode complexes

Chelation is a type of bonding between ligands and metal centres, characterised by a polydentate ligand bonded to a central metal atom, resulting in a 6 membered ring motif bridging the S and O on the sulfonylthiourea, shown in Figure 1.13. Metal atoms have an affinity for chelating ligands due to thermodynamic stability[38], known as the chelate effect.

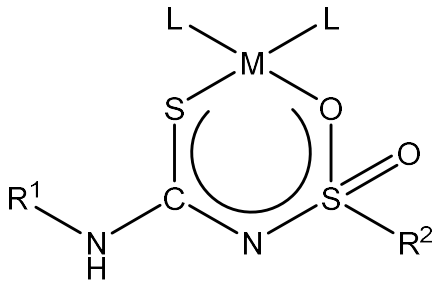

Figure 1.13: Chelation of sulfonylthiourea with a metal centre

A literature search for sulfonylthiourea structures containing a chelating S and O coordination mode to a metal centre gives a total of 33 results at the time of writing, the majority of which are L_2 complexes. L_3 complexes are also observed but are in the minority. Mono ligand complexes are very rare with only three reported structures being observed with Only Ag, Cu, Pd, Co, Ti and Ni being reported to coordinate in this mode. However, no structures were given.

1.5.1.1 Chelating S-O dansylthioureas

Dansyl derived thiourea (Dansyl = 5-(dimethylamino)-1-naphthylsulfonyl), shows mono and L_2 complexes with transition metal centres forming 6 member chelating rings[39] shown in Figure 1.14. The ligand is synthesised by a reaction of dansylamide with a corresponding acyl isothiocyanate (ethyl or butyl). The resulting ligand is reported to be a stable for an array of metal ions. The majority of these complexes are of the ligand *N*-butyl-*N`*-dansylthiourea reported by König *et al* who was investigating the fluorescent effects of the metal complexes created from this ligand. Chelating 6 membered ring complexes were formed with metals Ag, Cu, Pt and Pd. Cu was commented to form stable structures in both 6 and 4 member ring coordination modes.

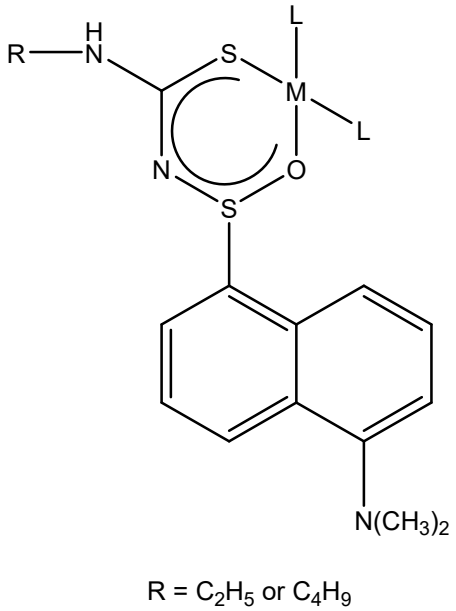

Figure 1.14: General chelating dansylthiourea structure.

Later, in 1995, Schuster *et al*, also studying fluorescent effects of these ligands with metal centres, investigated *N*-dansyl-*N`*-ethylthiourea coordinated with transition metal centres[40], of which only Ni and Ti formed stable 6 member chelate rings, *via* S and O as depicted above in Figure 1.14. The remaining metals examined predominantly formed 4 member rings *via* N and S. This observation follows the expected coordination trends as discussed above. It was noted that platinum group metals only formed complexes at temperatures above 60°C due to kinetic effects.

1.5.1.2 Chelating S-O mono-arenesulfonylthioureas

Similar in structure to the dansyl complexes above, mono-arene sulfonylthiourea complexes also exhibit 6 membered, chelating coordination modes. All of the mono-arene ligands reported were synthesised from benzenesulfonamide or an arene derivative and a corresponding acyl amide. The general mono-arene structure is shown in Figure 1.15.

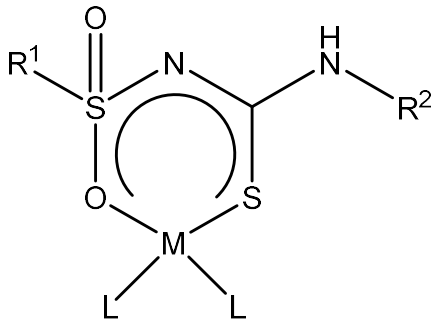

R^1 = Arene substituent. R^2 = NHR

Figure 1.15: General mono-arene sulfonylthiourea structure

One of these mono-arene ligands, bis [4-amino-N-(3-methyl-2(3H)-thiazolylidene) benzenesulfonamide], was reported by Gogorishvili *et al*, who was investigating coordination compounds of some sulfanilamides[41]. Chelating L_2 complexes were reported for metals Co, Cu and Ni; the general structure of these complexes is given in Figure 1.16. Formation of this coordination mode is likely due to steric effects and not related thermodynamic effects which traditionally governs the formation of this coordination mode. This assumption is due to the ligand 5 membered internal ring bridging the primary sulfur binding site and a nitrogen binding site. This connection sterically prevents the formation of a 4 member ring.

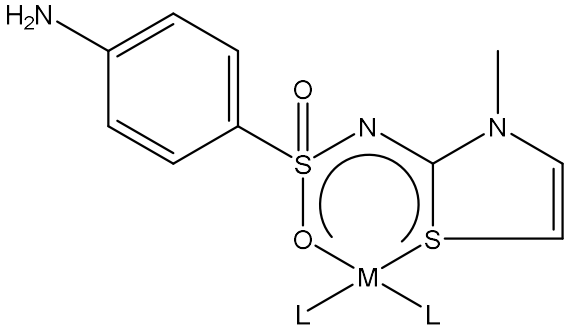

Figure 1.16: General structure of bis[4-amino-N-(3-methyl-2(3H)-thiazolylidene)benzenesulfonamide] metal complexes

Other mono-arenesulfonylthioureas ligands include arenesulfonylmonothio-$TolSO_2NHC(S)NHR$ (R = allyl, C_3H_5 or methyl, CH_3)[42], and the structurally similar arenesulfonyldithio-carbamic acid esters $RSO_2NHC(S)NHC_3H_5$ (R = $(CH_3)_2OC_6H_4$ or $CH_3OC_6H_4Cl$)[42], both shown in Figure 1.17. These complexes are L_2 complexes in which both coordinated ligands are sulfonylthioureas.

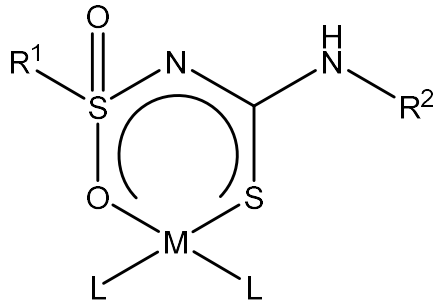

R1 = Tol, $(CH_3)_2OC_6H_4$ or $CH_3OC_6H_4Cl$
R2 = C_3H_5 or CH_3

Figure 1.17: General mono-arenesulfonylthioureas structure

It was reported that both these ligands showed affinity for Cu, Ni and Co. Only Ni was reported to have formed exclusively 6 membered chelated coordination modes. Co coordinated in the 6 membered chelate coordination mode as well as the 4 membered N-S bidentate coordination mode (due to the formation of both high spin and low spin complexes). Copper coordinated exclusively in the bidentate coordination mode.

1.5.1.3 Chelating S-O di-arenesulfonylthioureas

The two predominant di-arenesulfonylthioureas within the literature are $PhSO_2NHC(S)NHPh$ and $TolSO_2NHC(S)NHPh$, both shown in Figure 1.18[43, 44].

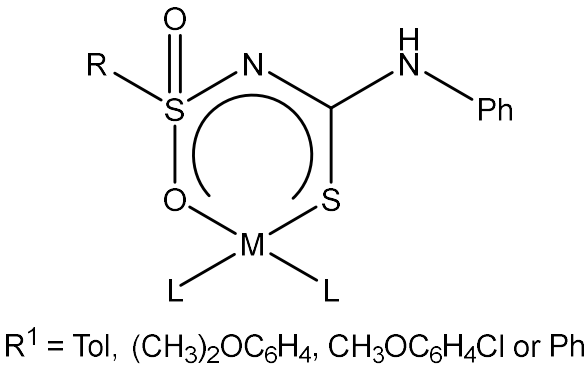

Figure 1.18: General structure of di-arenesulfonylthiourea complex

Both structures can be synthesised by equal molar amounts of tol-*p*-sulfonamide (or benzenesulfonamide) and phenol isothiocyanate. Both ligands show coordination to Co, Ni and Cu. Complexes of other transition metals have also been reported, however coordinate in the bidentate N and S coordination mode, as will be discussed below. The structurally similar di-arenesulfonyldithiocarbamic acid esters $RSO_2NHC(S)NHPh$ ($R = (CH_3)_2OC_6H_4$ or $CH_3OC_6H_4Cl$), are also reported and follow the same coordination, shown in Figure 1.18.

1.5.2 Bidentate S-N coordination mode complexes

Bidentate coordination mode complexes of sulfonylurea compounds are 4 member, square-planar rings with a metal atom bridging the soft sulfur and hard nitrogen binding sites. Due to the sulfonyl substituent, both nitrogen atoms are not equivalent therefore complexes formed can exist in two isomers. However, only the *proximal* isomer is observed within the literature, the two isomers, *proximal* and *distal* are shown in Figure 1.19. This coordination mode appears to be the dominant mode for sulfonylthiourea complexes with 42 reported complexes within the literature. It also appears a larger array of transition metal complexes are formed than the 6 member chelating coordination mode, which only reported complexes with Ag, Cu, Pd, Co and Ni.

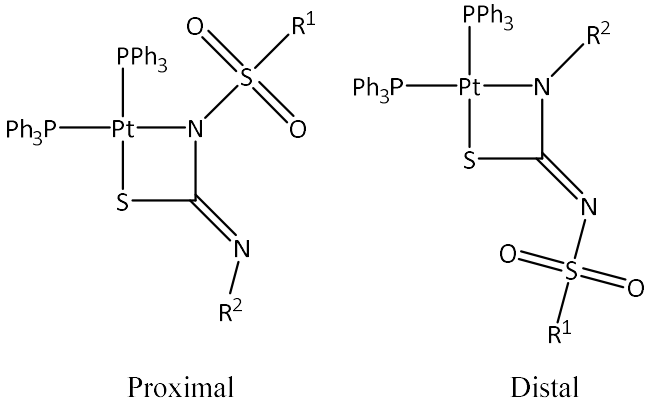

Figure 1.19: Proximal and Distal isomers of 4 member bidentate complexes

Isomerisation of these complexes is also possible and has been reported for the structurally similar acylthioureas[25]. The isomerisation process is likely due to the initial kinetically favourable product being produced followed by isomerisation to the thermodynamically more stable isomer. Due to only one conformation being reported it is likely this is the most stable structure, or no isomerisation takes place. This is yet to be explored for sulfonylthioureas.

1.5.2.1 Bidentate S-N dansylthioureas

All of the reported dansylthiourea complexes were synthesised and reported by Schuster *et al*[40], who investigated the metal complexes formed. While some of the complexes created formed 6 member chelating rings, namely Ni an Ti, the majority of the transition metal complexes coordinated in the 4 member ring, square-planar bidentate coordination mode. The general structure for this dansylthiourea coordination mode is given in Figure 1.20. It was noted that dansylthiourea shows a particular affinity for this coordination mode, following the prediction that such complexes would follow the more traditional S and N coordination shown by thioureas.

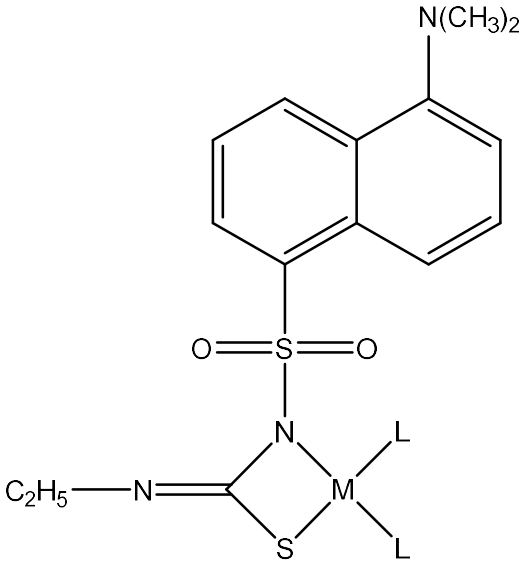

Figure 1.20: General S-N bidentate dansylthiourea structure.

Transition metal complexes in this coordination mode also show a larger array of transition metal complexes than the chelating coordination mode. While the chelating coordination mode showed only complexes with Ag, Cu, Pt and Pd, this coordination mode shows stable complexes with Bi, Sb, Pb, In, Mn, Hg, Cd, Zn, Ag, Cu, Pt, Ir, Rh, Co, Os, Ru, W, Mo and Cr. This is clear indication that this coordination mode is preferred.

1.5.2.2 Bidentate S-N mono-arenesulfonylthioureas

Transition metal complexes of bidentate mono-arenesulfonylthioureas ligands, shown in Figure 1.21, are present in both L_1 and L_2 arrangements. Complexes reported for this ligand are predominately formed with the metals Cu, Ni and Co. Some complexes of Ag and Ti are reported but are in the minority. It was noted by Uhlig *et al* that the copper complexes formed were observed in both the chelating and bidentate coordination[44] (both high and low spin complexes).

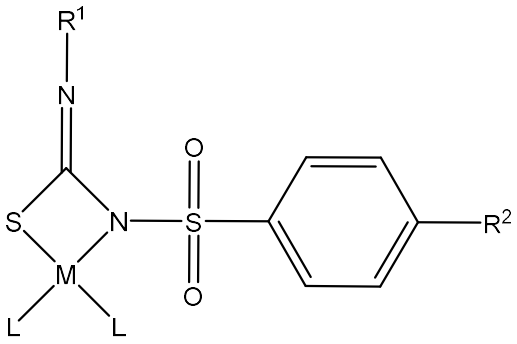

Figure 1.21: General bidentate L_1 arenesulfonylthioureas

Holzner *et al* reported the *N*-butyl-*N'*-benzenesulfonylthiourea complexes[45] of Cu(I), Ag(I) and Ti(I). The trend of copper forming stable complexes in both coordination modes was also reported by Schuster *et al* while discussing dansylthiourea complexes[40], synthesis of mono-arenesulfonylthiourea (where R = CH_3) is most likely achieved using toluene-*p*-sulfonamide and a corresponding isothiocyanate, a usual synthetic route as mentioned above. Addition of an arene isothiocyanate instead of an acyl isothiocyanate would create a poly-arenesulfonylthiourea, discussed below.

1.5.2.3 Bidentate S-N poly-arenesulfonylthioureas

Only three 4 membered bidentate complexes are present within the literature, all of which contain phenyl as the arene substituent, shown in Figure 1.22. Complexes reported are reported for metals Co, Ni, and Cu with Fe and Mn being attempted but unsuccessful[42].

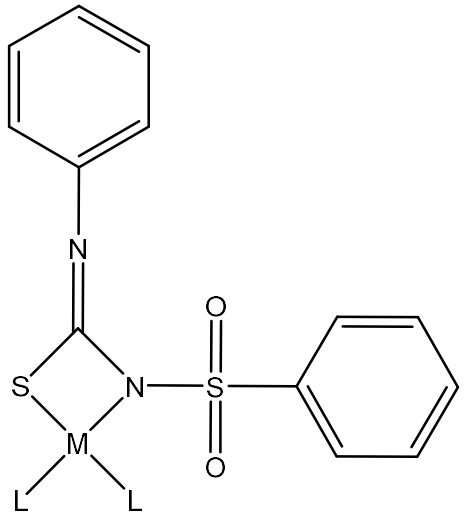

Figure 1.22: Bidentate diphenylsulfonylthiourea complex

It was reported that Cu has an affinity for this coordination mode while Ni and Co form both the four membered and six membered coordination modes with the 6 membered being of obvious favour. Co in particular was able to be isolated in both four and four membered ring isomers[46].

1.6 Thesis overview

Literature relating to the coordination chemistry of thiourea and acylthioureas ligands is well represented with a myriad of recent publications focusing on both the coordination and applications of the corresponding metal complexes. Surprisingly, while known for more than a century, studies involving the coordination chemistry of sulfonylthioureas is relatively unexplored. This is most likely due to the initial assumption that the coordination chemistry between sulfonylthioureas and the closely related acylthioureas would be analogous. However, the limited literature available for sulfonylthioureas suggests otherwise, indicating instead that the coordination mode adopted by these ligands would more closely resemble the substituted thiourea. Although, no dedicated study on the coordination chemistry of sulfonylthioureas has been conducted. Moreover, if the metal complexes derived from sulfonylthioureas do coordinate in the traditional S and N bidentate mode, then two isomers would be possible, due to the non-equivalency created by the sulfonyl group. Discussion on the adopted isomer or isomerisation of sulfonylthiourea complexes could not be found.

To this extent, it would be of interest to examine the coordination chemistry of the metal complexes derived from sulfonylthioureas for the purpose of comparing and contrasting the adopted coordination mode and structures with similar literature reported structures of thiourea and acylthiourea complexes. This comparison can be achieved using comparably modern direct and indirect methods such as ^{31}P and ^{1}H NMR, single crystal x-ray diffraction, Electrospray-ionisation mass spectrometry and infrared spectroscopy. Therefore, the aims of this thesis were to examine, compare and contrast the coordination chemistry of sulfonylthiourea derived ligands with an array of metal centres, particularly Ni(II), Pd(II), Pt(II), Au(III) and Ru(II).

1.7 References

1. A. Shakeel, A. A. Altaf, A. M. Qureshi and A. Badshah, *J. Drug Des. Med. Chem*, 2016, **2**, 10-20.
2. M. George, G. Tan, V. T. John and R. G. Weiss, *Chemistry–A European Journal*, 2005, **11**, 3243-3254.
3. D. C. Schroeder, *Chemical Reviews*, 1955, **55**, 181-228.
4. M. Shkir, S. AlFaify, V. Ganesh, I. Yahia, H. Algarni and H. Shoukry, *Journal of Materials Science: Materials in Electronics*, 2016, **27**, 10673-10683.
5. A. A. Atia, *Hydrometallurgy*, 2005, **80**, 98-106.
6. A. Kausar, S. Zulfiqar, L. Ali, M. Ishaq and M. Ilyas Sarwar, *Polymer International*, 2011, **60**, 564-570.
7. B. Wang, Y. Ma, L. Xiong and Z. Li, *Chinese Journal of Chemistry*, 2012, **30**, 815-821.
8. W. Winkler, *Journal of the Association of Official Agricultural Chemists*, 1955, **38**, 555.
9. A. A. Aly, E. K. Ahmed, K. M. El-Mokadem and M. E.-A. F. Hegazy, *Journal of Sulfur Chemistry*, 2007, **28**, 73-93.
10. R. del Campo, J. J. Criado, E. García, M. a. R. Hermosa, A. Jimenez-Sanchez, J. L. Manzano, E. Monte, E. Rodrıguez-Fernández and F. Sanz, *Journal of Inorganic Biochemistry*, 2002, **89**, 74-82.
11. S. Swaminathan, J. Haribabu, N. K. Kalagatur, R. Konakanchi, N. Balakrishnan, N. Bhuvanesh and R. Karvembu, *ACS Omega*, 2019, **4**, 6245-6256.
12. R. F. de Souza, G. A. da Cunha, J. C. Pereira, D. M. Garcia, C. Bincoletto, R. N. Goto, A. M. Leopoldino, I. C. da Silva, F. R. Pavan and V. M. Deflon, *Inorganica Chimica Acta*, 2019, **486**, 617-624.
13. U. Flörke, A. Ahmida, H. Egold and G. Henkel, *Acta Crystallographica Section E: Structure Reports Online*, 2014, **70**, m397-m398.
14. L. Shadap, S. Diamai, V. Banothu, D. Negi, U. Adepally, W. Kaminsky and M. R. Kollipara, *Journal of Organometallic Chemistry*, 2019, **884**, 44-54.
15. H. S. Sullivan, J. D. Parish, P. Thongchai, G. Kociok-Köhn, M. S. Hill and A. L. Johnson, *Inorganic Chemistry*, 2019, **58**, 2784-2797.
16. A. Saeed, U. Flörke and M. F. Erben, *Journal of Sulfur Chemistry*, 2014, **35**, 318-355.
17. M. Nencki, *Berichte der deutschen chemischen Gesellschaft*, 1873, **6**, 598-600.
18. K. R. Koch, *Coordination Chemistry Reviews*, 2001, **216**, 473-488.
19. M. M. Habtu, S. A. Bourne, K. R. Koch and R. C. Luckay, *New Journal of Chemistry*, 2006, **30**, 1155-1162.
20. P. Anastas and N. Eghbali, *Chemical Society Reviews*, 2010, **39**, 301-312.
21. I. B. Douglass and F. Dains, *Journal of the American Chemical Society*, 1934, **56**, 719-721.
22. G. Weber, J. Hartung and L. Beyer, *Journal für Praktische Chemie*, 1988, **330**, 241-247.
23. N. Kurnakow, Journal für Praktische Chemie, 1898, **50**, 234.
24. H. A. Nkabyo and K. Koch, *Journal of Molecular Structure*, 2019, **1190**, 47-53.
25. H. A. Nkabyo, D. Hannekom, J. McKenzie and K. R. Koch, *Journal of Coordination Chemistry*, 2014, **67**, 4039-4060.
26. L. Beyer, E. Hoyer, J. Liebscher and H. Hartmann, *ZEITSCHRIFT FUR CHEMIE*, 1981, **21**, 81-91.
27. K. Koch, C. Sacht, T. Grimmbacher and S. Bourne, *South African Journal of Chemistry*, 1995, **48**, 71-77.
28. A. Dago, Y. Shepelev, F. Fajardo, F. Alvarez and R. Pomés, *Acta Crystallographica Section C: Crystal Structure Communications*, 1989, **45**, 1192-1194.

29. K. R. Koch, C. Sacht and S. Bourne, *Inorganica Chimica Acta*, 1995, **232**, 109-115.
30. H. Hartmann and I. Reuther, *Journal für Praktische Chemie*, 1973, **315**, 144-148.
31. K. H. König, M. Kuge, L. Kaul and H. J. Pletsch, *Chemische Berichte*, 1987, **120**, 1251-1253.
32. C. Kharbanda, M. S. Alam, H. Hamid, K. Javed, S. Bano, Y. Ali, A. Dhulap, P. Alam and M. Pasha, *New Journal of Chemistry*, 2016, **40**, 6777-6786.
33. Y. Takahashi, M. Nishioka, K. Toyofuku and K. Uchida, *US 5314859A*, 1992.
34. C.-W. Ding, H.-F. Yu, R.-M. Li, X.-F. Jiang and B. Luo, *Arkivoc*, 2012, **9**, 254-261.
35. A Maurice and C. Paul, *US Patent 2,498,782*, 1950.
36. M. Shah, M. Y. Mhasalkar, V. M. Patki and C. V. Deliwala, *Journal of Scientific & Industrial Research*, 1959, **12B**, 202-204.
37. D. Tan, V. Štrukil, C. Mottillo and T. Friščić, *Chemical Communications*, 2014, **50**, 5248-5250.
38. M. Calvin and N. C. Melchior, *Journal of the American Chemical Society*, 1948, **70**, 3270-3273.
39. K. Koenig, J. Bosslet and C. Holzner, *ChemInform*, 1989, **20**.
40. M. Schuster and M. Šandor, *Fresenius' Journal of Analytical Chemistry*, 1996, **356**, 326-330.
41. A. Bult, *Pharmaceutisch weekblad*, 1981, **3(1)**, 213-223.
42. M. Doering, E. Uhlig, V. Nefedov and I. Salyn, *ChemInform*, 1988, **19**.
43. P. S. Thomas, *Journal fuer Praktische Chemie (Leipzig)*, 1991.
44. E. D. Uhlig, M.; Trishkina, E. M.; Nefedov, V. I., *Koordinatsionnaya Khimiya*, 1988.
45. C. Holzner, K.-H. König and H. Goesmann, *Monatshefte für Chemie/Chemical Monthly*, 1994, **125**, 1339-1352.
46. E. D. Uhlig, M., *Conference on Coordination Chemistry*, 1985, **10**.

2 Coordination chemistry of *N*-tolyl sulfonyl-*N`*-phenylthiourea [$TolSO_2NHC(S)NHPh$] with platinum(II), palladium(II), nickel(II) and gold(III) metal centres

2.1 Introduction

As previously discussed in Chapter 1, while there has been a relatively recent increase of interest in thiourea compounds due to their numerous uses in both industrial and pharmaceutical applications, very few examples of sulfonylthiourea complexes can be found within the literature. The vast majority of the reported complexes are from relatively few studies which focused on a single ligand with multiple metal centres. This observation is due to the vast majority of inorganic and coordination studies of thioureas being focused on the core thiourea moiety and on the closely related acylthioureas. To this point, little focus has been placed on sulfonylthioureas for these coordination studies.

When examining the coordination of the complexes which have been previously reported, a clear coordination trend can be observed. Of these reported complexes only two coordination modes are observed, bidentate 4 member ring complexes (*via* N and S) and 6 member bidentate complexes (*via* S and O).

Heavy transition metals with larger radii and which are chemically soft tend to coordination to one of the non-equivalent thiourea nitrogen atoms. This coordination mode results in a slightly skewed 4 member ring structure, shown in Figure 2.1.

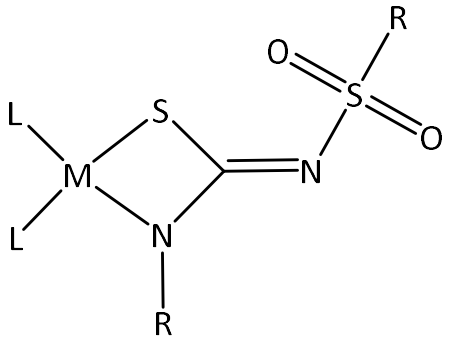

Figure 2.1: Bidentate 4 member ring structure of sulfonylthiourea complexes.

The second primary coordination mode observed within the literature is the bidentate 6 membered ring coordination structure, resulting in a delocalised chelate ring, shown in Figure: 2.2.

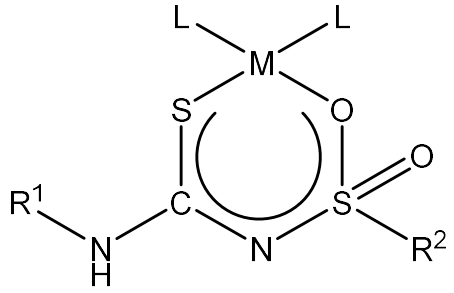

Figure: 2.2: Bidentate 4 coordinate structure of sulfonylthiourea complexes.

This bidentate S and O coordination mode predominately forms with soft metal centres with small radii such as Ag, Cu, Pd, Co and Ni. While this coordination mode can be argued as being more stable due to it containing less steric strain than the 4 membered ring, literature reported structures indicate this coordination mode to be less likely to form. This observation can be expected to be primarily due to the observed resistance to reactivity of the sulfonyl group, which would be required to form a 6 member ring. In some cases, both coordination modes were observed for the same complex, such as the case of Ni and Pd metal centres.

Metal complexes synthesised from the title ligand, $TolSO_2NHC(S)NHPh$, **2** shown in Figure 2.3, have been produced herein for the d^8 metal centres of platinum(II), palladium(II), nickel(II) and gold(III) for the purpose of examining their coordination, in particular the effects of these various metal centres on the coordination of a ligand with consistent substituents.

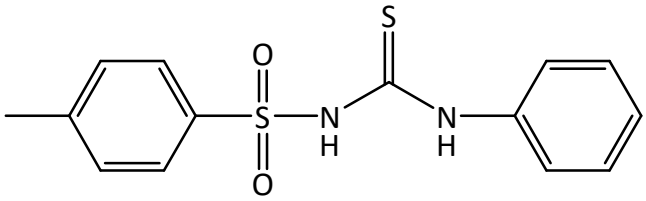

Figure 2.3: Structure of $TolSO_2NHC(S)NHPh$

2.2 Experimental

2.2.1 General procedures and instrumentation

Chemicals:

Toluene-*p*-sulfonamide and diphenylthiourea were sourced from BDH chemicals. Phenyl isothiocyanate, deuterated chloroform and general solvents were sourced from Sigma Aldrich. *cis*-$[PtCl_2(PPh_3)_2]$[1], $[AuCl_2(BP)]$[2] (BP = 2-benzylpyridyl) and $[NiCl_2(Dppe)]$[3] (Dppe = 1,2-bis(diphenylphosphino)ethane) were prepared by previously reported literature methods and used as is. $[PdCl_2(Dppe)]$[1] and $[PtCl_2(Dppp)]$[4] (Dppp = 1,3-bis(diphenylphosphino)propane) were prepared and supplied using literature reported methods.

NMR spectroscopy:

$^{31}P\{^1H\}$, ^1H and ^{13}C NMR spectra were recorded using a 400 MHz Bruker Avance DRX400 FT-NMR spectrometer using $CDCl_3$ as the solvent unless otherwise states and a temperature of 298K. Spectra were processed using Bruker topspin software.

Mass spectrometry:

Mass spectra were recorded in methanol using a Bruker Daltonics Microtof electrospray ionisation mass spectrometer. Sodium formate was used for calibration. Samples were prepared in Eppendorf tubes by dissolving the solid sample in 1 drop of dichloromethane and making up to 1.5 ml with methanol. Samples were centrifuged before use to ensure separation of undissolved solids. Spectra were recorded with a capillary exit voltage of 150V and a skimmer 1 voltage of 50V unless otherwise stated.

Infrared spectroscopy:

Infrared spectra were recorded using a Perkin Elmer Spectrum 100 Fourier transform IR spectrometer with an observed range of 4000-450cm^{-1}. Samples were prepared as KBr disks.

Melting point:

Melting points were recorded on a Reichert-Jung thermovar as solid samples placed on glass slides. Temperatures were recorded at the first signs of liquifying.

Elemental analysis:

Elemental analysis of all compounds was performed externally by the Campbell Microanalytical Laboratory, Department of Chemistry, University of Otago.

X-Ray crystallography:

Structural data was generated using a SuperNova, Single source at offset, Atlas diffractometer at a temperature of 100K with Cu Kα X-Ray radiation (6.390 mm, 1.5406 Å). The structure was solved by direct methods using Olex2[5] with the olex2.solve[6] structure solution program using Charge Flipping and refined with the olex2.refine[6] refinement package using Gauss-Newton minimisation.

2.2.2 Synthesis of [TolSO$_2$NHC(S)NHPh], 2.

The synthesis of the title ligand was carried out using an adapted procedure given by Shah *et al*[7]. *p*-Toluene sulfonamide (10 g, 0.058 mol) (TolSO$_2$NH$_2$) was dissolved in acetone (70 ml). To this mixture, NaOH (2.34 g, 0.058 mol) dissolved in distilled water (20 ml) was added. The resulting slightly opaque pale-yellow solution was stirred for 10 minutes followed by the addition of phenyl isothiocyanate (7.89 g, 0.058 mol) (PhNCS) added portionwise. The resulting yellow solution was stirred at room temperature for 48 hours, filtered to remove any unwanted reaction solids followed by acidification with glacial acetic acid to achieve a pH of 4. A white solid precipitate was obtained by addition of excess distilled water (approx. 200 ml). The product was separated by vacuum filtration and washed with distilled water (2 x 30 ml) followed by cold EtOH (2 x 30 ml). The solid was recrystallised from hot EtOH to give a white crystalline solid. A reaction scheme is shown in Figure 2.4. Yield, 6 g, 35%. m.p 145-148°C (lit[8]. 144-146°C); ESI-MS: Capillary exit voltage 90V, *m/z* $[M+H]^+$ 307.06 (calculated 307.41); ^{1}H NMR (400.13 MHz, chloroform-d$_1$) δ ppm 2.47 (3H, s, CH$_3$), 7.30 (1H, tt, *p*-Ph), 7.40 (6H, m), 7.86 (2H, d, *m*-tol) 8.86 (1H, s, NH) 9.79 (1H, s, NH); FT-

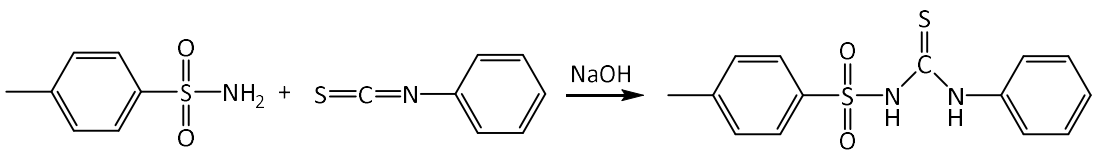

Figure 2.4: Reaction scheme of TolSO$_2$NHC(S)NHPh from p-tolyl sulfonamide and phenyl isothiocyanate

IR (cm^{-1}): υ(NH) 3304 (m) and 1597 (w), υ(S=O) 1381 (s) and 1146 (s). υ(CN) 1481 (m) and 1179 (m).

2.2.2.1 Synthesis of [$TolSO_2NHC(S)NHPh$] in non-aqueous conditions.

p-Toluene sulfonamide (10 g) ($TolSO_2NH_2$) was dissolved in dichloromethane (50 ml). To this mixture, triethylamine (6 g) was added. The resulting clear pale-yellow solution was stirred while phenyl isothiocyanate (7.89 g) (PhNCS) was added portionwise. The reaction mixture was left to stand at room temperature without stirring for 24 hours followed by evaporation of the solvent to give a crystalline solid which was then washed with water (2 x 10 ml) and cold methanol (3 x 50 ml) to give a white crystalline solid, 9.5 g, 55%, ESI-MS: Capillary exit voltage 90 V, *m/z* $[M+H]^+$ 307.06 (calculated 307.05).

2.2.2.2 Synthesis of diphenyl thiourea by the self-reaction of phenyl isothiocyanate in basic aqueous conditions.

Phenyl isothiocyanate (7.89 g) was added to acetone (70 ml). To this solution, NaOH (2.34 g) dissolved in distilled water (20 ml) was added. The resulting clear yellow solution was left to sit for 48 hours followed by acidification with glacial acetic acid to a pH of 4. The product was separated as a white solid by precipitation with excess distilled water (approx. 200 ml) and separated by filtration. The resulting solid was dried in vacuum, 7.6 g, 58%. ESI-MS: capillary exit voltage 90V, *m/z* $[M+H]^+$ 229.08 (calculated, 229.08) . The structure of diphenylthiourea is given below in Figure 2.5

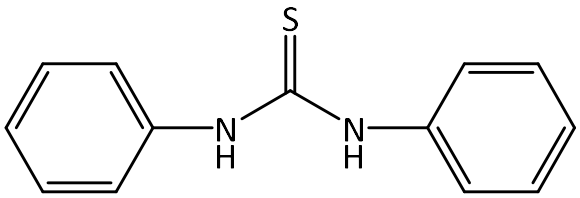

Figure 2.5: Structure of diphenylthiourea

2.2.3 Synthesis of *cis*-[$PtCl_2(PPh_3)_2$]

cis-[$PtCl_2(PPh_3)_2$] was prepared by a modified procedure[1] by a 2:1 reaction of triphenylphosphine and [$PtCl_2$(COD)] as follows, [$PtCl_2$(COD)] (0.5 g) was dissolved in CH_2Cl_2 (20 ml). While stirring, PPh_3 (0.700 g) was added, stirred for five minutes followed by the addition of petroleum sprits (*ca* 50 ml) to facilitate precipitation. The product was filtered and washed with petroleum spirits (2 x 15 ml) and dried in air to give the product as a white powder solid. 0.93 g, 95%.

2.2.4 Synthesis of [$AuCl_2$(BP)]

[$AuCl_2$(BP)] was prepared by a modified previously reported method[2]. The 1:1 reaction of 2-benzylpyridine and $Me_4N[AuCl_4]$ was carried as follows. $Me_4N[AuCl_4]$ (1.00 g) was suspended in distilled water (55 ml). To this, 1 mol equivalent of 2-benzylpyridine (0.460 g) was added in a single addition. The mixture was refluxed for 16 hours by which time the yellow suspension had turned white with a purple hue. The white solid was filtered while the solution was still hot (*ca.* 60°C). The white solid was washed with hot water (2 x 30 ml) and dried by vacuum, 0.78 g, 68%. ^{1}H NMR (400.13 MHz, chloroform-d_1) δ ppm 8.2-7.2 (m, aromatic), 4.59 (H_a, d, CH_2), 4.06 (H_b, d, CH_2) [J(AB) =15].

2.2.5 Synthesis of [$NiCl_2$(Dppe)]

[$NiCl_2$(Dppe)] was prepared using a previously reported literature method[3] in a 1:1 molar ratio reaction of 1,2-bis(diphenylphosphino)ethane (0.5 g) in warm ethanol with hydrated nickel(II) chloride (0.4 g). The product precipitated out of solution as a crystalline orange-brown solid, separated from solution by vacuum filtration and dried in air. Yield 0.48 g, 80%.

2.2.6 Synthesis of platinum(II), palladium(II) and gold(III) metal complexes of $TolSO_2NHC(S)NHPh$

The general procedure for all metal complexes synthesised from the title ligand is as follows. Equal molar amounts of the ligand [$TolSO_2NHC(S)NHPh$] and metal starting material were suspended in MeOH (30 ml) in a 250 ml round bottom flask with stirring. The solution was brought to reflux temperature followed by the addition of triethylamine (0.8 ml, excess). The solution was refluxed for 10 minutes followed by the addition of distilled water (40 ml) to precipitate any solid. The mixture was cooled rapidly using an ice bath to facilitate precipitation and coagulation. Where stated, NaCl (0.4 g) was added and allowed to stir for 1 hour to aid in coagulation. The solids were filtered and washed with 2 x 20 ml (4 x 50 ml if NaCl added) hot water and dried under vacuum. Details pertaining to each compound synthesised by this method are given in Table 2.1

*Table 2.1: Synthesis of sulfonylthiourea complexes from TolSO2NHC(S)NHPh, **2**.*

** = NaCl was used.*

				2		**Yield**			**NaCl**
Starting material	Code	mg	mmol	mg	mmol	mg	%	Colour	
$[PtCl_2(PPh_3)_2]$	**2a**	100	0.126	40	0.127	101	78	pale yellow	*
$[AuCl_2(BP)]$	**2b**	100	0.229	71	0.229	115	75	deep yellow	*
$[PdCl_2(Dppe)]$	**2c**	100	0.173	54	0.174	112	80	orange-brown	
$[PdCl_2(Bipy)]$	**2d**	100	0.300	95	0.300	97	57	orange-red	*
$[PtCl_2(Dppp)]$	**2e**	100	0.147	45	0.147	108	77	off white	
$[NiCl_2(Dppe)]$	**2f**	100	0.189	60	0.189	126	87	orange	

2.2.7 Synthesis of $[Pd_3S_2(Dppe)_3]^{2+}$

[Pd{$TolSO_2C(S)NPh$}(Dppe)] (**2c**) (20 mg) was dissolved in methanol (20 ml) and heated slightly below boiling for a duration of 7 hours.

Alternatively, [Pd{$TolSO_2NC(S)NPh$}Dppe] (20 mg) was dissolved in chloroform (0.5 ml) and let sit at room temperature for a duration of 14 days.

2.3 Characterisation

Only ESI-MS peaks of $[M+H]^+$ are presented unless otherwise stated. Elemental analysis of complex **2c** and **2d** were unavailable due to further reaction of the product to form trinuclear aggregates as will be discussed below in Section 2.4.3.

2.3.1 [Pt{TolSO$_2$NC(S)NPh}(PPh$_3$)$_2$], 2a

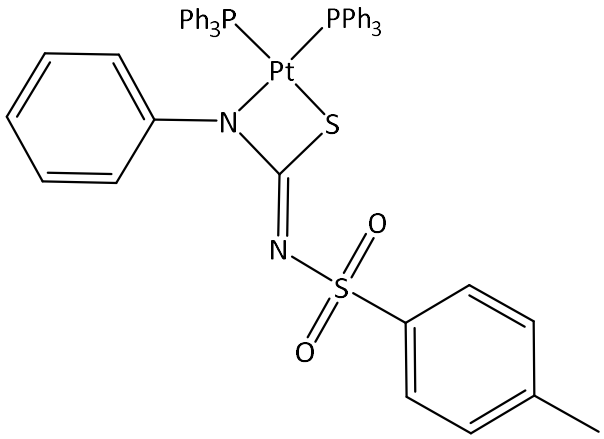

*Figure 2.6: Complex **2a***

Elemental analysis: Found (%) C 58.89; H 4.73; N 2.72. Calculated (%) C 58.65; H 4.14; N 2.74.

Melting point: 277-280°C

ESI-MS: *m/z* $[M+H]^+$ 1025.09 (calculated, 1025.06).

FT-IR (cm^{-1}): 3204 (w, broad), 3047 (w, broad), 1600 (s), 1563 (vs), 1486 (s), 1434 (s), 1312 (s), 1098 (s), 754 (s), 693 (vs), 544 (s).

NMR: $^{31}P\{^1H\}$ δ (ppm) 15.6 (d, P(1), ^1J[PtP(1)] 3039 Hz, ^2J[P(1)P(2)] 21 Hz) and 10.7 (d, P(2), ^1J[PtP(2)] 3380 Hz, ^2J[P(1)P(2)] 22 Hz). ^1H δ 7.7-6.2 (m, aromatic), 2.35 (3H, s, CH_3).

2.3.2 [Au{TolSO$_2$NC(S)NPh}(BP)], 2b

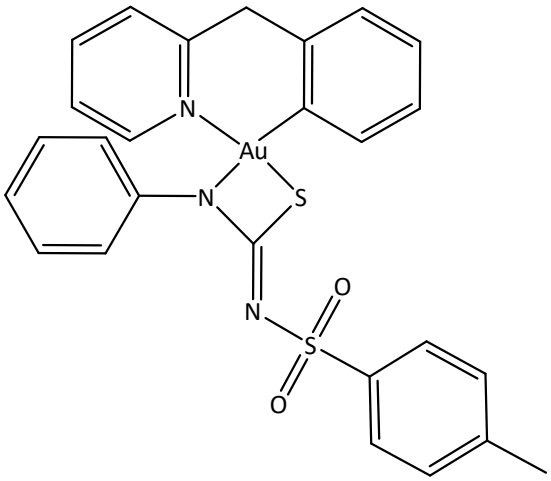

*Figure 2.7: Complex **2b***

Elemental analysis: Found (%) C 46.14; H 3.31; N 6.22. Calculated (%) C 46.63; H 3.31; N 6.28.

Melting point: 121-127°C

ESI-MS: *m/z* $[M+H]^+$ 669.97 (calculated, 670.09) and $[M+Na]^+$ 691.95 (calculated 692.06)

FT-IR (cm^{-1}): 1611 (w), 1592 (w), 1493 (vs, broad), 1447 (m), 1336 (s), 1281 (w), 1145 (s), 1185 (m), 690 (m), 545 (m).

NMR: ^1H δ 8.9-6.7 (m, aromatic), 3.41 (2H, s, CH_2) and 2.40 (3H, s, CH_3).

2.3.3 [Pd{TolSO$_2$NC(S)NPh}(Dppe)], 2c

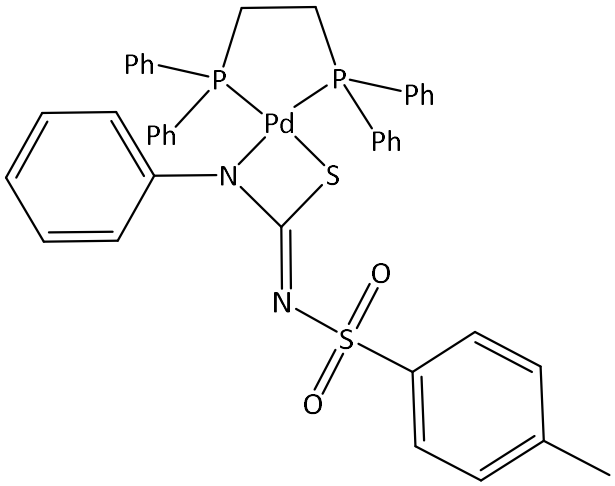

*Figure 2.8: Complex **2c***

Melting point: 129-132°C

ESI-MS: *m/z* $[M+H]^+$ 808.98 (calculated, 809.08).

FT-IR (cm^{-1}): 1589 (w), 1471 (vs), 1446 (s), 1325 (s), 1276 (w), 1140 (s), 1103 (m), 1089 (s), 691 (s), 530 (m).

NMR: $^{31}P\{^1H\}$ δ (ppm) 56.9 (d, P(2), ^2J[P(1)P(2)] 34 Hz) and 49.5 (d, P(1), ^2J[P(1)P(2)] 35 Hz) ^1H δ 8.0-6.5 (m, aromatic), 2.34 (3H, s, CH_3).

2.3.4 [Pd{TolSO$_2$NC(S)NPh}(Bipy)], 2d

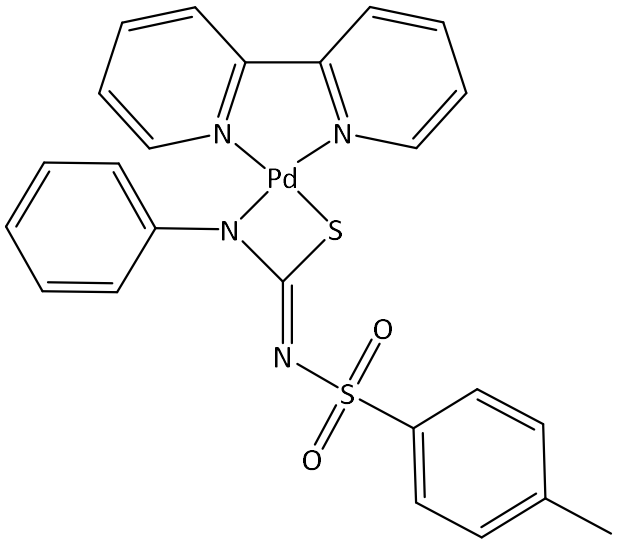

*Figure 2.9: Complex **2d***

Melting point: 143-146°C

ESI-MS: *m/z* $[M+H]^+$ 567.20 (calculated, 967.01) and $[M+Na]^+$ 589.90 (calculated, 589.00)

FT-IR (cm^{-1}): 1601 (w), 1487 (s), 1446 (m), 1330 (m), 1276 (w), 1208 (vw), 1140 (s), 1088 (s), 766 (w), 692 (w)

NMR: ^1H δ 8.4-6.8 (m, aromatic), 2.37 (3H, s, CH_3).

2.3.5 [Pt{TolSO$_2$NC(S)NPh}(Dppp)], 2e

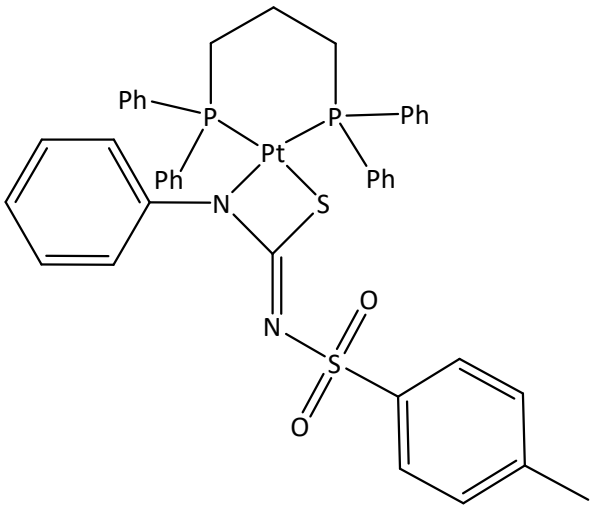

*Figure 2.10: Complex **2e***

Elemental analysis: Found (%) C 55,69; H 3.76; N 2.81. Calculated (%) C 53.99; H 4.20; N 3.07.

Melting point: 147-150°C

ESI-MS: *m/z* $[M+H]^+$ 912.02 (calculated, 912.16) and $[M+Na]^+$ 934.00 (calculated, 934.14).

FT-IR (cm^{-1}): 1590 (w), 1473 (vs), 1364 (s), 1328 (s), 1277 (m), 1140 (s), 1102 (m), 1089 (m), 690 (s), 545 (m), 514 (s).

NMR: $^{31}P\{^1H\}$ δ (ppm) -2.89 (d, P(1), ^1J[PtP(1)] 2906 Hz, ^2J[P(1)P(2)] 33 Hz) and -11.22 (d, P(2), ^1J[PtP(2)] 3024 Hz, ^2J[P(1)P(2)] 33 Hz). ^1H δ 7.8-6.3 (m, aromatic), 2.35 (3H, s, CH_3).

2.3.6 [Ni{TolSO$_2$NC(S)NPh}(Dppe)], 2f

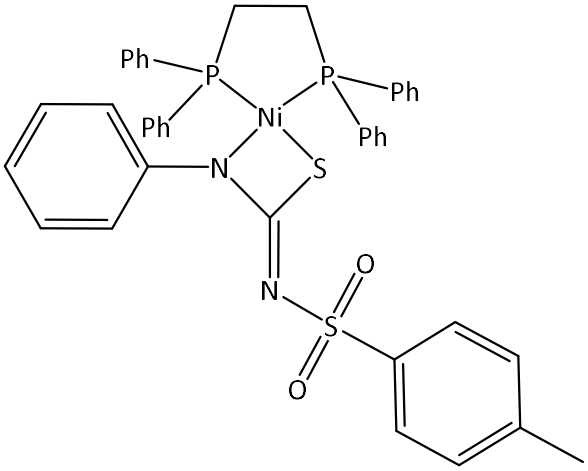

*Figure 2.11: Complex **2f***

Elemental analysis: Found (%) C 63.01; H 4.82; N 3.53. Calculated (%) C 63.09; H 4,77; N 3.68.

Melting point: 140-145°C

ESI-MS: *m/z* $[M+H]^+$ 760.80 (calculated, 761.11).

FT-IR (cm^{-1}): 1626 (w), 1591 (w), 1484 (vs), 1435 (s), 1328 (s), 1289 (m), 1126 (s), 1097 (s), 693 (s).

NMR: $^{31}P\{^1H\}$ δ (ppm) 58.4 (d, P(2), ^2J[P(1)P(2)] 38 Hz) and 53.5 (d, P(1), ^2J[P(1)P(2)] 38 Hz) ^1H δ 8.1-6.4 (m, aromatic), 2.34 (3H, s, CH_3).

2.4 Results and discussion

2.4.1 Synthesis

Synthesis of the sulfonylthiourea ligand *via* the RSO_2NH_2 + RNCS route in acetone with aqueous sodium hydroxide reported here resulted in both the target ligand ($TolSO_2NHC(S)NHPh$) and a secondary product in high yield. This by-product was later confirmed by ^1H NMR and ESI-MS characterisation to be the disubstituted 1,3-diphenylthiourea (PhNHC(S)NHPh). Successful separation of the target sulfonylthiourea ligand was achieved by two consecutive crystallisations in hot EtOH and multiple washings with cold EtOH, resulting in a large loss of yield.

ESI-MS of the first crystallisation of the ligand, shown in Figure 2.12, showed both an *m/z* of 229, relating to the diphenylthiourea $[M+H]^+$ ion and a *m/z* 307 ion relating to the target *p*-tolyl sulfonylthiourea $[M+H]^+$ ion. The addition of sodium formate produced the $[M+Na]^+$ peaks of both compounds with elevated relative intensities.

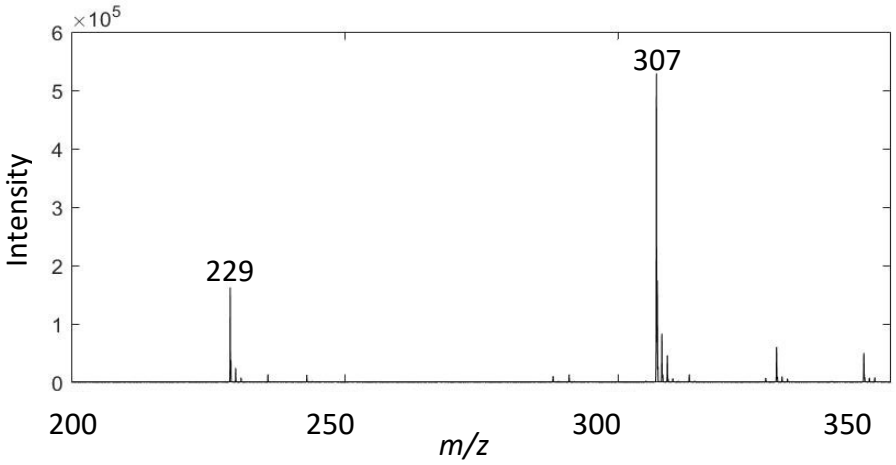

Figure 2.12: ESI-MS spectrum of p-tolyl sulfonylthiourea and diphenylthiourea

Evaporation of the crystallisation filtrate of the sulfonylthiourea ligand yielded a white crystalline solid of diphenylthiourea. To confirm the identity of the by-product the sample was then reacted with *cis*-$[PtCl_2(PPh_3)_2]$ to produce the platinum triphenylphosphine diphenylthiourea complex $[Pt\{PhNC(S)NPh\}(PPh_3)_2]$, a known thiourea complex[9]. ESI-MS of this complex resulted in a $[M+H]^+$ ion with

an *m/z* of 946 which is consistent with the expected diphenylthiourea complex. The isotope pattern of the $[M+H]^+$ ion peak also matches with the calculated isotope pattern. The isotope pattern also confirms the presence of platinum due to its distinctive pattern. Both the ESI-MS of the diphenylthiourea complex and the experimental and calculated splitting patterns is shown in Figure 2.13. ESI-MS and ^1H NMR of both the by-product and subsequent platinum complex confirms the identity of the by-product to be diphenylthiourea.

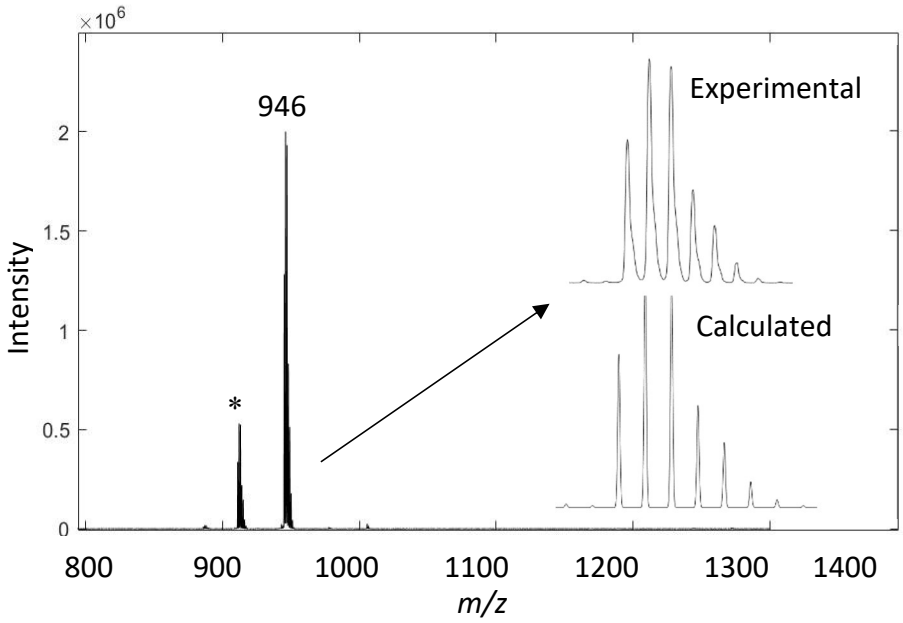

Figure 2.13: ESI-MS and Isotope patterns of [Pt{PhNC(S)NPh}(PPh$_3$)$_2$]

** = unknown Pt containing ion (m/z = 912)*

2.4.1.1 Synthesis of diphenylthiourea by hydrolysis of phenyl isothiocyanate in aqueous conditions.

As previously discussed, the formation of disubstituted thioureas was noted to have formed during the sulfonylthiourea ligand synthesis. Discussion relating to this formation of disubstituted thioureas during the synthesis of sulfonylthioureas is notably absent from relevant literature. However, the method used for the synthesis of the *p*-tolyl substituted sulfonylthiourea presented by Shah *et al*[10] reports low yields of 50%, possibly due to the competing thiourea synthesis. Other related methods for the synthesis of sulfonylthioureas also make no mention of this reaction and report similar or lower yields[8].

As the substituent of the produced thiourea by-product is the same as the isothiocyanate it can be assumed that this starting material is involved in the formation. Literature regarding the synthesis of di-substituted thioureas is dominated almost exclusively by the reaction of primary amines with isothiocyanate in a similar synthetic route to that of sulfonylthiourea, as discussed in Section 1.4. Although seldom reported, examples of the synthesis of 1,3-disubutiuted thioureas by isothiocyanates in the absence of amines is reported[11, 12].

It has also been noted that reactions involving isothiocyanates as a starting material or reagent frequently produce disubstituted thioureas as by-products whose formation is commonly associated with the presence of water[12, 13]. Interestingly, the nucleophilic addition of water to the central carbon atom is a main decomposition route of isothiocyanates. This addition results in an adduct (RNHC(S)OH) which further undergoes elimination of COS to give the corresponding primary amine[14]. The scheme is shown in Figure 2.14.

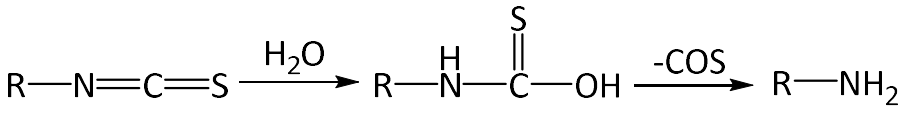

Figure 2.14: Formation of a primary amine via hydrolysis of isothiocyanate

It could then be proposed that this primary amine then reacts with a second isothiocyanate molecule to produce a disubstituted thiourea by a simple nucleophilic addition which has been reported[15].

An alternative scheme has been proposed by Blanco *et al*[12] who reports an amine free synthesis of symmetric urea's and thioureas by the self-condensation of isothiocyanates. In this reaction the isothiocyanate is activated by water to produce an anhydride type intermediate (RNHC(S)OC(S)NHR) which proceeds to be converted into substituted symmetrical disubstituted urea, as shown in Figure 2.15

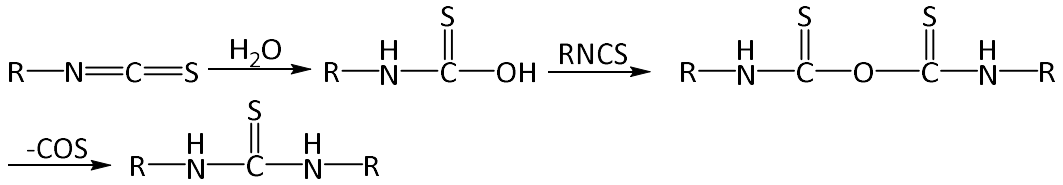

Figure 2.15: Synthesis of disubstituted thiourea via an anhydride type intermediate

This scheme was produced as it was discovered that the proportion of symmetric thiourea significantly increased during an attempted reaction of isothiocyanates in damp pyridine[16], in which no products arising from O and N acyl migration were detected in the reaction mixtures when carbohydrate substrates were employed. This suggested a different amine free mechanistic pathway. It was reasoned that in basic aqueous conditions the thiocarbamate intermediate (RNHC(S)OH) may be stabilised and act directly as the nucleophile, with no generation of free primary amines in solution.

A later study by Perveen *et al*[11] reported a synthesis of symmetrical 1,3-disubutiuted thioureas in aqueous conditions from corresponding isothiocyanates. It was noted that the rate of reaction is promoted by the presence of tertiary amines. It was commented by the author that the previous reported scheme by Blanco *et al*[12] lacked any indication of involvement of tertiary amines in their synthesis which this study deemed essential. Therefore, a new scheme was proposed for the formation of symmetrical thioureas, the thiocyanate variation of which is shown in Figure 2.16.

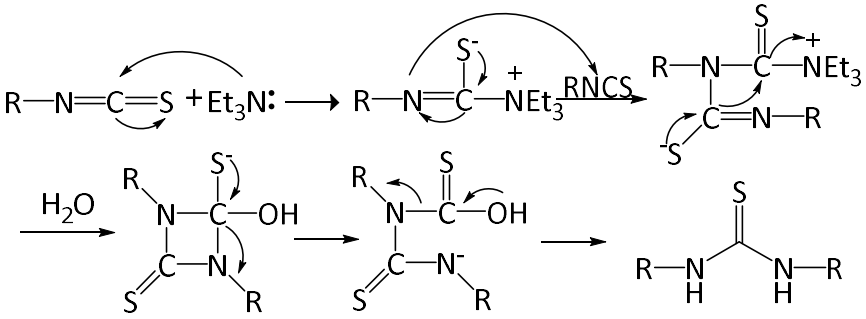

Figure 2.16: Reaction scheme for the synthesis of disubstituted thiourea from isothiocyanate

It can be seen that reactions that use of isothiocyanate as a reagent, including the sulfonylthiourea synthesis reported here, suffer from decomposition of the starting material in aqueous conditions to form symmetrical disubstituted thioureas. It may also be expected that even synthesis of non-symmetrical disubstituted thioureas by nucleophilic addition of an amine to thiocyanate would still suffer from the formation of symmetric thiourea by-products through the decomposition route discussed above, although this is yet to be explored. It should be noted that if the formation does occur it should be expected to be minor in comparison to the expected non-symmetrical thiourea as reported synthesis methods are in high yield and purity. In an attempt to determine the yield of diphenylthiourea from the sulfonylthiourea reaction used to synthesis the title ligand, given in Section 2.2.2, a parallel reaction was done to self-react phenyl isothiocyanate in acetone with aqueous sodium hydroxide in the absence of *p*-tolyl sulfonamide. The resulting diphenylthiourea was formed with a 58% yield indicating that a significant portion of the isothiocyanate starting material in the sulfonylthiourea reaction was being decomposed to diphenylthiourea and therefore reducing the yield of the target ligand.

2.4.1.2 Synthesis of *p*-tolyl sulfonylthiourea, [TolSO$_2$NHC(S)NHPh] in water-free conditions

An attempt to minimise the formation of diphenylthiourea during the *p*-tolyl sulfonylthiourea reaction was made for the purpose of increasing the product yield. Standard drum grade dichloromethane was used as a replacement for acetone to reduce potential water content in the solvent as well as to aid in removal of the solvent by evaporation. The chosen base was changed to triethylamine to significantly reduce the water content. The reaction time remained constant with the solvent being partially evaporated slowly over a further 24 hours to yield a crystalline solid of the deprotonated sulfonylthiourea ligand. After washing with methanol, the white crystalline solid was dried in vacuum. ESI-MS of the product showed diphenyl thiourea in significantly less intensity. ^{1}H NMR of the crystalline solid also indicated no mixture of ligands by integration of aromatic protons relative to the tolyl CH_3 protons, however Et_3N was present. The product yield was 55%, increased by 20% from 35% yield in aqueous conditions.

2.4.2 NMR Characterisation

2.4.2.1 Isomerisation

Isomerisation between the bidentate coordination modes of thiourea and acylthiourea complexes have been reported for asymmetrically di-substituted ligand metal complexes[17] namely that of the *cis-trans* isomerisation of ML_2 complexes of acylthioureas[18, 19]. Sulfonylthiourea ligands contain non-equivalent nitrogen binding sites which create two distinct S-N bidentate coordination modes. The nitrogen attached to the sulfonyl group may be involved in bonding to the metal centre causing the sulfonyl group to be close to the metal centre (*proximal*). Alternatively, this nitrogen may point away from the metal centre when the second nitrogen is involved in the bonding (*distal*). These two isomers are shown in Figure 2.17. It can be expected that due to these distinct isomers, isomerisation may be observed as is seen with the closely related acylthiourea and thiourea complexes.

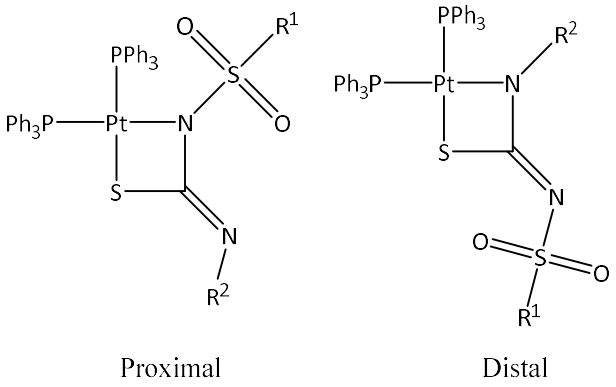

Figure 2.17: Proximal and Distal isomers of sulfonylthioureas

The isomerisation process is likely due to the initial kinetically favourable product being produced followed by isomerisation to the thermodynamically more stable coordination. Alternatively, the kinetically favoured and thermodynamically favoured isomer may be the same and no isomerisation will be observed. Furthermore, steric constraints may be an influencing factor in the synthesised isomers. For example, ether the bulky sulfonyl group or a sterically large substituent attached to this group may prevent the *proximal* isomer from being produced. To date no literature relating to isomerisation of sulfonylthiourea complexes has been reported.

$^{31}P\{^{1}H\}$ NMR characterisation of the phosphorus-containing complexes synthesised here (**2a, 2c, 2e** and **2f**) was used to monitor possible isomerisation between coordination modes by comparing the phosphorus peak chemicals shifts and relative intensities over a duration of time. It was expected that if isomerisation of the complex took place the phosphorus peaks of the initial coordination mode would decrease while a new set of peaks corresponding to the new coordination mode would increase.$^{31}P\{^{1}H\}$ NMR was chosen for this observation due to the relatively simple spectra which aided in monitoring changes of both chemical shift and peak intensity. This is in contrast to the complicated and often unresolved ^{1}H spectra of some metal complexes, in particular complexes with a large number of aromatic protons. Additional information such as purity and symmetry can also be inferred from phosphorus NMR.

Examination of the initial $^{31}P\{^{1}H\}$ NMR spectra of complex **2a** reveals the expected doublet of doublets each with satellite peaks due to ^{195}Pt splitting, as will be discussed below in Section 2.4.2.3. After a period of 48 hours the spectrum was recorded again with no notable change. After 8 days with consecutive scans every 48 hours no isomerisation was noticed to have taken place. A series of $^{31}P\{^{1}H\}$ spectra for complex **2a** is shown in figure Figure 2.18.

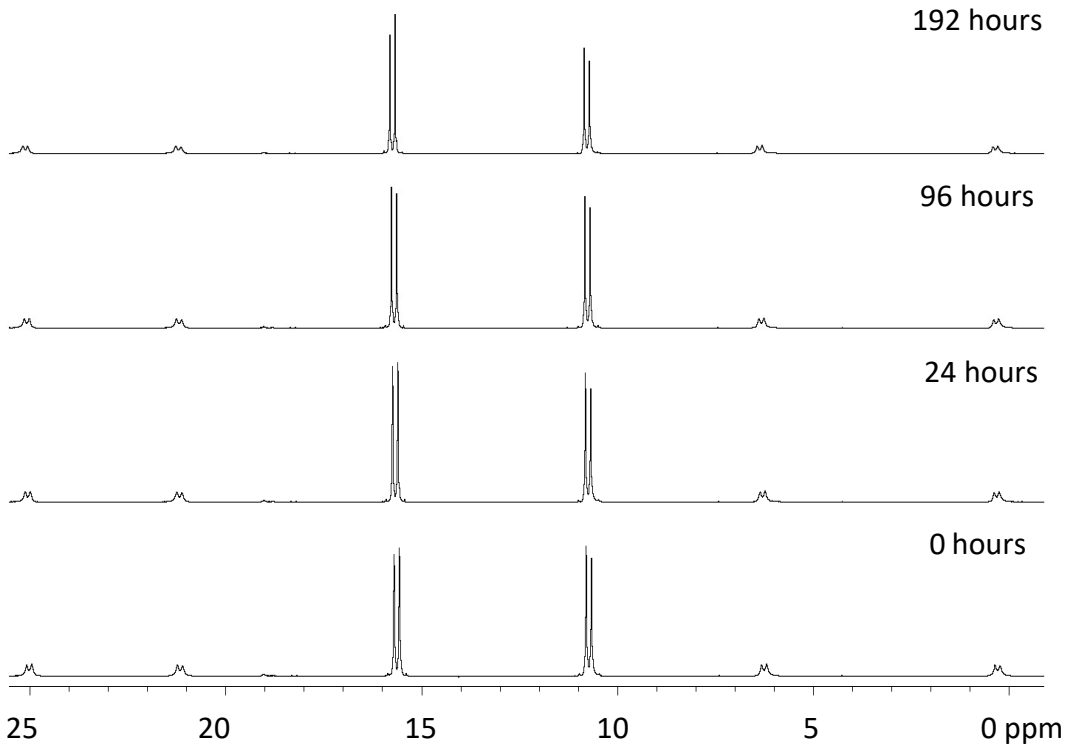

*Figure 2.18: $^{31}P\{^{1}H\}$ NMR comparison of complex **2a** over a duration of 192 hours.*

2.4.2.2 Proton NMR characterisation of complex 2b

Examination of the ^{1}H NMR spectrum of the [$AuCl_2$(BP)] starting material shows a proton which is strongly deshielded with a shift of 9.3 ppm. This doublet can be attributed to H_6, The CH_2 protons of the 2-benzylpyridyl ligand, ^{1}H spectra of the corresponding complex show the peak corresponding to H_6 has moved upfield signalling a decrease electronegativity of coordinated atoms in proximity. The non-equivalent CH_2 protons of the starting material show the standard quartet AB pattern of doublets as reported in the literature[2, 20]. This indicates slow inversion of the boat conformation of the 6 member chelated ring of the BP substituent at room temperature, in relation to the NMR time-scale. This slow inversion allows for the protons in the axial and equatorial conformations to be resolved. Interestingly, the corresponding complex (**2b**) shows these protons as an unresolved broad singlet peak at near equal distance between the doublet peaks. This broad peak indicates the inversion of the boat conformation is faster in the complex than that of the starting material. A comparison of these peaks is shown in Figure 2.19.

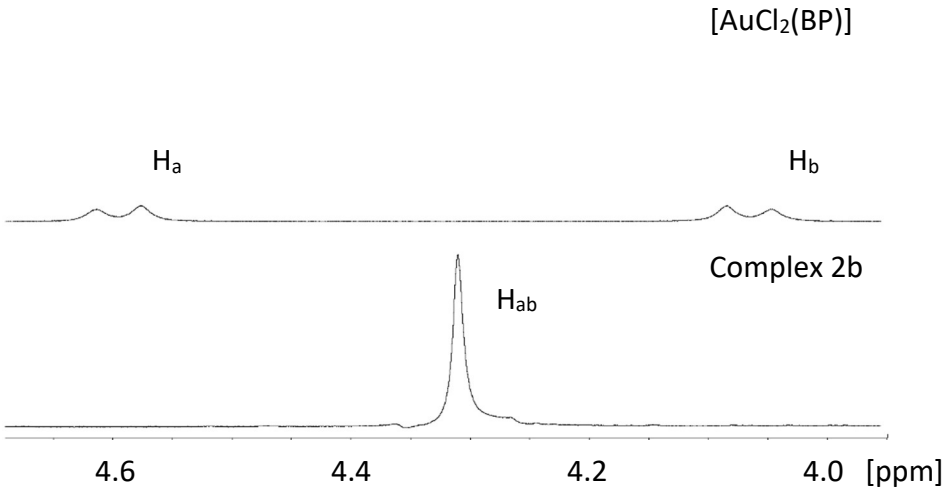

*Figure 2.19: H_6 comparison between complex **2b** and the starting material [$AuCl_2$(BP)] at room temperature.*

2.4.2.3 $^{31}P\{^{1}H\}$ NMR spectroscopy of platinum complexes.

The $^{31}P\{^{1}H\}$ NMR spectra of the platinum containing complexes **2a** and **2e** show the expected AB doublet of doublets with the corresponding satellites. These peaks represent two inequivalent phosphorus environments. Phosphorus coupling with ^{195}Pt provided J-coupling constants indicative of the degree of *trans* influence of the donor ligand atoms. These *trans* influence J-coupling value indications provide valuable information on the coordination mode adopted by the structure especially in absence of x-ray crystallographic information, such is the case with complex **2e**.

The $^{31}P\{^{1}H\}$ NMR spectrum of complex **2a**, shown in Figure 2.20, revealed a clean baseline with only one set of AB doublets indicating only one compound or isomer is present. ^{195}Pt J coupling values were 3038 Hz (PPh_3 *trans* to S) and 3380 Hz (PPh_3 *trans* to N). These values confirm the complex to be in the expected S-N bidentate coordination mode. The sulfur atom is expected to have a slightly higher *trans* influence and is therefore used to assign the phosphorus with the smaller coupling constant to the sulfur *trans* position. Isomeric information from the J-coupling values could not be concluded due to a lack of relevant literature values for comparison.

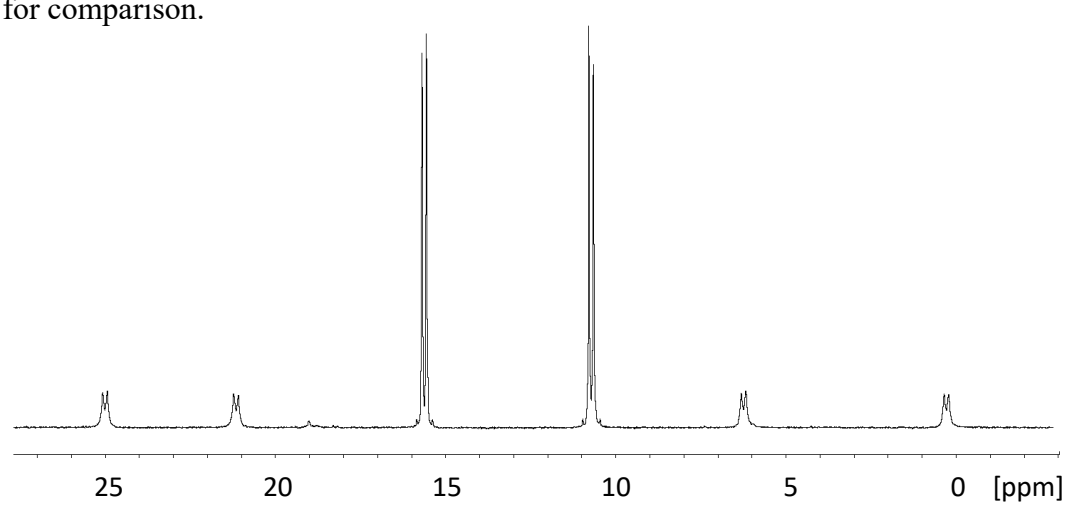

*Figure 2.20: $^{31}P\{^{1}H\}$ NMR spectrum of complex **2a***

The $^{31}P\{^{1}H\}$ NMR spectrum of complex **2e** gave a similar AB doublet of doublets with ^{195}Pt J-coupling values of 2906 Hz (P *trans* to S) and 3024 Hz (P *trans* to N). The difference in $^{1}J(PtP)$ coupling constants is 118 Hz and complex **2e** 342 Hz. This significant difference is an indication of a difference phosphine environments which is to be expected.

2.4.3 Trinuclear d^8 metal aggregates of palladium(II) formed from sulfonylthiourea ligand metal complexes.

Phosphorus NMR characterisation of complex **2c** [Pd{$TolSO_2NC(S)NPh$}(Dppe)] over a duration of four weeks was done in order to observe possible isomerisation of the complex, as is explained previously in Section 2.4.2.1. While no isomerisation was observed, a change in phosphorus peak intensities was noted to have taken place over the duration which indicates possible decomposition or further reaction, as shown in Figure 2.21.

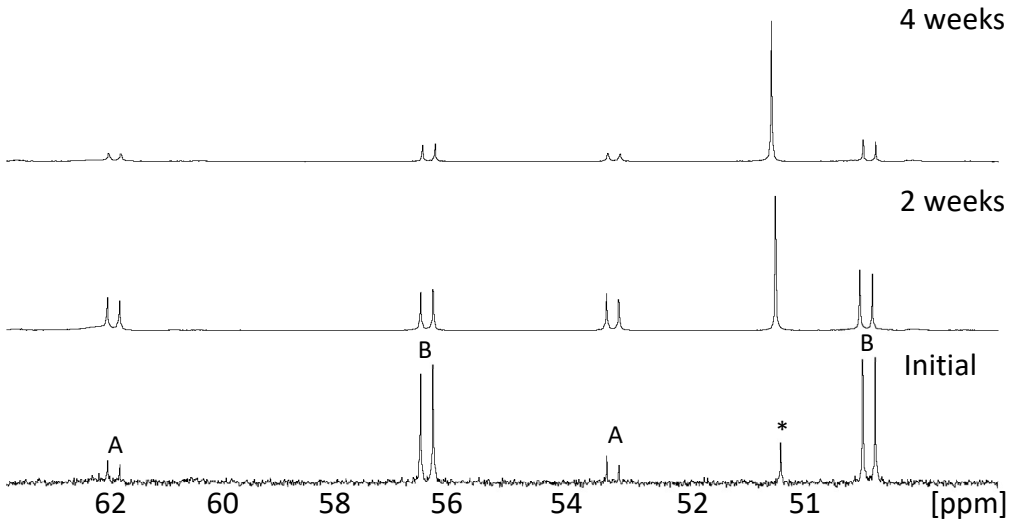

*Figure 2.21: $^{31}P\{^1H\}$ NMR comparison of complex **2c** over a duration of 4 weeks*

Initial $^{31}P\{^1H\}$ NMR spectra showed two sets of doublets corresponding to both the thiourea complex **2c**, which contains two phosphorus environments due to the bidentate coordination mode and an unknown second compound. A singlet peak at 51 ppm was also observed. The palladium starting material used in the synthesis of the complex, 1,2-bis(diphenylphosphino)ethane]dichloropalladium(II) [$PdCl_2$(Dppe)], is expected to give a singlet peak, however literature values for this have been reported to be closer to 25 ppm, significantly lower than the observed peak at 55 ppm. Furthermore, two consecutive experiments were performed over the duration which showed the intensity of the singlet peak rising as the intensity of the set of doublets corresponding to complex **2c** decreased. This observation indicates the singlet peak is the product of or related to the complex and also indicates a distinct change in chemical environment is taking place.

ESI-MS of the complex **2c** freshly dissolved in methanol was compared to the mass spectrum of the NMR sample at the end of the 4 week duration to observe the formation of any new ions which may relate to the increase in intensity of the unknown compound. The comparison of both mass spectra revealed a large intensity drop of the complex $[M+H]^+$ ion at an *m/z* of 809 as well as the appearance of 2^+ ions in the NMR sample, the most notable of which was a 2^+ ion with an *m/z* of 788, therefore a mass of 1576, which is much higher than that of complex **2c** which has a $[M+H]^+$ *m/z* of 809. Thus, it can be indicated that the source of the 2^+ ion is not due to fragmentation of the complex and is likely its own compound.

In order to confirm the hypothesis that **2c** was converting into the new compound a fresh sample of complex **2c** dissolved in methanol and the ESI-MS spectrum was recorded. The sample was then heated for a duration of 7 hours at reflux to promote the decomposition of the complex. ESI-MS spectra were recorded at 3 and 7 hour intervals, shown in Figure 2.22. Comparison of the mass spectra over the time period reveals a decrease in intensity for the $[M+H]^+$ ion of complex **2c** and a dramatic increase in intensity for the 2^+ ion *m/z* 788. The remaining mass range of the spectra remained relatively unchanged. These spectra strongly indicate a relationship between the two ions of interest.

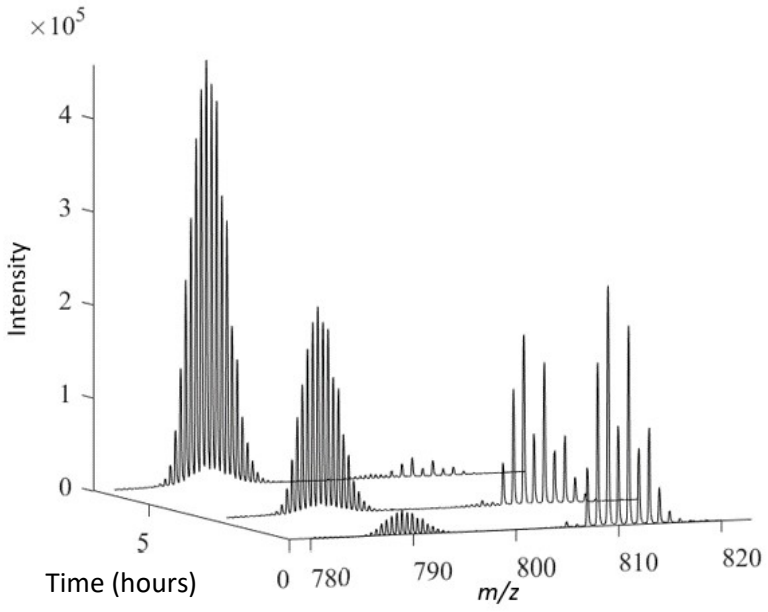

*Figure 2.22: Time comparison of complex **2c** in solution*

Literature pertaining to complexes synthesised from the starting material, [1,2-Bis(diphenylphosphino)ethane]dichloropalladium(II) [$PdCl_2$(Dppe)], revealed

a tendency for the complexes formed with sulfur containing ligands to undergo further rearrangement to form a more stable multinuclear aggregate[21] of the formula $[Pd_3S_2(Dppe)_3]^{2+}$. These d^8 M_3S_2 aggregates contain bridging sulphide ligands and are similar to the closely related to M_2S_2 aggregates which are some of the most powerful metalloligands currently within the literature. Both M_3S_2 and M_2S_2 aggregates have had considerable interest[22]. Based on this observation it was initially thought the compound formed from complex **2c** was the $[Pd_3S_2(Dppe)_3]^{2+}$ cation, one of these multinuclear aggregates. The structure of this ion has been previously reported[21, 23, 24] and is given in Figure 2.23[23]. The counter-anions are reported to be two residual chloride atoms resulting from the $[Pd(Dppe)]Cl_2$ starting material resulting in the neutral compound $[Pd_3S_2(Dppe)_3]Cl_2$

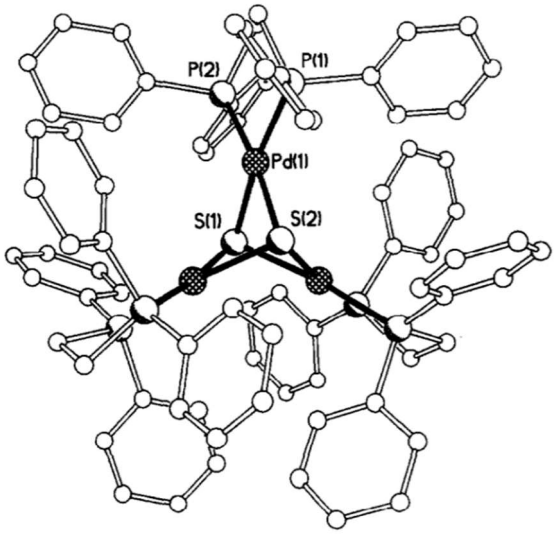

Figure 2.23: Structure of $[Pd_3S_2(Dppe)_3]^{2+}$. Hydrogens and two chloride counter-anions are obmited[18].

The structure of this cationic complex contains a triangle of palladium ions capped with sulfur atoms with a Dppe group attached at each palladium in a bidentate chelating coordination mode. X-Ray crystal structure of the neutral compound ($[Pd_3S_2(Dppe)_3]Cl_2$) shows a high degree of symmetry due to the threefold axis passing through the two bridging sulfur atoms[23].

While analogues of this structure have been reported for Pt[25] and Ni[24] only that of $[Pd_3S_2(Dppe)_3]^{2+}$ contains exact crystallographic three-fold rotation symmetry. This high degree of symmetry would produce a singlet in the phosphorus

NMR spectrum as the phosphorus atoms are all in identical chemical environments. Due to molecular vibrations in the liquid state, the Pt and Ni analogues are also expected to produce singlet peaks.

The mass and charge of the $[Pd_3S_2(Dppe)_3]^{2+}$ complex produced a *m/z* of 790, matching the mass spectra observations reported earlier. Isotopic patterns from the ESI-MS were also compared to calculated patterns for both complex **2c** and that of the multinuclear aggregate. Both the calculated and observed patterns for both complexes matched exactly. A comparison of calculated and observed patterns for the spectrum recorded after 3 hours is given in Figure 2.24. The observed isotope pattern of the aggregate confirms the presence of palladium and the 0.5 *m/z* separation of peaks is also observed indicating a 2^+ charge.

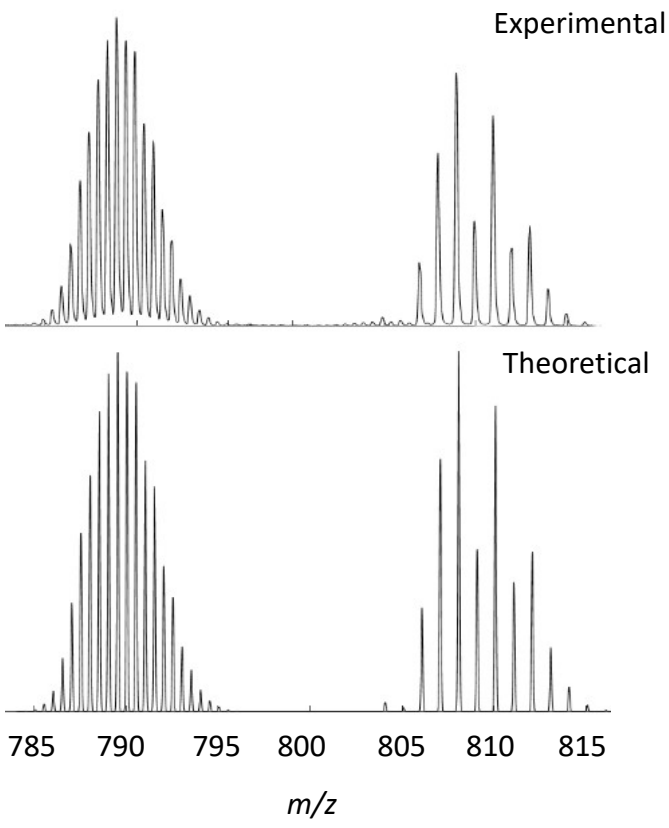

*Figure 2.24: Comparison between experimental and theoretical isotope patterns of complex **2c** and $[Pd_3S_2(dppe)_3]^{2+}$*

Complex **2d** may also be expected to form trinuclear aggregate in the same manner as complex **2c**. No phosphorus atoms are present in the complex limiting NMR experiments however a time-temperature experiment can be performed. The experiment was done following ta similar procedure outlined for complex **2c** above by gentle warming of the sample dissolved in methanol to promote the formation of the aggregate. The experiment was left for a duration of 7 hours with three spectra being recorded. The expected *m/z* for the complex and aggregate $[Pd_3S_2(Dppe)_3]^{2+}$ were 566 and 427, respectively. Comparison of the spectra revealed the presence of the expected 427 ion following the same trend of an increase in intensity over the duration of the experiment as the complex **2d** $[M^+H]^+$ ion decreased. Examples of palladium bipyridine aggregates are known and observed within the literature[26].

Synthesis of the $[Pd_3S_2(Dppe)_3]Cl_2$ aggregate as reported by Capdevila *et al*[23] was achieved by a reaction between $[Pd(Dppe)Cl_2]$ and an excess of Na_2S. In contrast the synthesis of this aggregate reported here is by decomposition of the sulfonylthiourea metal complex *via* what is expected to be a hydroxide induced C-S bond clavation. Examples of dinuclear (M_2S_2) and trinuclear (M_3S_2) aggregates forming from thiourea has been well documented within the literature[27-30] and it is well known that thioureas may act as a source of sulfide in reactions with metal ions[31, 32]. However, no relevant literature could be found specifically relating to sulfonylthioureas. The synthetic route of these aggregates from the sulfonylthiourea complexes can be expected to be a result of desulfurisation resulting from the hydrolysis of the C-S thiourea bond of the metal complex. This desulfurisation would result in a sulfonylurea product ($RSO_2NHC(O)NHR$) which may also act as the counter anion for the cationic aggregate, alternatively hydroxide anions may also act as the counter anion. Interestingly, while desulfurisation is observed for thioureas, the electron withdrawing sulfonyl group of the ligand may promote hydrolysis due to a reduction of electron density around the carbon making it more susceptible to nucleophilic attack. This susceptibility is further promoted by the single C-S bond of the complex as opposed to the double bond of the lone ligand. It can therefore be expected that sulfonylureas would more readily undergo desulfurisation compared to their thiourea counterparts, even in the case for presumably stable metal complexes.

2.4.4 Single crystal XRD structure of complex 2a.

Single crystal XRD quality crystals were grown by diffusion of diethyl ether into dichloromethane which grew in the monoclinic space group $P2_1/n$ with four molocules in the asymteric unit. The crystal structure of complex **2a**, shown in Figure 2.25, shows a slightly distorted square-planar geometry formed from a bidentate coordination of the thiourea S and N atoms with the Pt atom. This distortion can be observed with the comparison of the relevant square-planar bond lengths, notably S1-Pt 2.322(2) Å, N1-Pt 2.105(5) Å, C1-N1 1.330(8) Å, C1-S1 1.770(6) Å. A full list of bond lengths is given in Table 2.2. These square-planar bond lengths match very closely to the reported lengths of the related diphenylthiourea complex which are 2.332 Å, 2.052 Å, 1.353 Å and 1.8782 Å, respectively[9]. This indicates the core thiourea moiety of both complexes are near identical with little to no influence from the addition of the sulfonyl group of complex **2a**.

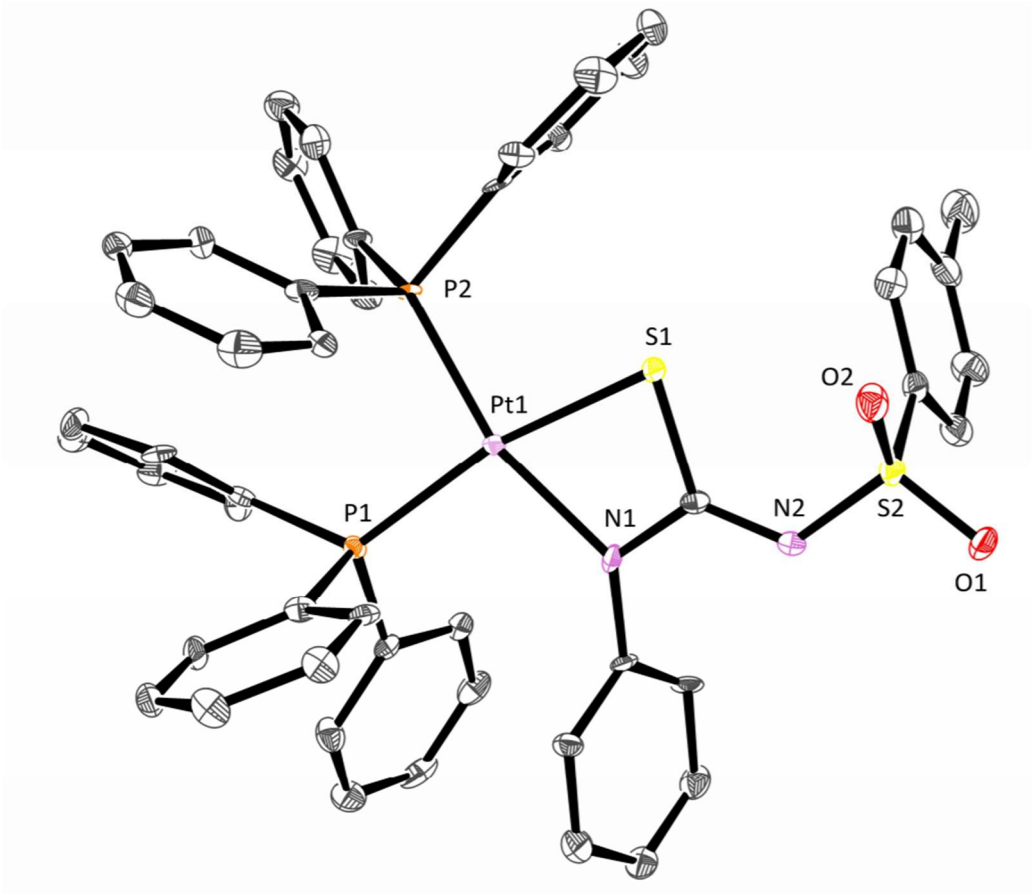

*Figure 2.25: ORTEP structure of complex **2a** generated from single crystal XRD data. Hydrogens are omitted for clarity. Ellipsoids at 50% probability.*

Bond angles of the central thiourea carbon atom shows a S1-C1-N2 bond angle of 121.1(4)°, close to the expected trigonal planar bond angle of 120°. However, the S1-C1-N1 bond angle is observed as 108.1(4)°, due to bonding with the platinum metal atom. Relevant bond angles are given in Table 2.2.

Table 2.2: Relevant bond lengths and angles of complex **2a**

Complex **2a**	Length (Å)
P1 – Pt	2.297(2)
P2 - Pt	2.263(1)
S1 - Pt	2.322(2)
N1 - Pt	2.105(5)
C1 – N1	1.330(8)
C1 – S1	1.770(6)
C1 – N2	1.326(8)

	Angle (°)
P1 – Pt – P2	98.19(5)
S1 – Pt – N1	69.3(2)
S1 – C1 – N1	108.1(4)
C1 – N2 – S2	121.1(4)

The crystal structure of the complex confirms the complex to be in the distal isomer, showing N1 (Ph) bonded to the metal with the phenyl ring sitting somewhat parallel to one of the triphenylphosphine aromatic rings in an almost π–π stacked manner. Observation of the crystal geometry indicate this to be sterically favoured as the SO_2-Tol substituent would be sterically hindered in the *proximal* position. This gives further evidence to the lack of observed isomerisation as one isomer is clearly and unambiguously sterically favoured.

The sulfonylthiourea moiety of the complex sits on a flat plane with the Pt, P1 and P2 atoms. This plane is defined by the square-planar coordination. N2-S2-Tol bond angles are observed as 106.3° placing the tolyl substituent into its own plane defined by the tolyl carbon ring. A thiourea-tolyl interplanar angle of 80.03° is observed. A C1-N1-Ph angle of 120.63° is observed and sits parallel to a triphenylphosphine aromatic ring with offset carbon atoms. Both phenyl rings have

a centroid distance of 3.650 Å from each other. This relatively close proximity is aided by the aromatic rings tendency to be able to stack together spatially as the phenyl ring has little steric hindrance. Crystallographic information pertaining to the crystal structure of complex **2a** is given in Table 2.3

Table 2.3: Crystallographic single crystal XRD data of complex **2a**

Complex **2a**.	
Formula	$C_{50}H_{42}N_2O_2P_2PtS_2$
Formula weight	1024.06
Crystal system	monoclinic
Space group	$P2_1/n$
a/Å	9.69052(13)
b/Å	20.4713(3)
c/Å	21.2268
α/°	90
β/°	96.9343(12)
γ/°	90
Volume/Å^3	4180.12(10)
Z	4
ρ_{calc}g/cm^3	1.6271
μ/mm^{-1}	8.284
Crystal size/mm^3	0.079 x 0.038 x 0.03
Radiation	Cu Kα (λ = 1.54184 Å)
2Θ range for data collection/°	8.1 to 147.78
Reflections collected	23539
Independent reflections	8188 [R_{int} = 0.0378, R_{sigma} = 0.0421]
Data/restraints/parameters	8188/0/533
Goodness-of-fit on F^2	1.044
Final R indexes [I>=2σ (I)]	R_1 = 0.0379, wR_2 = 0.1021
Final R indexes [all data]	R_1 = 0.0507, wR_2 = 0.1086
Largest diff. peak/hole / e Å^{-3}	2.36/-2.31

2.5 Conclusions

Examination of the d^8 metal complexes formed from the title ligand have been observed in this chapter for the metal centres platinum(II), palladium(II), nickel(II) and gold(III). Coordination modes of these complexes were determined by both direct and indirect methods and show a distinct favour towards a 4 member bidentate coordination mode in the *distal* isomeric position. Comparison of the sulfonylthiourea complexes with the structurally similar thiourea complexes reveal little to no influence of the sulfonyl substituent on the coordination modes observed. This coordination mode is hypothesised to be the most stable both sterically and thermodynamically, this hypothesis is aided by the lack of observed isomerisation and steric influence of the substituents. While stable in the solid phase, in solution complexes **2c**, **2d** and **2e** show a tendency to decompose into trinuclear aggregates promoted by the reduced electron density of the carbon-sulfur bond of the complex, as opposed to the lone ligand. The synthesis of sulfonylthiourea was also observed to form disubstituted thioureas as a result of the self-reaction of isothiocyanate in aqueous conditions. In conclusion the dominant coordination mode for sulfonylthioureas with d^8 transition metals was observed to be a 4 member bidentate coordination mode with the sulfonyl substituent *distal* from the metal centre.

2.6 References

1. D. Drew, J. Doyle and A. G. Shaver, *Inorganic Syntheses: Reagents for Transition Metal Complex and Organometallic Syntheses*, 1990, **28**, 346-349.
2. M. Agostinaá, M. Agostina-Chinellu, A. Zucca, S. Stoccoro, G. Minghetti, M. Manassero and M. Sansioni, *„Journal of the Chemical Society, Dalton Transactions*, 1995, 2865-2872.
3. G. Booth and J. Chatt, *Journal of the Chemical Society (Resumed)*, 1965, 3238-3241.
4. J. X. McDermott, J. F. White and G. M. Whitesides, *Journal of the American Chemical Society*, 1976, **98**, 6521-6528.
5. O. V. Dolomanov, L. J. Bourhis, R. J. Gildea, J. A. K. Howard and H. Puschmann, *Journal of Applied Crystallography*, 2009, **42**, 339-341.
6. L. J. Bourhis, O. V. Dolomanov, R. J. Gildea, J. A. K. Howard and H. Puschmann, *Acta Crystallographica Section A: Foundations and Advances*, 2015, **71**, 59-75.
7. M. H. Shah, M. Y. Mhasalkar, V. M. Patki and C. V. Deliwala, *Journal of Scientific & Industrial Research*, 1959, **18B**, Pages202-204.
8. H. Ulrich, B. Tucker and A. Sayigh, *Tetrahedron*, 1966, **22**, 1565-1573.
9. W. Henderson, R. D. W. Kemmit, S. Mason, M. R. Moore, J. Fawcett and D. R. Russell, *Journal of the Chemical Society, Dalton Transactions*, 1992, 59-66.
10. M. Shah, M. Y. Mhasalkar, V. M. Patki and C. V. Deliwala, *Journal of Scientific & Industrial Research*, 1959, **12B**, 202-204.
11. S. Perveen, S. M. Hai, R. A. Khan, K. M. Khan, N. Afza and T. B. Sarfaraz, *Synthetic Communications*, 2005, **35**, 1663-1674.
12. J. J. Blanco, C. S. Barría, J. M. Benito, C. O. Mellet, J. Fuentes, F. Santoyo-González and J. G. Fernández, *Synthesis*, 1999, 1907-1914.
13. V. B. Joseph, D. P. Satchell, R. S. Satchell and W. N. Wassef, *Journal of the Chemical Society, Perkin Transactions 2*, 1992, 339-341.
14. W. D. Ollis, *Comprehensive Organic Chemistry: The Syntesis and Reactions of Organic Compounds*, Pergamon, 1979.
15. D. C. Schroeder, *Chemical Reviews*, 1955, **55**, 181-228.
16. C. Ortiz‐Mellet, J. M. Benito, J. M. García Fernández, H. Law, K. Chmurski, J. Defaye, M. L. O'Sullivan and H. N. Caro, *Chemistry–A European Journal*, 1998, **4**, 2523-2531.
17. J. E. Spenceley, W. Henderson, J. R. Lane and G. C. Saunders, *Inorganica Chimica Acta*, 2015, **425**, 83-91.
18. H. A. Nkabyo, D. Hannekom, J. McKenzie and K. R. Koch, *Journal of Coordination Chemistry*, 2014, **67**, 4039-4060.
19. K. Koch, C. Sacht, T. Grimmbacher and S. Bourne, *South African Journal of Chemistry*, 1995, **48**, 71-77.
20. K. J. Kilpin, W. Henderson and B. K. Nicholson, *Polyhedron*, 2007, **26**, 204-213.
21. B.-C. Tzeng, S.-C. Chan, M. C. Chan, C.-M. Che, K.-K. Cheung and S.-M. Peng, *Inorganic Chemistry*, 2001, **40**, 6699-6704.
22. I. Dance and K. Fisher, *Progress in Inorganic Chemistry*, 1994, **42**, 637-803.
23. M. Capdevila, W. Clegg, R. A. Coxall, P. González-Duarte, M. Hamidi, A. Lledós and G. Ujaque, *Inorganic Chemistry Communications*, 1998, **1**, 466-468.
24. K. Matsumoto, N. Saiga, S. Tanaka and S. i. Ooi, *Journal of the Chemical Society, Dalton Transactions*, 1991, 1265-1271.
25. G. W. Bushnell, K. R. Dixon, R. Ono and A. Pidcock, *Canadian Journal of Chemistry*, 1984, **62**, 696-702.
26. B. C. Tzeng, Y. L. Wu and J. H. Kuo, *Journal of the Chinese Chemical Society*, 2006, **53**, 1033-1038.
27. M. B. Dinger, W. Henderson, B. K. Nicholson and W. T. Robinson, *Journal of Organometallic Chemistry*, 1998, **560**, 169-181.

28. L. A. Hoferkamp, G. Rheinwald, H. Stoeckli-Evans and G. Süss-Fink, *Organometallics*, 1996, **15**, 704-712.
29. G. Süss-Fink, U. Bodensieck, L. Hoferkamp, G. Rheinwald and H. Stoeckli-Evans, *Journal of Cluster Science*, 1992, **3**, 469-478.
30. W. Henderson, B. K. Nicholson, R. G. Fortney-Zirker, S. Patel, J. R. Lane, M. J. Wyllie and E. R. T. Tiekink, *Inorganica Chimica Acta*, 2015, **425**, 154-163.
31. Y. Liang, P. Bai, J. Zhou, T. Wang, B. Luo and S. Zheng, *CrystEngComm*, 2016, **18**, 6262-6271.
32. N. Bao, L. Shen, T. Takata, K. Domen, A. Gupta, K. Yanagisawa and C. A. Grimes, *Journal of Physical Chemistry C*, 2007, **111**, 17527-17534.

3 Coordination of *cis*-[$PtCl_2(PPh_3)_2$] with a variety of substituted sulfonylthiourea ligands containing Me, Et, Tolyl and Allyl substituents

3.1 Introduction

Since its increase in popularity by Rosenburg[1], cisplatin (*cis*-[$PtCl_2(NH_3)_2$]) and its cytotoxic effects have increased interest and awareness in investigating other *cis*-coordinated platinum group complexes[2, 3] most of which intend to overcome some of the limitations and disadvantages of cisplatin. Some of these limitations include poor water solubility, high toxicity, and cellular resistance[4]. To this extent many metal complexes with mono and bidentate ligands have been prepared in with the hope that they may be able to replicate the renowned anti-cancer effects of cisplatin while simultaneously employing ligands with various substituents which may aid in limiting any potential disadvantages. Furthermore, the use of bidentate ligands allows for the decrease in premature reactivity of the platinum complexes and hinder any possible *cis-trans* isomerism that may take place in the complexes, which is a particular problem with metal complexes in which the ligand coordinates to the metal in a monodentate coordination mode[5]. Many of these prepared complexes are sterically hindered and contain bidentate nitrogen ligands[6]. As discussed in previous chapters, thioureas and the derivatives thereof, acylthioureas, have shown the ability to coordinate to a wide range of metal centres[7] and have a large variety of substituents[8, 9] which makes these ligands ideal for investigation of platinum metal centres. The coordination chemistry of metal complexes derived from *cis*-[$PtCl_2(PPh_3)_2$] with thioureas[10-13] has been investigated however no literature specifically relating to sulfonylthioureas could be found.

The results of the previous chapter indicated a strong tendency for the metal complexes formed with sulfonylthiourea ligands to coordinate in a square-planar S and N coordination mode. This coordination mode was determined by both direct and indirect methods including, single crystal XRD and $^{31}P\{^1H\}$ NMR which was

aided by ^{195}Pt J-coupling values to examine the *trans* influence of the coordinated substituents. These results follow the trend observed within the literature for the same class of ligands, further cementing the difference in coordination modes from that of the similarly structured acylthioureas. It may therefore be expected that the coordination mode observed, specifically that of the *distal* isomer, may be due to the tolyl substituent which remained constant in all of the complexes synthesised. Literature pertaining to the effects of the substituent on the coordination of sulfonylthioureas is non-existent as the previously reported complexes focused primarily on applications. However, it can be hypothesised that the steric nature of the substituent, combined with intermolecular interactions. It would therefore be of interest to observe the effects of altering both the ligand substituents on the coordination chemistry of sulfonylthiourea metal complexes and observe the intermolecular interactions of the ligands. The aim of this chapter was to synthesise sulfonylthiourea metal complexes derived from *cis*-$[PtCl_2(PPh_3)_2]$ with a variety of sulfonylthiourea substituents with the intention to observe the substituent effects on the coordination chemistry of the resulting platinum metal centres. The general structure of complexes derived from *cis*-$[PtCl_2(PPh_3)_2]$ with sulfonylthiourea in both *distal* and *proximal* isomers is given in Figure 3.1.

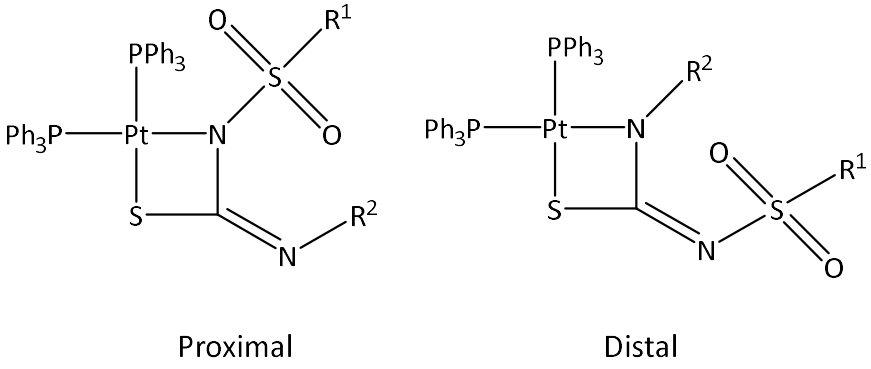

Figure 3.1: General structure of a complex derived from cis-$[PtCl_2(PPh_3)_2]$ with disubstituted sulfonylthiourea $[RSO_2NHC(S)NHR`]$in both distal and proximal isomers

3.2 Experimental

3.2.1 Chemicals

Triethylamine was sourced from Unilab chemicals. Toluene-*p*-sulfonamide was sourced from BDH chemicals. Deuterated chloroform, general solvents, phenyl isothiocyanate, methane sulfonic acid and ethane sulfonic acid were sourced from Sigma Aldrich. Thionyl chloride was sourced from Scharlau and methane sulfonyl chloride was sourced from Honeywell Riedel-de Haën AG. All previously listed chemicals were used as is. Allyl isothiocyanate was sourced from Fluka and steam distilled before use. *cis*-[$PtCl_2(PPh_3)_2$] was prepared previously in Section 2.2.3. For general procedures and instrumentation refer to Section 2.2.1

3.2.2 Synthesis of *N*-methylsulfonyl-*N*`-phenylthiourea [$CH_3SO_2NHC(S)NHPh$], 3a`

The title ligand, [$CH_3SO_2NHC(S)NHPh$], was synthesised by an adapted literature procedure[14] from methane sulfonic acid *via* a simple multistep synthesis resulting in methyl sulfonamide which was then reacted with phenyl isothiocyanate to produce [$CH_3SO_2NHC(S)NHPh$]. A synthetic route for this reaction is given below as Figure 3.2. Alternatively, the synthesis began from methane sulfonyl chloride.

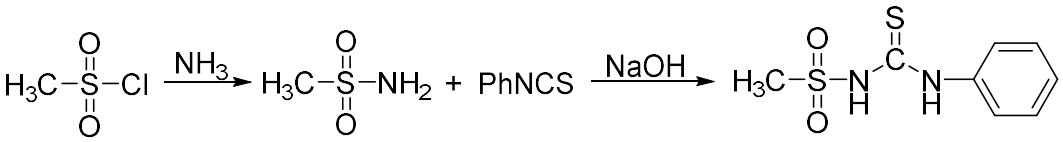

Figure 3.2: Synthesis of [$CH_3SO_2NHC(S)NHPh$] from methane sulfonic acid.

3.2.2.1 Synthesis of methyl sulfonamide.

Methane sulfonyl chloride (15 g, 0.13 mol) was added dropwise into rapidly stirring aqueous ammonia (150 ml, 30%, excess). The temperature of the ammonia solution was allowed to rise to 80°C during the addition. Once the addition was completed the mixture was let to sit at 80°C for 1h and while still hot (*ca* 50°C) the product was isolated by two consecutive liquid-liquid separations into acetonitrile (2 x 150 ml). The combined organic phases were evaporated to give methyl sulfonamide (8 g, 64%) used without further purification.

3.2.2.2 Synthesis of [$CH_3SO_2NHC(S)NHPh$], 3a`

Methyl sulfonamide (5 g, 0.052 mol) was dissolved in acetone (50 ml) and sodium hydroxide (1.5 g dissolved in 5 ml water) was then added. The mixture was stirred for 15 minutes followed by the addition of phenyl isothiocyanate (7.1 g, 0.052 mol, in approximately 1 ml portions). The mixture was stood at room temperature for 48 hours followed by acidification with glacial acetic acid (15 ml). A white solid was precipitated using excess water (200 ml), filtered by vacuum filtration, and washed with cold ethanol (2 x 25 ml). Yield, 7.38 g, 60%. ESI-MS: Capillary exit voltage 90V, *m/z* $[M+H]^+$ 231.06 (calculated, 231.03).

3.2.3 Synthesis of *N*-ethanesulfonyl-*N*`-phenylthiourea [$CH_3CH_2SO_2NHC(S)NHPh$], 3b`

Ethane sulfonyl chloride (5 g, 0.038 mol) was added dropwise to aqueous ammonia (150 ml, 30%, excess) with rapid stirring. The temperature was allowed to rise to 80°C during the addition and held for 1 hour. While still hot (*ca* 50°C), the product was isolated by two consecutive liquid-liquid separations into acetonitrile (2 x 150 ml). The combined organic phases were evaporated to near dryness to give ethyl sulfonamide as an off-white oil. CH_2Cl_2 (100 ml) was added to dissolve the product followed by triethylamine (5 g). The solution was stirred for 20 minutes followed by the dropwise addition of phenyl isothiocyanate (6 g, 0.044 mol) with stirring. The reaction mixture was allowed to evaporate slowly over 42 hours to give what is expected to be, the triethylammonium salt of the target ligand as a crystalline solid which was then filtered by vacuum filtration and washed with isopropyl alcohol (15 ml) and cold ethanol (25 ml) and used as is without further purification. The structure of [$CH_3CH_2SO_2NHC(S)NHPh$] is given in Figure 3.3. Yield, 3.7 g, 34%. ESI-MS: Capillary exit voltage -90V, *m/z* $[M-H]^-$ 243.08 (calculated, 243.03).

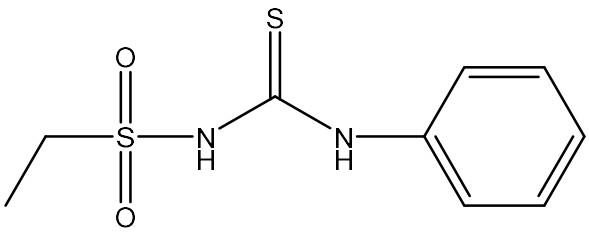

Figure 3.3: Structure of [$CH_3CH_2SO_2NHC(S)NHPh$].

3.2.4 Synthesis of *N*-tolylsulfonyl-*N*`-allylthiourea [$TolSO_2NHC(S)NHCH_2CHCH_2$], 3c`

Toluene sulfonamide (5 g, 0.029 mol) was dissolved in CH_2Cl_2 (150 ml) followed by the single addition of triethylamine (3 g). The solution was raised to reflux followed by the single addition of allyl isothiocyanate (2.9 g, 0.029 mol) with stirring. The reaction mixture was refluxed for 30 minutes and without delay evaporated to dryness by rotary evaporation to give an off-white solid which was then washed with isopropyl alcohol (25 ml) and cold ethanol (25 ml) resulting in a white solid powder which is expected to be the triethylammonium salt of the target ligand, used as is without further purification. The structure of [$TolSO_2NHC(S)NHCH_2CHCH_2$] is given in Figure 3.4. Yield, 4.17 g, 38%. ESI-MS: Capillary exit voltage -90V, *m/z* $[M-H]^-$ 269.01 (calculated 269.04).

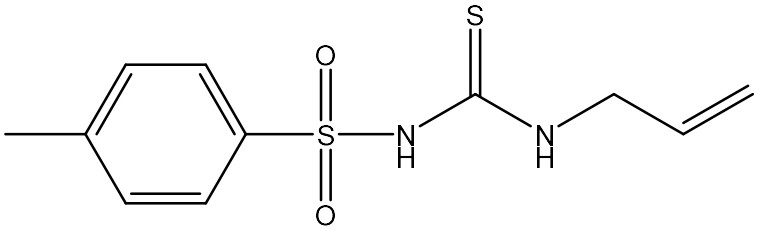

Figure 3.4: Structure of [$TolSO_2NHC(S)NHCH_2CHCH_2$]

3.2.5 Synthesis of methyl, ethyl and allyl substituted sulfonylthiourea complexes derived from *cis*-[$PtCl_2(PPh_3)_2$]

The general procedure for the sulfonylthiourea complexes derived from *cis*-[$PtCl_2(PPh_3)_2$] has been adapted from the previously reported method in Section 2.2.6. The adapted procedure is as follows. A weighed portion of the ligand (or the triethylammonium salt thereof) was dissolved in MeOH (30 ml) in a round bottom 250 ml and brought to reflux with stirring. Once reflux was achieved, triethylamine (0.8 ml, excess) was added followed by *cis*-[$PtCl_2(PPh_3)_2$]. The solution was refluxed for 5 minutes followed by the rapid addition of distilled water (40 ml) to precipitate any solid. The mixture was cooled rapidly using an ice bath to aid in precipitation and coagulation. Solids were collected by vacuum filtration and washed with hot water (2 x 20 ml) and dried under vacuum. Details pertaining to each compound prepared by this method are given in Table 3.1.

Table 3.1: Synthesis of complexes of methyl, ethyl, tolyl and allyl substituted sulfonylthioureas

Ligand			*cis*-[$PtCl_2(PPh_3)_2$]		Product yield			
R =, R` =	mg	mmol	mg	mmol	mg	%	Code	Colour
CH_3, Ph	23.4	0.101	80	0.101	70	73	**3a**	Pale yellow
CH_3CH_2, Ph	17.2	0.049	40	0.050	37	77	**3b**	Pale yellow
Tol, Allyl	17.9	0.048	40	0.050	39	81	**3c**	Pale yellow

3.3 Characterisation

Only ESI-MS peaks of $[M+H]^+$ for complexes **3a**, **3b** and **3c** (at an exit voltage of 150V and skimmer 1 voltage of 50V) and characteristic ^1H NMR and IR peaks are reported unless otherwise stated. Complexes **3b** and **3c** were only characterised spectroscopically.

3.3.1 [Pt{$CH_3SO_2NC(S)NPh$}(PPh_3)$_2$], 3a

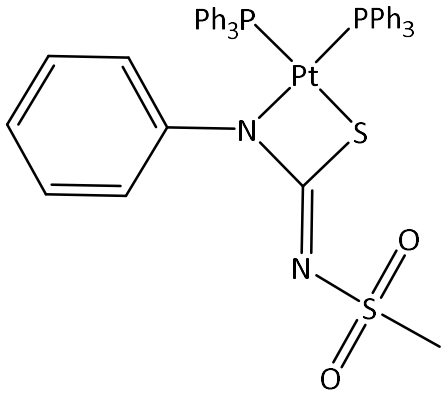

*Figure 3.5: General structure of **3a***

Elemental analysis: Found (%) C 55.72; H 3.54; N 2.77. Calculated (%) C 55.75; H 4.04; N 2.96.

Melting point: 260-266°C

ESI-MS: *m/z* $[M+H]^+$ 948.08 (calculated, 948.16), $[M+Na]^+$ 970.00 (calculated, 970.14).

FT-IR (cm^{-1}): 1591 (w), 1484 (vs), 1436 (s), 1131(s), 1098 (m), 694 (s), 526 (s).

NMR: $^{31}P\{^{1}H\}$ δ (ppm) 15.5 (d, P(1), ^{1}J[PtP(1)] 3059 Hz, ^{2}J[P(1)P(2)] 22 Hz) and 10.4 (d, P(2), ^{1}J[PtP(2)] 3358 Hz, ^{2}J[P(1)P(2)] 22 Hz). ^{1}H δ 7.7-6.2 (m, aromatic), 2.88 (3H, s, CH_3).

3.3.2 [Pt{$CH_3CH_2SO_2NC(S)NPh$}(PPh_3)$_2$], 3b

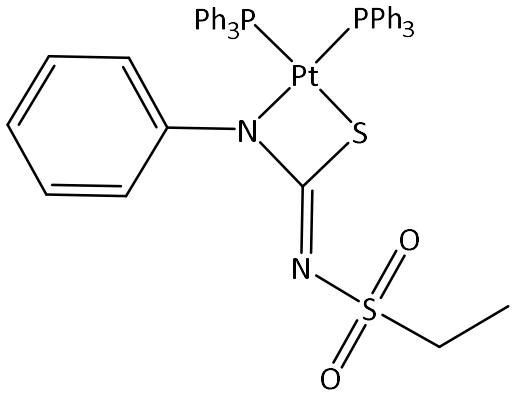

*Figure 3.6: General structure of **3b***

Melting point: 220-227°C

ESI-MS: *m/z* $[M+H]^+$ 962.34 (calculated, 962.17).

FT-IR (cm^{-1}): 3053 (w), 2922 (w), 1631 (w, broad), 1591 (m), 1484 (vs), 1328 (s), 1289 (s), 1126 (vs), 1097 (s), 997 (m), 693 (vs, broad), 547 (s).

NMR: $^{31}P\{^{1}H\}$ δ (ppm) 15.57 (d, P(1), ^{1}J[PtP(1)] 3043 Hz, ^{2}J[P(1)P(2)] 21 Hz) and 10.5 (d, P(2), ^{1}J[PtP(2)] 3366 Hz, ^{2}J[P(1)P(2)] 21 Hz). ^{1}H δ 7.7-6.2 (m, aromatic), 2.89 (2H, q, CH_2), 1.17 (3H, t, CH_3).

3.3.3 [Pt{TolSO$_2$NC(S)NCH$_2$CHCH$_2$}(PPh$_3$)$_2$], 3c

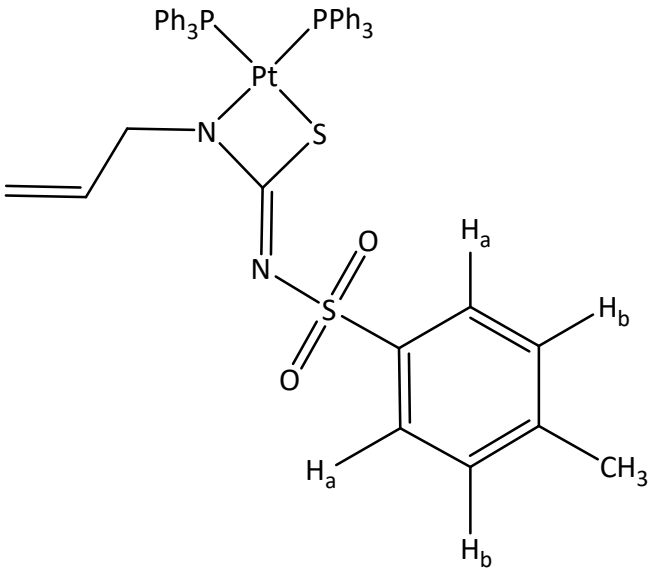

*Figure 3.7: General structure of **3c***

Melting point: 226-230°C

ESI-MS: *m/z* $[M+H]^+$ 989.27 (calculated, 989.18), $[M+Na]^+$ 1010.11 (calculated, 1010.17).

FT-IR (cm^{-1}): 1633 (w, broad), 1500 (s), 1436 (m), 1141 (m), 1091 (s), 693 (s).

NMR: $^{31}P\{^1H\}$ δ (ppm) 17.25 (d, P(1), ^1J[PtP(1)] 3038 Hz, ^2J[P(1)P(2)] 21 Hz) and 12.1 (d, P(2), ^1J[PtP(2)] 3308 Hz, ^2J[P(1)P(2)] 21 Hz). ^1H δ 7.8 (CH_3-PhH_{aa}, d, 2H), 7.78 (PhH_{bb}, d, 2H), 7.5-7.0 (PPh_3, m aromatic, 30H), 5.2 (allyl-CH, m, 1H), 4.5 (allyl-NCH_2, d, 2H), 4.2 (C=CH_2, m, 2H), 2.19 (CH_3-Ph, s, 3H).

3.4 Results and discussion

3.4.1 Synthesis

N-methylsulfonyl-*N`*-phenylthiourea [$CH_3SO_2NHC(S)NHPh$], **3a`** was synthesised using an adapted procedure from Section 2.2.2 which involved full work up of the anionic ligand using acetic acid followed by precipitation with water to give the neutral ligand **3a`** in high purity. Previously reported synthesis of [$TolSO_2NHC(S)NHPh$], **2** resulted in a mixture of both the target ligand and the diphenylthiourea ligand by-product due to decomposition of isothiocyanate in aqueous conditions as discussed in Section 2.4.3. Separation of these two ligands proved difficult and required successive crystallisations to achieve adequate purity. This difficulty in achieving a pure product can be attributed to the extremely similar structures which both contain similar arene substituents, this would result in the solubility of the two thiourea ligands to be smiler and therefore would make separation by traditional methods, including column chromatography difficult. **3a`** however did not suffer from the same difficulties of separation. While the negative ESI-MS of the ligand mixture pre-workup showed the presence of both the diphenylthiourea anion and target ligand in high intensity, the post workup ligand sample of **3a`** showed only the intended without the need for further purification by crystallisation. This contrasting separation can be attributed to the considerable difference in structure with the methyl substituent altering the solubility enough to allow for isolation of the pure ligand by simple means.

Previous attempts to synthesise substituted sulfonylthiourea ligands using the method reported for **2** and **3a`** resulted in an unprecedented decomposition of the ligands by unknown means. Pre-workup ESI-MS of the ligand mixture showed clear and strong negative ions of the anionic ligands. However, post-workup ESI-MS and ^1H NMR of both the isolated solid and the solution show no presence of the ligands. Due to insufficient time to investigate the cause of this decomposition, ligands **3b`** and **3c`** were isolated pre-workup by slow evaporation of the solvent to give the anionic ligand as a salt with the corresponding cation being triethylammonium which was present in the positive ESI-MS spectrum of the **3b`** and **3c`** ligand samples ($[M]^+ = 102$). The anionic ligands were used as is without further purification and successfully formed the corresponding platinum complexes, **3b** and **3c**.

3.4.2 Mass spectrometry

Complexes **3a**, **3b** and **3c** all readily formed strong $[M+H]^+$ ions in the ESI-MS spectrum at an capillary exit voltage of 150V and a skimmer 1 voltage of 50V. **3a** and **3c** also displayed strong $[M+Na]^+$ peaks in the 150V spectra which increased in intensity relative to an increase in exit voltage (90-180V). These peaks displayed the typical elemental pattern associated with platinum containing complexes and were compared to calculated elemental patterns of the expected complex. An example of the $[M+H]^+$ and $[M+Na]^+$ ion peaks including isotope pattern and the calculated isotope patterns for complex **3a** is given in Figure 3.8.

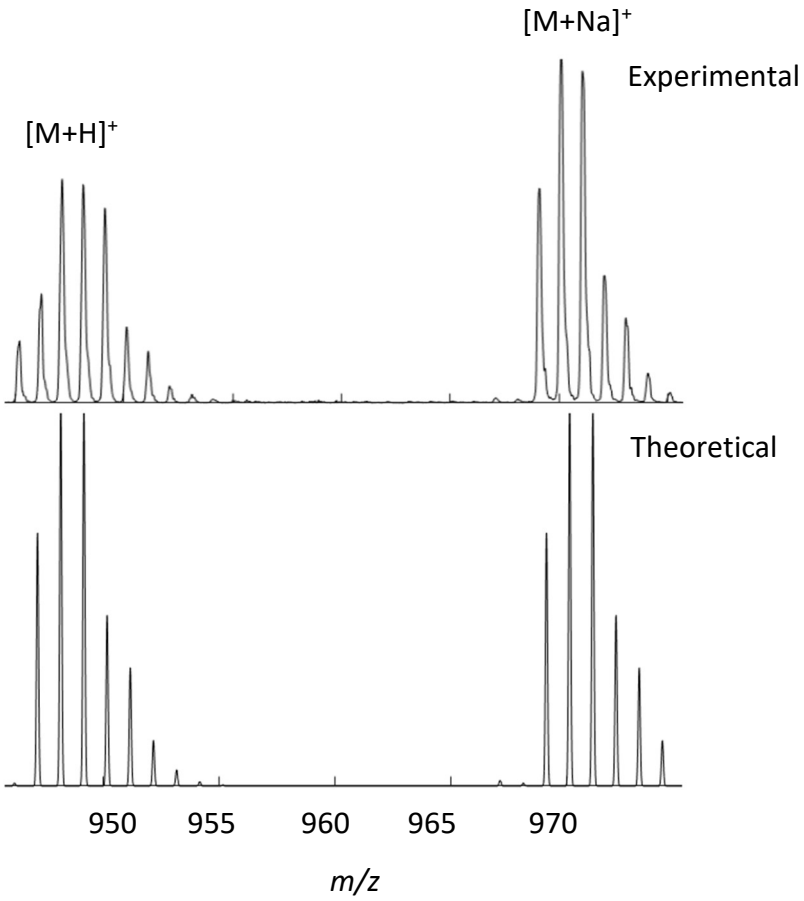

*Figure 3.8: Comparison between experimental and theoretical isotope patterns of complex **3a***

$[2M+Na]^+$ of complex **3a** and **3c** was also observed however no corresponding peak of complex **3b** could be found. All complexes were stable and resisted fragmentation, including the expected loss of PPh_3 which could not be observed regardless of the increase in voltage.

3.4.3 NMR spectroscopy

3.4.3.1 $^{31}P\{^{1}H\}$ NMR spectroscopy

As discussed briefly in Section 2.4.2.3 in the previous chapter, $^{31}P\{^{1}H\}$ spectroscopy of square-planar platinum complexes can provide an indication on the coordination of the platinum metal centre by use of ^{195}Pt J-coupling values. This is due to the J-coupling values of the ^{195}Pt satellites being directly correlated to the environment *trans* to each atom and can therefore be used to assign coordination and in some cases give an indication of bond length[15]. Coupling values of complex **2a** were assigned on the basis of the sulfur atom having a slightly higher *trans* influence than that of nitrogen and were 3039 Hz (PPh_3 *trans* to S) and 3380 Hz (PPh_3 *trans* to N). This indicated the complex to be in an S-N bidentate coordination mode however insufficient information for comparison meant that the isomer of the complex could not be conclusively determined by NMR means. The isomer was later discovered to be in the *distal* position, which is to say that the non-coordinated N atom (NSO_2R) is facing away from the metal centre, as seen in Figure 3.1, by use of single crystal XRD methods. Therefore, the J-coupling values presented previously for complex **2a** may provide some structural information on the isomer of the complexes synthesised in this chapter by comparison of the coupling values. The J-coupling values for complexes **2a, 3a, 3b** and **3c** are given in Table 3.2

*Table 3.2: $^{31}P\{^{1}H\}$-^{195}Pt J-coupling values of complexes **2a** and **3a-c** (Hz)*

Complex	^{1}J[PtP(2)]	P(2) *trans* to	^{1}J[PtP(1)]	P(1) *trans* to
2a	3380	N-Ph	3039	S-C
3a	3358	N-Ph	3059	S-C
3b	3366	N-Ph	3043	S-C
3c	3308	N-Allyl	3038	S-C

As previously discussed, P(1) of complex **2a**, with a coupling constant of 3039 Hz, was determined to be *trans* to sulfur due to the smaller coupling constant associated with the slightly higher *trans* influence of the substituent. Comparison of the ^{1}J[PtP(1)] coupling constant of complexes **3a**, **3b** and **3c** show ^{195}Pt constants of 3059 Hz, 3043 Hz and 3028 Hz respectively, all of which are very similar to that of

2a with the largest difference being only 21 Hz. This clearly indicates P(1) of each complex is *trans* to S-C. ^{1}J[PtP(2)] of P(2) of complex **2a** was determined to be *trans* to N-R with a value of 3380 Hz and later confirmed by single crystal XRD analysis to be *trans* to N-Ph. ^{31}P{^{1}H} NMR spectra of complex **3a** with assigned P(1) and P(2) phosphorus atoms is given in Figure 3.9. The J-coupling value of P(2) of **2a** can be used to assign the P(2) *trans* substituent of the complexes prepared in this chapter which have the P(2) ^{1}J[PtP(2)] coupling values of **3a** 3358 Hz, **3b** 3366 Hz and **3c** 3308 Hz as seen in Table 3.2. Complexes **2a**, **3a** and **3b** share extremely close J-coupling values, with the largest difference being 14 Hz, and can therefore be assigned to N-Ph giving the complexes in the *distal* isomer. Interestingly complex **3c** which differs from the previous complexes by the change of the isothiocyanate substituent to an allyl group gives a P(2) ^{1}J[PtP(2)] J-coupling value of 3308 with a difference to the next closest value being 50 Hz. While expectably different, the value is not too dissimilar to assign this to a sulfonyl group which can be expected to give a much larger *trans* influence. Instead it can be argued that the P(2) J-coupling value falls within the alkyl range and indicates P(2) is *trans* to N-allyl which is to be expected following the trend of the previous complexes. From this, it can be concluded that there is a strong indication that the complexes prepared in this chapter are coordinated in an S-N bidentate fashion in the *distal* isomer shown in Figure 3.1

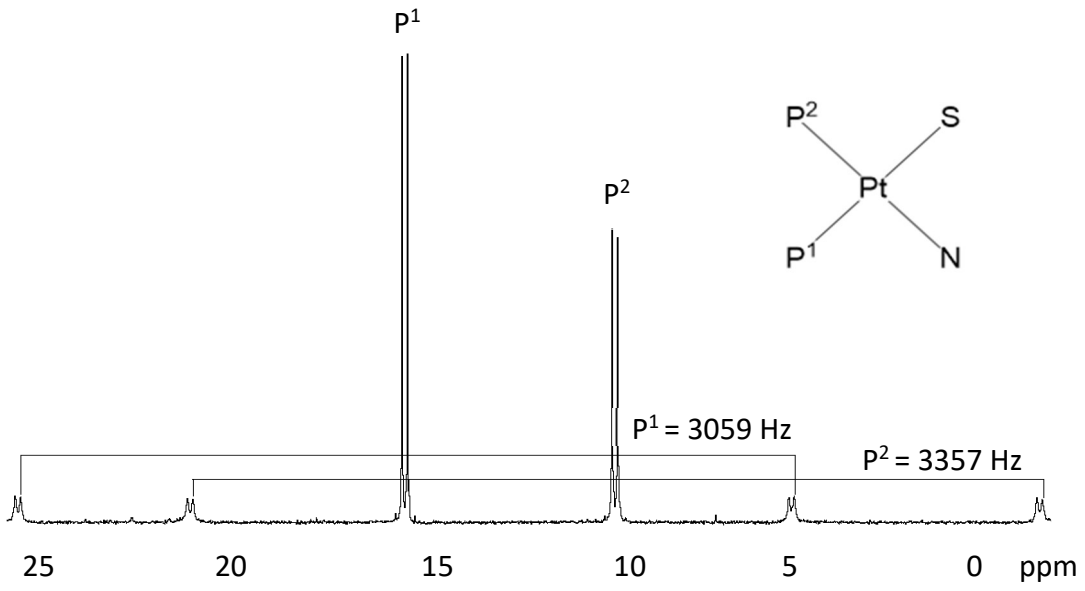

*Figure 3.9: ^{31}P{^{1}H} NMR spectrum of complex **3a** with P(1) and P(2) assigned phosphorus atoms.*

3.4.4 Single crystal x-ray diffraction.

3.4.4.1 Single crystal XRD structure of complex 3a.

Single crystal XRD quality crystals were grown by diffusion of diethyl ether into dichloromethane and grew in the triclinic P-1 space group. The asymmetric unit consists of two molecules of **3a** and two water molecules. As expected, the core thiourea moieties of complex **2a** and **3a** are near identical with S1-C1, C1-N1 and C1-N2 bond lengths of 1.770 Å, 1.330 Å, 1.326 Å and 1.791 Å, 1.326 Å, 1.323 Å, respectively. Selected bond lengths are given in Table 3.3 and the ORTEP structure of complex **3a** is given in Table 3.3. The coordination of the core platinum atom of complex **3a** also shares near identical geometry with complex **2a** with the sulfonylthiourea ligand coordinating to the platinum atom in a bidentate S-N coordination mode with S1-Pt and N1-Pt bond lengths of 2.3453 Å and 2.088 Å, which are comparable to those of complex **2a** [2.322 Å and 2.105 Å]. The two triphenylphosphines are coordinated to the core platinum atom in a *cis* fashion with bond lengths of 2.2912 Å (P1-Pt) and 2.2551 Å (P2-Pt).

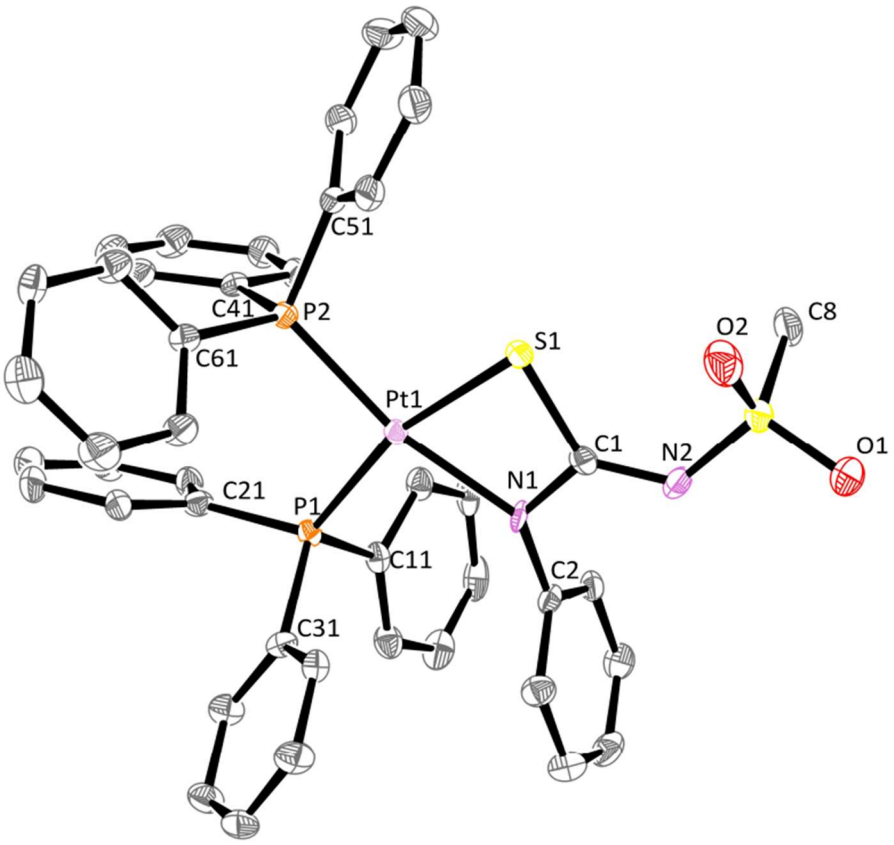

*Figure 3.10: ORTEP structure of complex **3a** generated from single crystal XRD data. Hydrogens and a water molecule are omitted for clarity. Thermal ellipsoids at 50% probability.*

*Table 3.3: Selected bond lengths and angles of complex **3a**.*

Complex 3a	Length (Å)
P1 – Pt	2.2912(9)
P2 - Pt	2.2551(9)
S1 - Pt	2.3453(8)
N1 - Pt	2.088(3)
C1 – N1	1.326(5)
C1 – S1	1.791(4)
C1 – N2	1.323(5)

	Angle (°)
P1 – Pt – P2	97.53(3)
S1 – Pt – N1	69.04(8)
S1 – C1 – N1	107.1(3)
C1 – N2 – S2	123.7(3)

Complex **3a** has square-planar geometry which is slightly distorted as evident from the comparison of P1-Pt-P2 and S2-Pt-N1 bond angles of 97.53° and 69.04° degrees. This distortion results in C1 bond angles of 129.26° (S1-C1-N2), 123.72° (N1-C1-N2) and 107.02° (S1-C1-N1). N2 also shows a standard geometric angle of 123.64°. The isomer of complex **3a** is shown from the crystallographic structure to be the *distal* isomer which is also shared by complex **2a**. $^{31}P\{^{1}H\}$ NMR observations of the platinum complexes reported in this chapter are reinforced by the crystal structure with the ^{1}J[PtP(1)] and ^{1}J[PtP(2)] J-coupling values being more accurately associated with P(1) (*trans* to S) and P(2) (*trans* to N) which in turn reinforces NMR J-coupling values for the complexes lacking single crystal structures, including complex **3c** which was tentatively assigned to the *distal* isomer.

Complex **3a** shows a clear and distinctive square-planar coordination geometry which is defined by the mean positions of P1, P2, Pt, S1, C1, N1, N2 and S2 which creates a near flat plane with the largest deviation being S1 with a deviation distance of 0.12 Å from the mean plane. The phenyl ring subsistent has inter-plane angle of 83.39°, nearly a 90° rotation from the thiourea plane. The methyl substituent also sits on its own plane with a N2-S2-C8 angle of 105° placing the methyl group a near 90° below the thiourea plane.

The similarities between the core thiourea moieties of complexes **3a** and **2a** are made more apparent when also comparing these complexes to the closely related

platinum triphenylphosphine diphenylthiourea complex, [Pt{PhNC(S)NPh}(PPh_3)$_2$][16], which contains comparable S1-Pt, N1-Pt, C1-N1 and C1-S1 bond lengths of 2.332 Å, 2.052 Å, 1.353 Å and 1.8782 Å, respectively. The complex is also square-planar with the core platinum atom having near identical coordination geometry to complexes **2a** and **3a** reported here. This further cements the observations made in Section 2.4.4 regarding the lack of involvement of the sulfonyl group on the adopted bidentate square-planar coordination mode which indicates sulfonylthiourea coordination to be more closely related to thiourea than to the more structurally close acylthioureas which favour 6-membered bidentate chelating rings with S and O.

3.4.4.2 Single crystal XRD structure of [$CH_3SO_2NHC(S)NHPh$], 3a`

Single crystal XRD quality crystals were grown by slow evaporation of dichloromethane and grew in the monoclinic space group P21/c. The asymetric unit consists of four molocules of **3a`**. While sulfonylthiourea ligands have been known since 1950[17] there are only 16 reported crystal structures and only 3 of which are the type H_2L, at the time of writing. This is unlike the structurally similar and more heavily studied acylthioureas which have numinous reported crystal structures including that of the acyl analogue[18] of ligand **3a`** ($CH_2CONHC(S)NHPh$). It was therefore of interest to compare and contrast **3a`** with both the acyl analogue as well

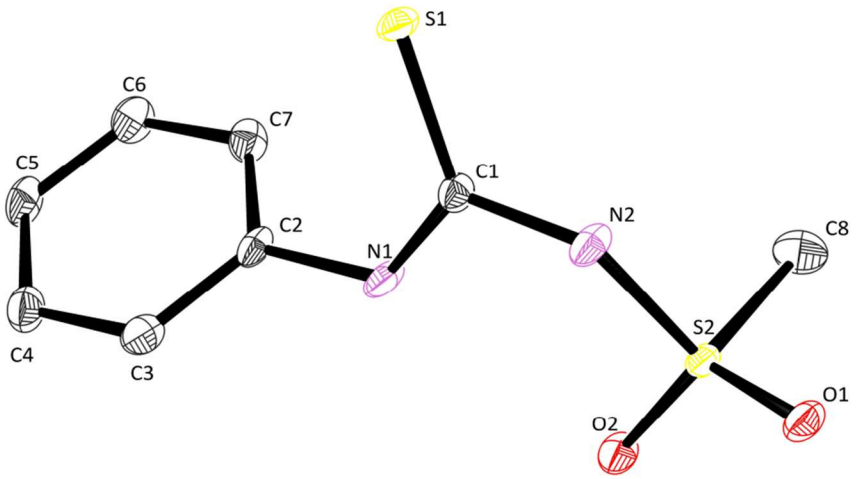

*Figure 3.11: ORTEP structure of compound **3a`** generated from single crystal XRD data. Thermal ellipsoids at 50% probability. Hydrogens are omitted.*

as the corresponding complex derived from *cis*-[$PtCl_2(PPh_3)_2$], **3a**. The ORTEP XRD structure of **3a`** is given in Figure 3.11.

Examination of the crystal structure of **3a`** reveals a standard trigonal-planar geometry of the thiourea carbon atom with S1-C1, C1-N1 and C1-N2 bond lengths of 1.675 Å, 1.327 Å and 1.387 Å respectivly and S1-C1-N1, S1-C1-N2 and N1-C1-N2 bond angles of 124.55°, 118.17° and 117.21° respcecivly, near the expected 120° trigonal-planar bond angles. Relevant bond lengths and angles for compound **3a`** are given in Table 3.4. C1-N1 and C1-N2 bond lengths of 1.327 Å and 1.387 Å are close to the literature reported average amide C-N bond length of 1.32 Å[19].

*Table 3.4: Relevant bond lengths and angles of compound **3a`***

Compound 3a`	**Length (Å)**
C1 – N1	1.327(2)
C1 – N2	1.387(2)
S1 – C1	1.6758(17)
N2 – S2	1.6530(14)
S2 – C8	1.7533(18)
N1 – C2	1.4316(19)
	Angle (°)
S1 – C1 – N1	124.55(12)
S1 – C1 – N2	118.17(12)
C1 – N1 – C2	125.38(14)
N1 – C1 – N2	117.21(14)
C1 – N2 – S2	129.72(12)
N2 – S2 – C8	104.25(8)

Interestingly, the sulfonyl group of the ligand is facing in the opposite direction with respect to S1 with a C1-N2-S2 bond angle of 129.72° which is in contrast to the observed orientation observed in complex **2a** and **3a** which place the sulfonyl group in the same orientation as S1. This orentation of S2 is most likely due to the intramolecular N-H· · ·O=S hydrogen bonding which results in a hydrogen bond stabilised pseudo 6-member ring motif. The hydrogen bond of ligand **3a`** in shown in Figure 3.12. Hydrogen bonding of this type has been observed and extensively reported for the acyl analogues including the methyl substituted

analogue of complex **3a`** which report N-H· · ·O=C intramolecular hydrogen bonding between the thiourea N−H and the amidic O donor atom of the acyl group[9, 18]. Of particular interest is the literature relating to the observed hydrogen bonding in acylthioureas in relation to the coordination mode adopted by the corresponding metal complexes. It has been suggested that the coordination mode adopted by acylthiourea complexes, particularly the monodentate (through S) are due to the hydrogen bonding which stabilises the thiourea moiety of the complexes into pseudo 6-membered ring[9, 20, 21]. The hydrogen bonding of the ligand has also been suggested to be responsible for the observed *proximal* isomers of the acyl complexes as the geometry of the ligand would encourage bonding to the exposed nitrogen. However, the presence of hydrogen bonding in **3a`** and the observed *distal* isomer of complex **2a** and **3a** indicate that hydrogen bonding is not the only defining factor of the coordination mode adopted by these complexes

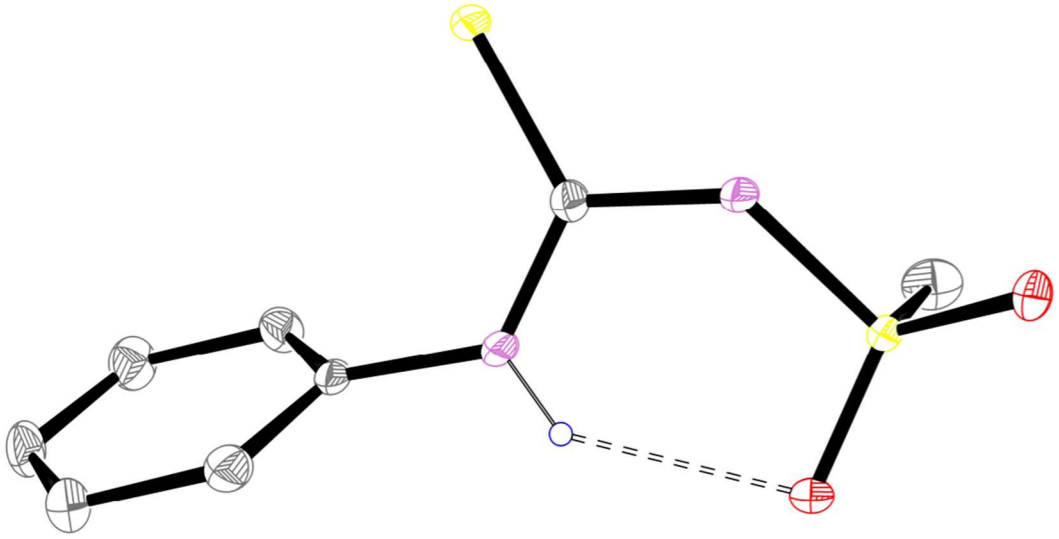

*Figure 3.12: Intramolecular hydrogen bonding of ligand **3a`**. Phenyl and methyl hydrogens are omitted.*

The geometry of ligand **3a`** reveals a near flat thiourea S-C-N1/N2 moiety with a large deviation of S2 with a distance 0.57 Å from the thiourea plane, which is defined by the mean positions of S1, C1, N1 and N2. The phenyl ring has an inter-plane angle of 61.24° and the methyl substituent sits below the thiourea plane with a N2-S2-C8 bond angle of 104.25°. Crystallographic information relating to **3a** and **3a`** is given in Table 3.5.

*Table 3.5: Crystallographic single crystal XRD data of complex **3a** and compound **3a`***

	Complex 3a`	**Complex 3a**
Formula	$C_8H_{10}N_2O_2S_2$	$C_{44}H_{39}N_2O_2P_2PtS_2$
Formula weight	230.31	959.947
Crystal system	Monoclinic	Triclinic
Space group	$P2_1/c$	P-1
a/ Å	5.63542(12)	11.9104(4)
b/ Å	8.87072(18)	12.7126(6)
c/ Å	20.3842(4)	14.9487(6)
α/°	90	67.617(4)
β/°	91.4698(17)	87.901(3)
γ/°	90	69.376(4)
Volume/ Å^3	1018.68(4)	1946.29(15)
Z	4	2
ρ_{calc}g/cm^3	1.5016	1.638
μ/mm^{-1}	4.564	8.861
Crystal size/mm^3	0.18 × 0.093 × 0.071	0.185 × 0.071 × 0.047
Radiation	Cu Kα (λ = 1.54184 Å)	Cu Kα (λ = 1.54184 Å)
2Θ range for data collection/°	8.68 to 148.16	7.98 to 148
Reflections collected	5704	21882
Independent reflections	1997 [R_{int} = 0.0186] [R_{sigma} = 0.0179]	7614 [R_{int} = 0.0301] [R_{sigma} = 0.0321]
Data/restraints/parameters	1997/0/128	7614/0/491
Goodness-of-fit on F^2	1.033	1.042
Final R indexes [I>=2σ (I)]	R_1 = 0.0279, wR_2 = 0.0714	R_1 = 0.0254, wR_2 = 0.0615
Final R indexes [all data]	R_1 = 0.0306, wR_2 = 0.0731	R_1 = 0.0288, wR_2 = 0.0655
Largest diff. peak/hole / e Å^{-3}	0.40/-0.55	1.15/-1.23

3.5 Conclusions

Substituted sulfonylthiourea ligands **3a`**, **3b`** and **3c`** and their subsequent metal complexes derived from *cis*-[$PtCl_2(PPh_3)_2$], **3a**, **3b** and **3c** were prepared in this chapter for the purpose of examining their coordination. These complexes were compared to both the tolyl sulfonylthiourea complex (**2a**), prepared previously in Chapter 2 and the structurally similar diphenylthiourea complex. The crystal structure of **3a** was the main source of this comparison which was supported by $^{31}P\{^1H\}$ NMR with ^{195}Pt J-coupling constants, mass spectrum analysis and IR analysis which was used in structural determination of complexes lacking crystal structure, **3b** and **3c**. To this extent, NMR J-coupling values showed a distinctive pattern of coordination and it was determined through these means that the complexes prepared here and in previous chapters (**2a**, **3a**, **3b** and **3c**) all share a bidentate S-N coordination mode to the central Pt atom in the *distal* isomer, regardless of substituent. These results indicate that the sulfonyl group of the ligands may contribute a larger role in the coordination mode adopted than the steric nature of the substituents. Furthermore, the crystal structure of **3a`** was compared to the analogous acylthiourea ligand which showed that both ligands share similar N-H· · ·O=R hydrogen bonding which holds the ligand into a pseudo 6-membered ring like structure. Literature relating to acylthioureas suggest that this hydrogen bonding was the source of the observed coordination, namely the monodentate (through S) and the bidentate *proximal* (S-N) coordination modes due to hydrogen bond stabilisation of the ligand structure. However, the complexes prepared here were observed to be in the *distal* isomer which lacks in this hydrogen bonding suggesting that ether the effects of this hydrogen bonding in sulfonylthioureas contribute less to the observed isomer or that hydrogen bonding alone is not the only driving factor.

3.6 References

1. B. Rosenberg, L. Van Camp and T. Krigas, *Nature*, 1965, **205**, 698-699.
2. I. Kostova, *Recent Patents on Anti-Cancer Drug Discovery*, 2006, **1**, 1-22.
3. F. K. Keter, S. Kanyanda, S. S. Lyantagaye, J. Darkwa, D. J. G. Rees and M. Meyer, *Cancer Chemotherapy and Pharmacology*, 2008, **63**, 127-138.
4. P. Bippus, M. Skocic, M. A. Jakupec, B. K. Keppler and F. Mohr, *Journal of Inorganic Biochemistry*, 2011, **105**, 462-466.
5. A. S. Abu-Surrah and M. Kettunen, *Current Medicinal Chemistry*, 2006, **13**, 1337-1357.
6. M. J. Bloemink, H. Engelking, S. Karentzopoulos, B. Krebs and J. Reedijk, *Inorganic Chemistry*, 1996, **35**, 619-627.
7. R. del Campo, J. J. Criado, E. García, M. a. R. Hermosa, A. Jimenez-Sanchez, J. L. Manzano, E. Monte, E. Rodrıguez-Fernández and F. Sanz, *Journal of Inorganic Biochemistry*, 2002, **89**, 74-82.
8. A. Saeed, U. Flörke and M. F. Erben, *Journal of Sulfur Chemistry*, 2014, **35**, 318-355.
9. K. R. Koch, *Coordination Chemistry Reviews*, 2001, **216**, 473-488.
10. J. E. Spenceley, W. Henderson, J. R. Lane and G. C. Saunders, *Inorganica Chimica Acta*, 2015, **425**, 83-91.
11. L. Battan, S. Fantasia, M. Manassero, A. Pasini and M. Sansoni, *Inorganica Chimica Acta*, 2005, **358**, 555-564.
12. W. Henderson, B. K. Nicholson and M. B. Dinger, *Inorganica Chimica Acta*, 2003, **355**, 428-431.
13. W. Henderson, B. K. Nicholson and C. E. F. Rickard, *Inorganica Chimica Acta*, 2001, **320**, 101-109.
14. S. M. Brown, J. P. Muxworthy and B. D. Gott, *WO 9825890 A1* 1998.
15. P. G. Waddell, A. M. Slawin and J. D. Woollins, *Dalton Transactions*, 2010, **39**, 8620-8625.
16. W. Henderson, R. D. W. Kemmit, S. Mason, M. R. Moore, J. Fawcett and D. R. Russell, *Journal of the Chemical Society, Dalton Transactions*, 1992, 59-66.
17. S. Petersen, *Chemische Berichte*, 1950, **83**, 551-558.
18. D. Shahwar, M. N. Tahir, M. M. Chohan and N. Ahmad, *Acta Crystallographica Section E: Structure Reports Online*, 2012, **68**, o508-o508.
19. L. Yao, B. Vögeli, J. Ying and A. Bax, *Journal of the American Chemical Society*, 2008, **130**, 16518-16520.
20. M. M. Sheeba, M. M. Tamizh, L. J. Farrugia, A. Endo and R. Karvembu, *Organometallics*, 2014, **33**, 540-550.
21. R. Gandhaveeti, R. Konakanchi, P. Jyothi, N. S. Bhuvanesh and S. Anandaram, *Applied Organometallic Chemistry*, 2019, **33**, e4899.

4 Coordination of (η^6-arene) ruthenium(II) piano-stool complexes with *N*-methylsulfonyl-*N`*-phenylthiourea [$CH_3SO_2NHC(S)NHPh$]

4.1 Introduction

Piano-stool complexes of the type [(η^6-arene)Ru(L)R] where the coordinated ligand is a deprotonated sulfonylthiourea are completely absent within the literature with the closest reported structures being those related to acylthioureas[1, 2]. These acylthiourea ligands coordinate to the metal centre in both the monodentate, through S and less commonly bidentate, through both S and N coordination modes. A second bidentate coordination mode is also observed with the ligand coordinating to the metal centre through S and the acyl O. However, ruthenium complexes of this type are seldom reported. The monodentate coordination mode is thought to be a result of intramolecular hydrogen bonding of the acylthiourea ligand between the N-H of the thiourea moiety with the amidic C-O donor atom which results in in a pseudo 6 membered ring motif, as shown in Figure 4.1. However, recently reported complexes with the bidentate S and N coordination mode of these acylthiourea ligands also show intramolecular hydrogen bonding between the N-H of the thiourea moiety with the amidic C-O donor atom in the crystal structure[1], also shown in Figure 4.1.

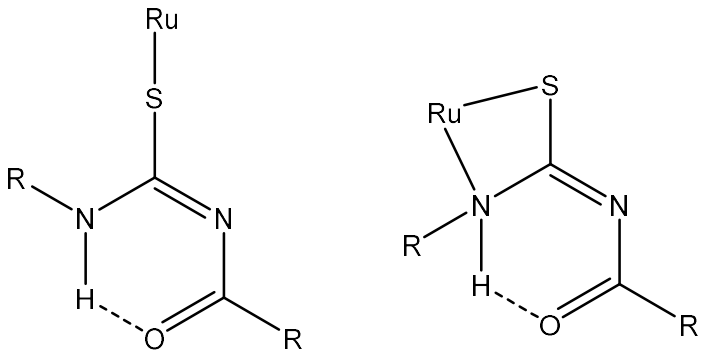

Figure 4.1: Acylthiourea mono and bidentate coordination modes with ruthenium(II) showing hydrogen bonding of the ligand

These observations indicate that the hydrogen bonding of this type is not the only influencing factor. The results of the previous chapter indicate a strong tendency for sulfonylthiourea ligands to coordination to the metal centre in a bidentate S and N fashion in the *distal* isomer. Furthermore, as previously discussed in Section 2.4.3, the S-C bond of the prepared sulfonylthiourea complexes was discovered to be prone to hydroxide induced cleavage, which was promoted by electron withdrawing effects of the sulfonyl group. For this reason, the monodentate coordination mode predominately observed with acylthiourea derived ruthenium complexes is expected to not be observed for the complexes prepared herein. It can therefore be expected, based on the results of both Chapters 2 and 3, that the sulfonylthiourea ligand would coordinate to the ruthenium(II) metal centre though S and N in a bidentate fashion in the *distal* isomer. For this reason, it can be expected that the coordination mode of the ruthenium(II) metal complexes derived from sulfonylthiourea ligands would be somewhat similar in coordination chemistry to the S and N bidentate coordinated complexes derived from acylthioureas. These acylthiourea derived complexes can be seen from the crystal structure to adopt the archetypical piano-stool shape of the Ru(II) half-sandwich structure in the *proximal* isomer (with respect to the C=O acyl group)[1, 2].

Recent interest in arene ruthenium complexes has been observed after the success of RAPTA-C, $[(\eta^6\text{-cymene})RuCl_2(PTA)]$[3, 4] (PTA = 1,3,5-Triaza-7-phosphaadamantane), an anti-cancer complex with a recent review by Kar *et al* highlighting an array of both ruthenium and iridium based metallopharmaceuticals[4] which aim to mimic its success. An attractive feature of these ruthenium complexes is the incorporation of π-conjugated arene moieties which are traditionally considered to occupy three of the ruthenium binding sites. These arene substituents have been observed to be highly stable in both acidic and basic conditions[5] while leaving three binding sites available for the incorporation of specific ligands. It has also been proposed that the hydrophobicity of these arene complexes facilitate the diffusion of the complexes through the lipophilic cell membrane where the change in chloride ion concentrations facilitates the hydrolyses of the complex, which can then undergo binding to DNA[6]. Two particular complexes which show significant results are RM175 $\{[(C_6H_5Ph)Ru(en)Cl][PF_6]$ (en = ethylenediamine)$\}$ and RAPTA-C mentioned above. Replacement of the two labile chlorines with chelating ligands has seen an increase in stability of the complexes against pre cell

diffusion hydrolysis which extremely enhances the effect on the cytotoxicity[3]. Recent studies in this field have shown promising results with the use of acylthiourea ligands[1] which form stable complexes with the added ability to have a wide range of substitutes. Since the remaining chlorine aids in the cytotoxic effects, the reported complexes with thioureas have not introduced variability at this site. One of the major draw backs of previous metallic based pharmaceuticals was the high toxicity of non-cancer cells and the development of tumour resistance[7-9]. Ruthenium based complexes are being developed to mitigate this[6 4].

Other applications of these complexes have shown interesting use as catalysts with a recent example being the efficient asymmetric transfer hydrogenation of ketones[2]. In this example monodentate acylthiourea complexes exhibit hydrogenation of simple ketones *via* an intermediate with both the ruthenium and acyl nitrogen atoms.

Due to the interesting coordination and useful applications shown by acylthiourea arene ruthenium complexes, it would be of interest to examine the coordination of similar sulfonylthiourea complexes for the purpose of differentiating the effect that the sulfonyl group will have on the coordination mode adopted by such complexes. Furthermore, recent literature on the phosphine complex $[(\eta^6\text{-cymene})RuCl_2(TCEP)]$[10] (where TCEP = tris(2-cyanoethyl)phosphine, $P(CH_2CH_2CN)_3$) show interesting coordination which is unlike the majority of other tertiary alkyl phosphines due to the small cone angle (132°) caused by possible intermolecular interactions between the cyano groups. This combined with the well-studied triphenylphosphine ligand give the possibility for novel ruthenium complexes with interesting coordination. Moreover, the isolation and employment of $[(arene)RuCl_2(Phosphine)]$ metal complexes may lay the groundwork for future ruthenium dichloride phosphine complexes and ruthenium sulfonylthiourea complexes. To this extent, the aim of this chapter is to synthesise a range of sulfonylthiourea ruthenium phosphine complexes for the purpose of examining their coordination in particular comparison and contrast to the closely related acylthioureas.

4.2 Experimental

4.2.1 Chemicals:

General solvents, deuterated solvents, α-terpinene and mesitylene were acquired from Sigma Aldrich and used as is. Triphenylphosphine was sourced from Strem chemicals. [$CH_3SO_2NHC(S)NHPh$] was prepared previously in Section 3.2.1. Ruthenium trichloride hydrate was acquired from Precious Metals Online (Australia). Tris(2-cyanoethyl)phosphine[11] and [(η^6-benzene)$RuCl_2]_2$[12] were prepared previously following the literature reported methods and provided. For general procedures and instrumentation refer to Section 2.2.1

4.2.2 Synthesis of [(η^6-cymene)$RuCl_2]_2$

The [(η^6-cymene)$RuCl_2]_2$ dimer[12] was synthesised by an adapted method given by Jensen *et al*[13] and is as follows. $RuCl_3 \cdot xH_2O$ (3.55 g) and α-terpinene (30 ml) were added to a 250 ml round bottom flask followed by ethanol (200 ml). The solution was brought to reflux with stirring for 5 hours before being removed from the heat. Upon cooling the product precipitated as a red-brown crystalline solid which was then filtered and washed with ice cold methanol (50 ml). The product was dried under vacuum to give a red crystalline solid, 3.2 g. The synthetic scheme of the dimer is given in Figure 4.2.

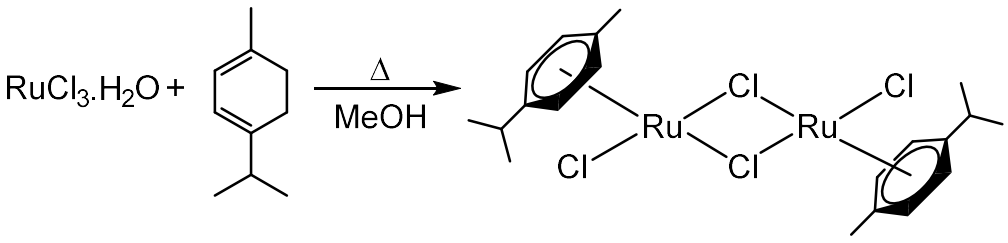

Figure 4.2: Synthetic scheme of the ruthenium cymene dimer.

4.2.3 Synthesis of [(η^6-cymene)$RuCl_2(PPh_3)$]

[(η^6-cymene)$RuCl_2(PPh_3)$] was prepared by a modified procedure given in Section 2.2.3. [(η^6-cymene)$RuCl_2]_2$ dimer (0.425 g), previously prepared, was dissolved in CH_2Cl_2 (20 ml) with rapid stirring. Two molar equivalents of PPh_3 (0.364 g) were

added in a single addition and stirred for a further 30 minutes followed by the rapid addition of petroleum sprits (*ca* 50 ml) to facilitate precipitation. The crystalline solid was filtered by vacuum and washed with petroleum spirits (2 x 25 ml) followed by drying in air to give the product as a red crystalline solid. A scheme for this reaction is given in Figure 4.3.

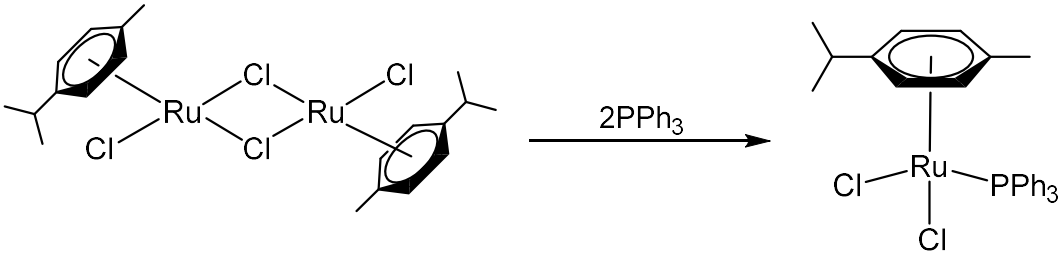

Figure 4.3: Synthesis of the [(η⁶-cymene)RuCl₂(PPh₃)] monomer

4.2.4 Synthesis of [(η⁶-cymene)RuCl₂(TCEP)]

[(η⁶-cymene)RuCl₂(TCEP)] was prepared using an adapted literature reported method by Henderson *et al*[10] and is given as follows. A mixture of the [(η⁶-cymene)RuCl₂]₂ dimer (0.5 g) and two molar equivalents of TCEP (TCEP = Tris(2-cyanoethyl)phosphine (0.315 g) in ethanol were brought to reflux in a 250 ml round bottom flask with moderate stirring for a total of 2 hours before being removed from the heat. After cooling to room temperature, the pink solid suspension was collected by vacuum filtration and washed with cold methanol (2 x 20 ml) and petroleum spirits (1 x 10 ml) followed by drying in air to give a pink powder solid (0.445 g)

4.2.5 Synthesis of [(η⁶-benzene)RuCl₂(TCEP)]

The synthesis of [(η⁶-benzene)RuCl₂(TCEP)] is given as follows. A mixture of the [(η⁶-benzene)RuCl₂]₂ dimer (0.5 g) and two molar equivalents of TCEP (0.389 g) in CH_2Cl_2 were brought to reflux in a 250 ml round bottom flask with moderate stirring for 5 hours before being removed from the heat. After cooling to room temperature, the light brown solid was collected by vacuum filtration. The solid sample was then suspended in CH_3CN and stirred for 3 hours, filtered to remove any undissolved solid and evaporated to give [(η⁶-benzene)RuCl₂(TCEP)] as an orange-brown solid. Yield, 0.3 g, 67% ESI-MS: Capillary exit voltage -90V, *m/z* $[M+Cl]^-$ 477.97 (calculated, 477.83), $[2M+Cl]^-$ 924.99 (calculated, 924.90).

4.2.6 Synthesis of η^6-arene ruthenium(II) phosphine metal complexes derived from [$CH_3SO_2NHC(S)NHPh$]

The general procedure for all metal complexes synthesised from the title ligand is as follows. Equimolar amounts of the ligand ($CH_3SO_2NHC(S)NHPh$) and metal complex starting material were suspended in MeOH (20 ml)/triethylamine (0.6 ml, excess). The solutions were slowly stirred at room temperature for 12 hours at which point the solution had turned black and the solid precipitate had changed colour, indicating the presence of the complex. In the case of the TCEP complexes, the temperature was held at 30°C for the duration. The solid precipitate was collected by vacuum filtration and washed with water (2 x 30 ml) to remove residue Et_3N and Et_3NHCl. The exact amounts used for each complex are given in Table 4.1

*Table 4.1: Synthesis of sulfonylthiourea ruthenium(II) complexes from $CH_3SO_2NHC(S)NHPh$, **3a**`*

Starting material			$CH_3SO_2NHC(S)NHPh$		Yield		Code	colour
Arene =, Phosphine =	mg	mmol	mg	mmol	mg	%		
Cymene, PPh_3	100	0.176	40	0.176	80	62	**4a**	orange-red
Cymene, TCEP	100	0.200	46	0.200	89	67	**4b**	orange-red
Benzene, PPh_3	100	0.195	45	0.195	91	69	**4c**	yellow-orange
Benzene, TCEP	100	0.225	51	0.225	58	42	**4d**	yellow-orange

4.3 Characterisation of ruthenium sulfonylthiourea complexes

Only ESI-MS peaks of $[M+H]^+$ at a capillary exit voltage of 150V and skimmer 1 voltage of 50V are reported unless otherwise stated. Complexes containing TCEP were dissolved in minimal DMF and made up to 1 ml with methanol. Due to time constraints (Covid19 lockdown) and unavailability of NMR at the time of writing, complex **4d** was only characterised by ESI-MS and IR analysis. Structures are drawn as the *proximal* isomer based on XRD observations of complex **4c**.

4.3.1 [(η^6-cymene)Ru{$CH_3SO_2NC(S)NPh$}(PPh_3)], 4a

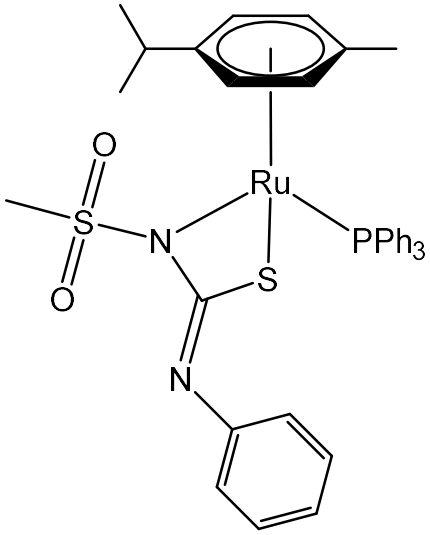

*Figure 4.4: Complex **4a***

Elemental analysis: Found (%) C 58.66; H 5.78; N 3.66. Calculated (%) C 59.57; H 5.14; N 3.86.

Melting point: 190-196°C

ESI-MS: *m/z* $[M+H]^+$ 727.06 (calculated, 727.12); $[(M+H)-PPh_3]^+$ 464.98 (calculated, 465.02)

FT-IR (cm^{-1}): 1638 (w, broad), 1570 (m), 1434 (m), 1383(m), 1287(m) 1124 (s), 1094 (w).

NMR: ($CDCl_3$) $^{31}P\{^1H\}$ δ (ppm) 40.48 (s, P). ^1H δ (ppm) 7.7-6.3 (m, PPh_3, 15H), 7.19 (para-NPh, t, J_{HH} = 7.8 Hz, 1H), 6.89 (ortho-NPh, t, J_{HH} = 7.3 Hz, 2H), 6.80 (meta-NPh, d, J_{HH} = 7.2 Hz, 2H), 6.3 (Cymene-H_a, d, J_{HH} = 5.69 Hz, 1H), 5.83 (Cymene-H_b, d, J_{HH} = 5.62 Hz, 1H), 5.16 (Cymene-H_c, d, J_{HH} = 6.14 Hz, 1H), 4.97 (Cymene-H_d, d, J_{HH} = 6.18 Hz, 1H), 3.26 (Isopropyl-CH, sx, J_{HH} = 6.7 Hz, 1H), 2.43 (SO_2-CH_3, s, 3H), 1.66 (cymene-*p*-CH_3, s, 3H), 1.39 (Isopropyl-CH_3(a), d, J_{HH} = 6.8 Hz, 3H), 1.26 (Isopropyl-CH_3(b), d, J_{HH} = 6.9 Hz, 3H)

4.3.2 [(η^6-cymene)Ru{$CH_3SO_2NC(S)NPh$}(TCEP)], 4b

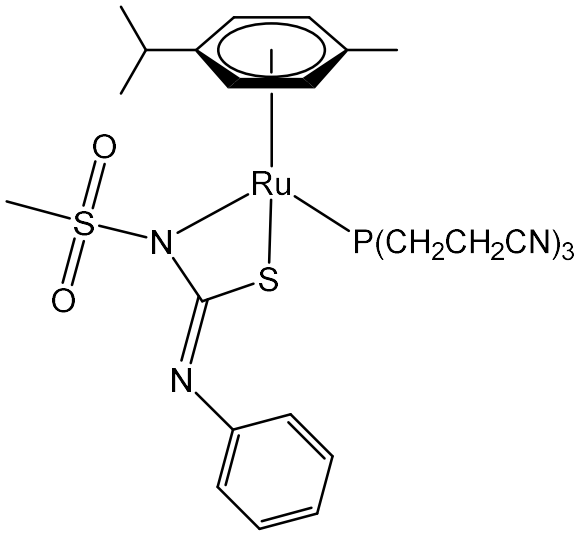

*Figure 4.5: Complex **4b***

Elemental analysis: Found (%) C 48.77; H 5.95; N 10.12. Calculated (%) C 48.38; H 5.22; N 10.66.

Melting point: >300°C

ESI-MS: *m/z (Positive)* $[M+H]^+$ 658.13 (calculated, 658.10); $[(M+H)\text{-TCEP}]^+$ 465.22 (calculated, 465.02); (Negative) $[M+Cl]^-$ 692.22 (calculated, 692.06).

FT-IR (cm^{-1}): 1637 (m, broad), 1575 (vs), 1290 (m), 1152(m), 1125 (s), 929 (m).

NMR: (DMF/$CDCl_3$) ^{31}P δ (ppm) 29.66 (s, P). (DMSO-d_6) ^1H δ (ppm) 7.19 (para-NPh, t, J_{HH} = 7.9 Hz, 1H), 6.89 (ortho-NPh, t, J_{HH} = 7.2 Hz, 2H), 6.8 (meta-NPh, d, J_{HH} = 8.1 Hz, 2H), 6.0 (cymene-H_a, d, J_{HH} = 6.3 Hz, 1H), 5.9 (cymene-H_b, broad, 1H), 5.88 (cymene-H_c, d, J_{HH} = 6.2 Hz, 1H), 5.35 (cymene-H_d, d, J_{HH} = 5.8 Hz, 1H), 4.16 (Isopropyl -CH, m, 1H), 3.26 (cymene-*p*-CH_3, s, 3H), 2.76 (PCH_2CH_2, m, 2H), 2.64 (PCH_2CH_2, m, 2H), 2.50 (SO_2-CH_3, s, 3H), 1.22 (Isopropyl-CH_3(a), d, J_{HH} = 7.0 Hz, 3H), 1.13 (Isopropyl-CH_3(b), d, J_{HH} = 6.8 Hz, 3H).

4.3.3 [(η^6-benzene)Ru{$CH_3SO_2NC(S)NPh$}(PPh_3)], 4c

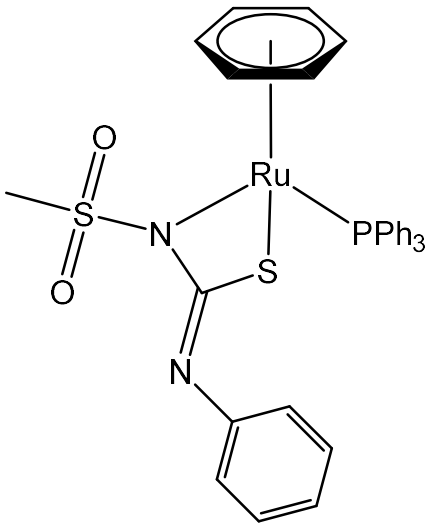

*Figure 4.6: Complex **4c***

Elemental analysis: Found (%) C 56.18; H 4.17; N 3.63. Calculated (%) C 57.39; H 4.36; N 4.18.

Melting point: 207-210°C

ESI-MS: *m/z* $[M+H]^+$ 671.07 (calculated, 671.05); $[(M+H)-PPh_3]^+$ 408.97. (Calculated, 408.95)

FT-IR (cm^{-1}): 1567 (vs), 1435 (m), 1292 (m), 1157 (m), 1126 (vs), 1091 (m), 919 (m), 701 (m), 528 (m).

NMR: ($CDCl_3$) $^{31}P\{^1H\}$ δ (ppm) 37.76 (s, P1). ^1H δ (ppm) 7.7-6.8 (m, aromatic), 2.55 (SO_2-CH_3, s, 3H).

4.3.4 [(η^6-benzene)Ru{$CH_3SO_2NC(S)NPh$}(TCEP)], 4d

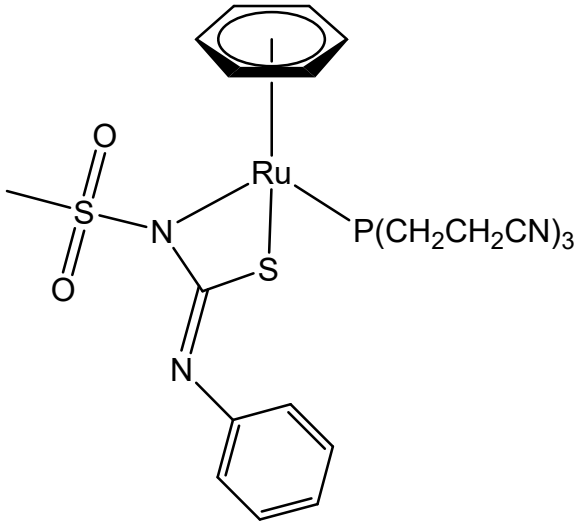

*Figure 4.7: Complex **4d***

Melting point: >300°C

ESI-MS: *m/z* $[M+Cl]^-$ 637.11 (calculated, 636.00).

FT-IR (cm^{-1}): 2248 (w), 1617 (s), 1584 (m), 1436 (m), 1304 (m), 1143 (w), 1125 (m), 917 (w), 516 (w).

4.4 Results and discussion

4.4.1 Synthesis

The $[(\eta^6\text{-cymene})RuCl_2]_2$ dimer was synthesised in high yield and purity by a simple reaction between $RuCl_3 \cdot xH_2O$ and α-terpinene in refluxing ethanol. This reaction was then followed by a tertiary phosphine induced cleavage of the chlorine bridge of the dimer using triphenylphosphine, which after precipitation of the product using petroleum spirits, gave the resulting $[(\eta^6\text{-cymene})RuCl_2(PPh_3)]$ monomer as a red crystalline solid in high yield and purity. Following this reaction, a second bridge splitting reaction of the ruthenium cymene dimer using tris(2-cyanoethyl)phosphine (TCEP) was conducted using a previously reported method by Henderson *et al*. Interestingly, this reaction required refluxing conditions and a longer reaction duration to produce the desired ruthenium monomer. A synthetic scheme for the preparation of the arene ruthenium phosphine monomers is given in Figure 4.8. The new TCEP arene ruthenium monomer of $[(\eta^6\text{-benzene})RuCl_2(TCEP)]$ was also prepared from $[(\eta^6\text{-benzene})RuCl_2]_2$ following the procedure given for the cymene complex. However, due to the benzene dimer's reduced solubility in common solvents, specifically ethanol, early attempts of producing the monomer afforded a mixture of the desired product and dimer starting material with successful preparation of the benzene TCEP monomer being produced in CH_2Cl_2 with a slightly longer reflux time of 5 hours with further purification by dissolving the product in CH_3CN and filtering to remove residue undissolved solids. This new complex was characterised by MS, discussed below

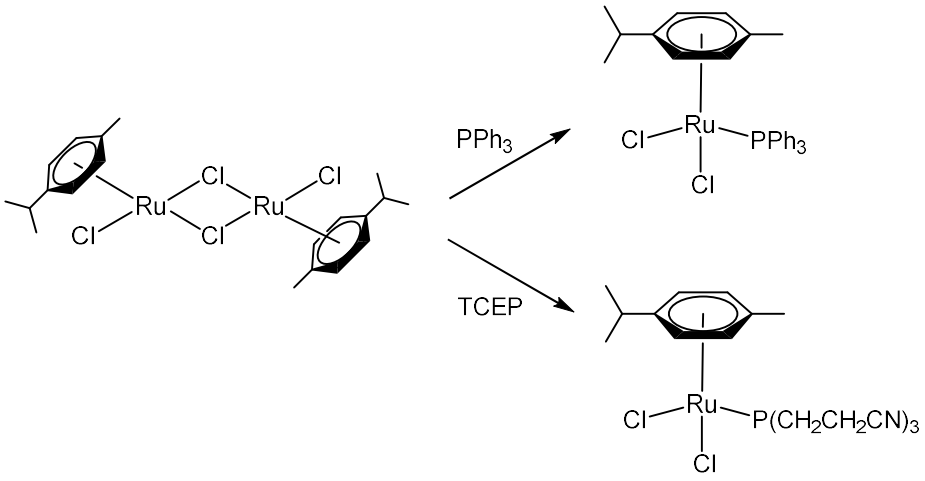

Figure 4.8:Synthetic scheme for the preparation of the arene ruthenium phosphine monomers from $[(\eta^6\text{-cymene})RuCl_2]_2$

and successfully formed the corresponding sulfonylthiourea complex.

Synthesis of the ruthenium(II) piano-stool complexes with the *N*-methylsulfonyl-*N*`-phenylthiourea ligand [$CH_3SO_2NHC(S)NHPh$] (**3a`**), deviated slightly from the method reported in the previous chapters. Due to the decreased solubility of the ruthenium piano stool complexes prepared here compared to the complexes prepared in the previous chapters, complexes **4a-4d** were synthesised without the need for precipitation by addition of water to the methanol reaction mixture. Instead, the complexes were isolated by vacuum filtration and washed with water to give the target complexes **4a-4c** in adequate purity to furnish micro analytical data without further purification. To compensate for the lower temperature, the reaction time was increased to 12 hours which was adequate for the full completion of complexes **4a** and **4c**. After 12 hours, ^{31}P NMR analysis of the TCEP containing complexes **4b** and **4d** showed a mixture of both the starting material and target complex. This can be attributed to the notable insolubility of the ruthenium TCEP starting material in methanol. It was found that a consistent temperature of 30°C was required for the 12 hours duration to ensure reaction completion. This can be observed in the comparison of ^{31}P NMR spectra of complex **4b** after 12 hours without heating followed by a further 1 hour at 30°C degrees, shown in Figure 4.9.

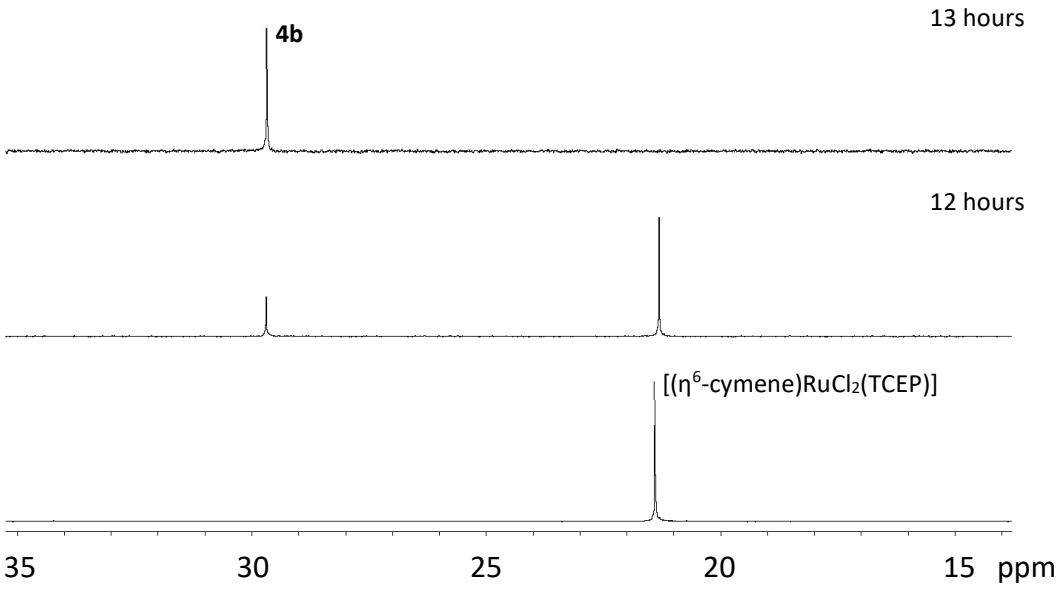

*Figure 4.9: ^{31}P NMR comparison of the reaction mixture for the synthesis of **4b**.*

4.4.2 Mass spectral analysis

The ESI mass spectra of the triphenylphosphine containing complexes (**4a** and **4c**) show the expected $[M+H]^+$ ions at an *m/z* of 727 and 671, respectively. These ions were most prominent at a capillary exit voltage of 90V and unlike the platinum(II) triphenylphosphine complexes reported in Chapter 3, were more prone to fragmentation and showed strong $[(M+H)\text{-}PPh_3]^+$ ion peaks at a capillary exit voltage of 150V with near equal intensity to the parent $[M+H]^+$ ion. At 180V the $[(M+H)\text{-}PPh_3]^+$ ion was clearly the most prominent peak. These observations may indicate that the Ru-P bond of the complex is much weaker than that of the Pt-P bond of complexes **3a-3c** reported earlier. A comparison of the 90V, 150V and 180V spectra of complex **4a** is given in Figure 4.10 which clearly show the increase in fragmentation in relation to increase in voltage.

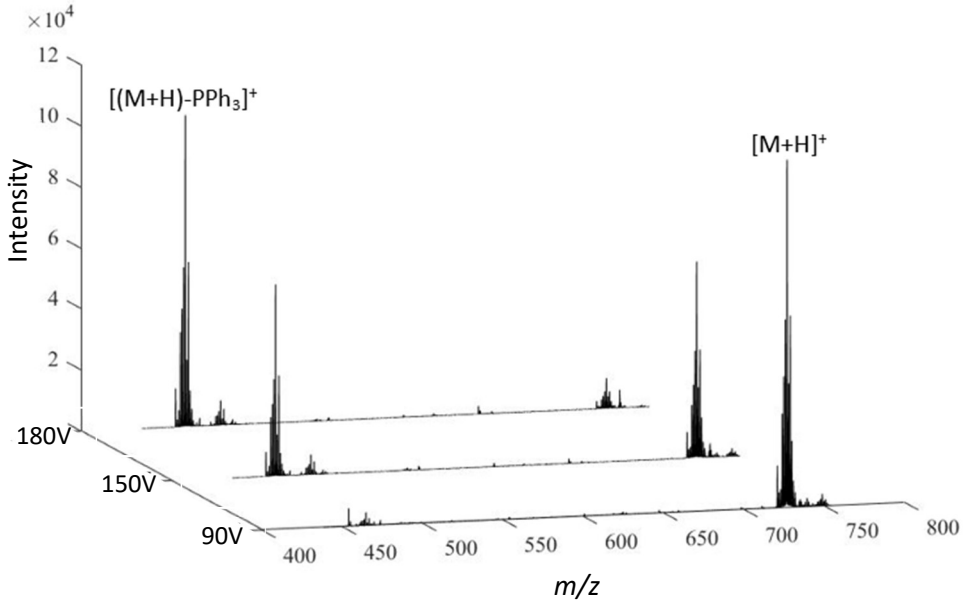

*Figure 4.10: Mass spectra comparison of complex **4a** at capillary exit voltages of 90V, 150V and 180V*

Interestingly, TCEP containing complexes, **4b** and **4d**, were more resistant to positive ionisation with only complex **4b** giving adequate intensity to confidently assign the ions $[M+H]^+$ (*m/z* 658) and $[(M+H)\text{-}TCEP]^+$ (*m/z* 465). The complexes did however give strong $[M+Cl]^-$ peaks in the negative-ion mode which is reminiscent of the observed ions of the starting material, $[RuCl_2\{P(CH_2CH_2CN)_3\}(\eta^6\text{-cymene})]$, which shows strong $[M+Cl]^-$ and $[2M+Cl]^-$

ion peaks[10]. Moreover, the benzene analogue of the cymene TCEP monomer prepared here, $[RuCl_2\{P(CH_2CH_2CN)_3\}(\eta^6\text{-benzene})]$ further exemplifies this observation by also showing $[M+Cl]^-$ and $[2M+Cl]^-$ ion peaks in the negative-mode which match with calculated isotope patterns, as shown for $[M+Cl]^-$ in Figure 4.12. Furthermore, both of these observations are consistent with the observed $[P(CH_2CH_2CN)_3+Cl]^-$ and $[2\{P(CH_2CH_2CN)_3\}+Cl]^-$ negative ion peaks of the free TCEP ligand as reported by Henderson *et al*[10]. This indicates that the source of this unprecedented ionisation of the complex is the TCEP itself, most likely due to interaction of a chloride ion to the alkyl protons. Interactions of chlorines with the alkyl protons of alkyl nitrates has been reported[14] and is further exemplified by the lack of corresponding $[M+Cl]^-$ negative ions for the triphenylphosphine containing complexes **4a** and **4c**. Interestingly, complex **4b** which showed both the positive $[M+H]^+$ and negative $[M+Cl]^-$ ion peaks gave $[M+Cl]^-$ in much lower intensity in relation to complex **4d** which only showed $[M+Cl]^-$.

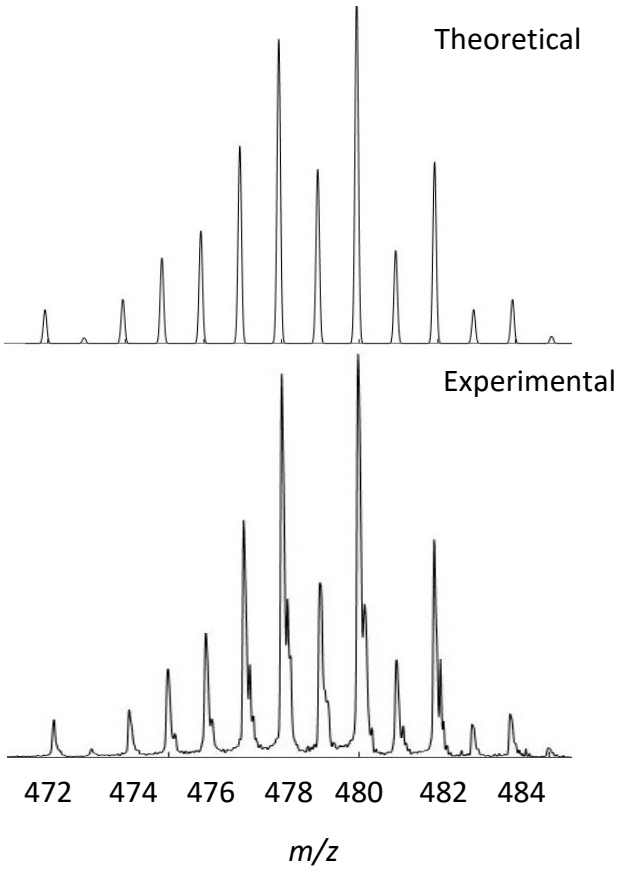

Figure 4.12: Theoretical and experimental $[M+Cl]^-$ ESI-MS spectrum of $[(\eta^6\text{-cymene})RuCl_2(TCEP)]$

4.4.3 ^{1}H NMR analysis of cymene containing complexes 4a and 4b

Proton NMR analysis of the cymene containing compounds (**4a** and **4b**) reveals the symmetry of the cymene substituent has been broken by coordination to the ruthenium centre. This in-turn creates well resolved and relatively simple spectra which aids in characterisation of the complexes. A full proton spectrum of complex **4a** is given in Figure 4.15. Firstly, the comparison of the ^{1}H NMR spectrum of the triphenylphosphine complex (**4a**) and the TCEP containing complex (**4b**) allowed for the assignment of the phenyl protons of the sulfonylthiourea ligand by comparison of the absent triphenylphosphine protons. A comparison of the aromatic regions of both complex **4a** and **4b** is given in Figure 4.13.

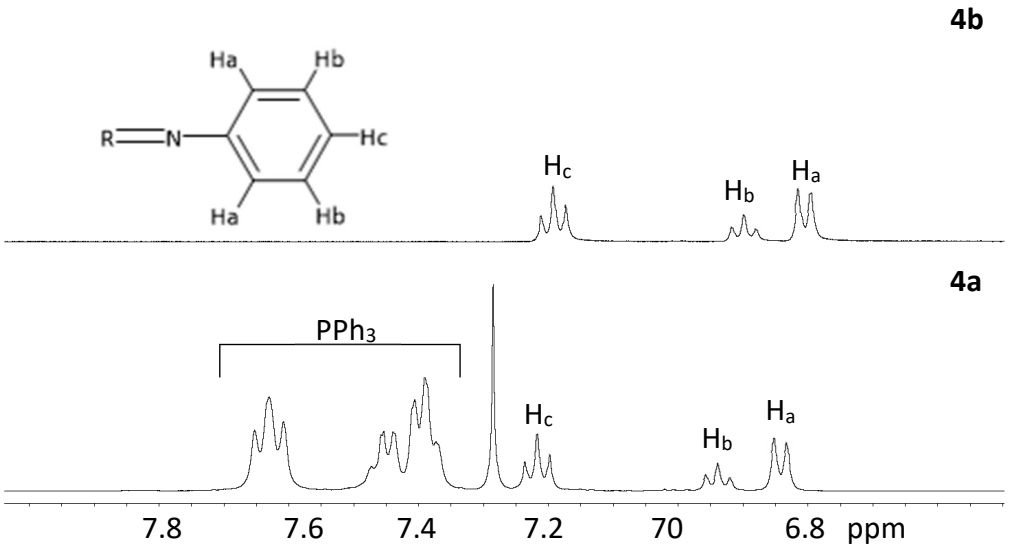

*Figure 4.13: Comparison of the aromatic regions of the ^{1}H NMR of complexes **4a** and **4b***

Moreover, the aromatic protons of the cymene are well resolved and give four doublet resonances between 6.3 and 4.9 ppm. Interestingly, one of these resonances for complex **4b** appears as a broad unresolved singlet, however the remaining peaks are unaffected. The lack of a fourth doublet in the region seems to confirm this resonance belonging to a cymene proton, however the reason for it being unresolved is unknown. A comparison of this region is given in Figure 4.14

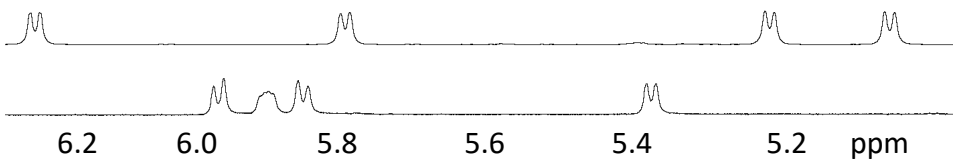

*Figure 4.14: Comparison of the cymene protons of complex **4a** (top) and **4b** (bottom)*

The isopropyl methyl groups (CH-**(CH$_3$)$_2$**) of the cymene substituent gives two doublet resonances in the alkyl region along with a well resolved sextet resonance slightly downfield corresponding to the isopropyl primary carbon. The remaining cymene *para*-methyl group gives a singlet in close proximity to the distinctive water resonance and was assigned based on integration. The methyl group of the ligand (**CH$_3$**SO$_2$) gives a strong intensity singlet at ~2.4 ppm for complex **4a** and ~2.5 ppm for complex **4b** which is reminiscent of the lone ligand. Interestingly only one set of cymene responses is seen for both complexes which indicates only one structural isomer is present.

Due to the decreased solubility of complex **4b** due to the TCEP ligand, ^{1}H NMR of the complex was obtained in DMSO-d$_6$ solvent. Because of this the spectrum was completely dominated by the strong intensity of the DMSO solvent resonance and required presaturation for adequate resolution. A side effect of this is the poorly resolved TCEP alkyl protons which appear as two sets of broad multiplets between 2.8 and 2.5 ppm. Assignment of these protons was achieved by comparison of the TCEP absent spectrum of complex **4a** and comparison of literature reported values for the [(η^6-cymene)RuCl$_2$(TCEP)] starting material.

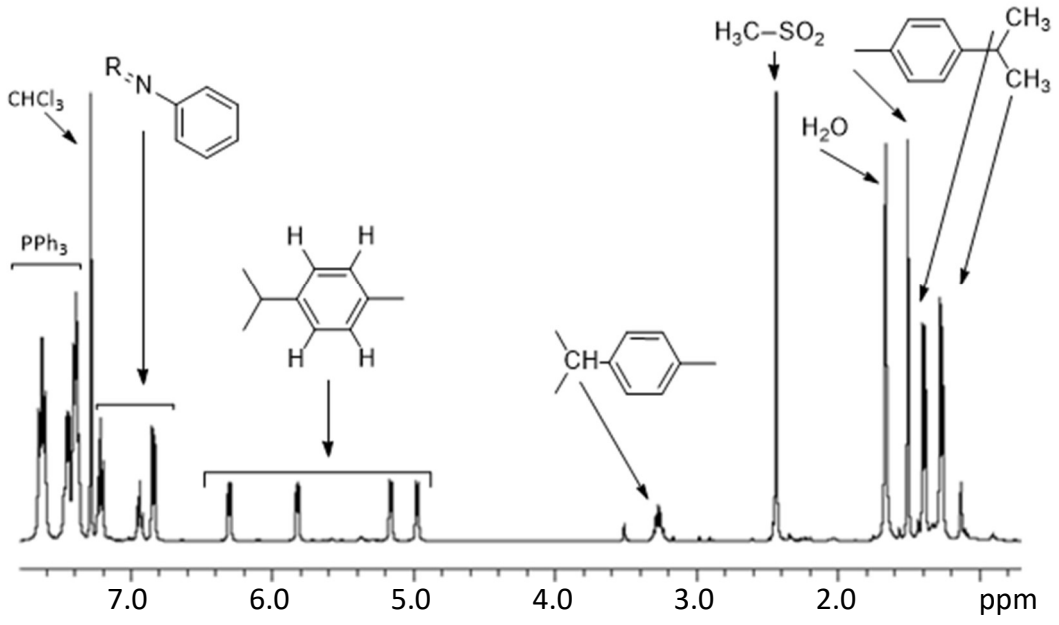

*Figure 4.15: Annotated ^{1}H NMR of complex **4a***

4.4.4 Single crystal XRD structure of complex 4c.

Single crystal XRD quality crystals of complex **4c** were grown by slow evaporation from an 80:20 mixture of CH_2Cl_2 and diethyl ether. The crystals grew in the monoclinic space group $P2_1/c$. The asymmetric unit consists of four molecules of **4c** and four CH_2Cl_2 solvent molecules, the latter of which adopts two conformations in a 55:45 ratio due to a slight rotation about the C1s - C11s bond. The coordination of the ruthenium metal centre of the complex shows an archetypal piano-stool structure with the ligand (**3a`**) coordinating to the ruthenium metal centre in a bidentate fashion through S1 and N2 with S-Ru and N-Ru bond lengths of 2.393(7) Å and 2.117(2) Å, respectively. A P-Ru bond distance of 2.331(7) Å is observed which creates the third leg of the piano stool structure. Selected bond lengths and angles is given in Table 4.2. Interestingly, the single crystal structure of complex **4c** reveals the unexpected *distal* isomer which is formed by coordination to the metal centre through NSO_2 (N2) as opposed to NPh (N1) which is observed for the structures reported in earlier chapters, this isomer places the sulfonyl SO_2CH_3 group in close proximity to the ruthenium metal centre. The ORTEP structure of complex **4c** is given in Figure 4.16.

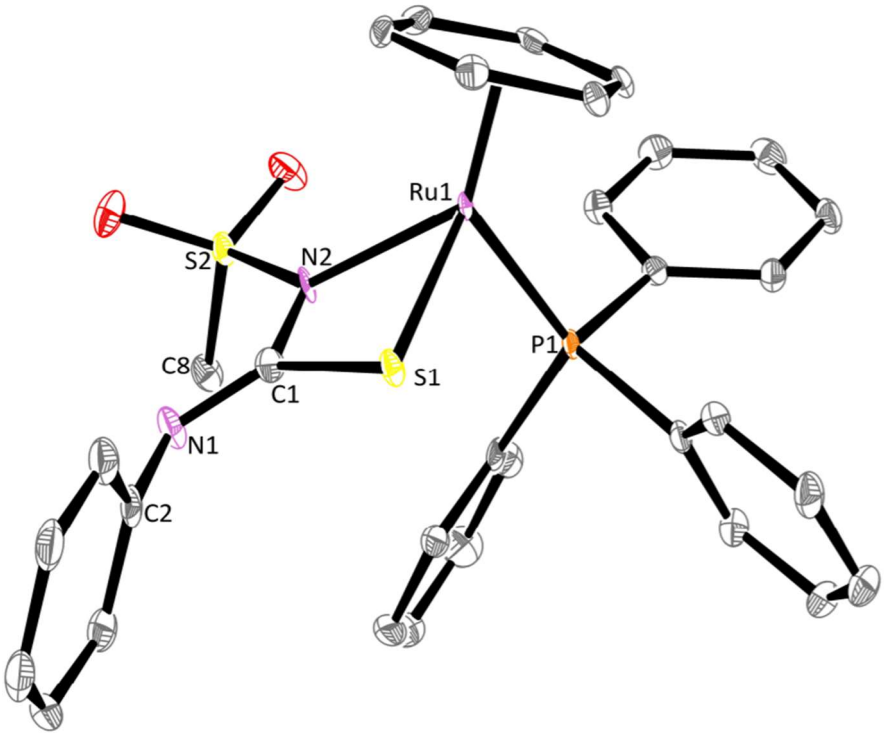

*Figure 4.16: ORTEP structure of complex **4c**. Hydrogens and one molecule of CH_2Cl_2 is removed for clarity. Thermal ellipsoids at 50% probability.*

*Table 4.2: Selected bond lengths and angles of complex **4c***

Complex **4c**	Length (Å)
C_6H_6 centroid - Ru	1.727
P1 – Ru	2.331(7)
S1 – Ru	2.393(7)
N2 – Ru	2.117(2)
C1 – N1	1.282(4)
C1 – S1	1.777(3)
C1 – N2	1.378(4)
N2 – S2	1.621(2)
	Angle (°)
N2 – Ru – S1	67.42(7)
C1 – N1 – C2	120.4(3)
C1 – N2 – S2	121.8(2)
S1 – Ru – P1	89.71(2)
N2 – Ru - P1	89.23(7)

In contrast to the crystal structures of the d^8 platinum complexes **2a** and **3a** which have a square-planar geometry, the d^6 ruthenium structure of **4c** shows a pseudo octahedral piano stool structure. This structure interestingly shows the *proximal* isomer which is in contrast to the *distal* isomers reported previously. Examination of the literature for the structurally similar ruthenium arene acylthiourea complexes reveals the most commonly adopted coordination mode is monodentate, through S[2, 15-17] and also commonly through S and O[18-20] which forms a 6 member ring around the central ruthenium atom. Although rare for acylthioureas, a 4 member ring bidentate coordination mode through S and N is observed with all reported structures being in the *proximal* isomer[1, 21]. This 4 member ring coordination mode resembles the coordination chemistry observed for simple thioureas[22]. Similar thiosemicarbazones (R_2N-NR`C(S)NR_2)[23-25] which form 5 member ring like structures also show S and N bidentate coordination modes with ruthenium. Bond lengths involved in the 4 member bidentate ring of complex **4c** were compared to relevant bond lengths of literature reported ruthenium arene thiourea complexes. Comparison bond lengths are given in Table 4.3, comparison structures are given in Figure 4.17.

Interestingly, the Ru-S bond lengths of the reported complexes are longer than that observed for complex **4c** with the exception of the acylthiourea complex reported by Ghandhaveetu *et al* which was comparably longer than that observed for **4c.**

Table 4.3: Comparison bond lengths of 4 member bidentate ring thiourea piano-stool structures

	Code	Ru-S1 (Å)	S-C (Å)	C-N (Å)	N-Ru (Å)
Complex **4c**	**4c**	2.393(7)	1.777(3)	1.282(4)	2.117(2)
Obradovic *et al*[26]	**1**	2.460(3)	1.708	1.324	2.209(6)
M.Aitali *et al*[27]	**2**	2.438	1.730	1.343	2.097
Gandhaveetu *et al*[1]	**3**	2.4232	1.711	1.325	2.118

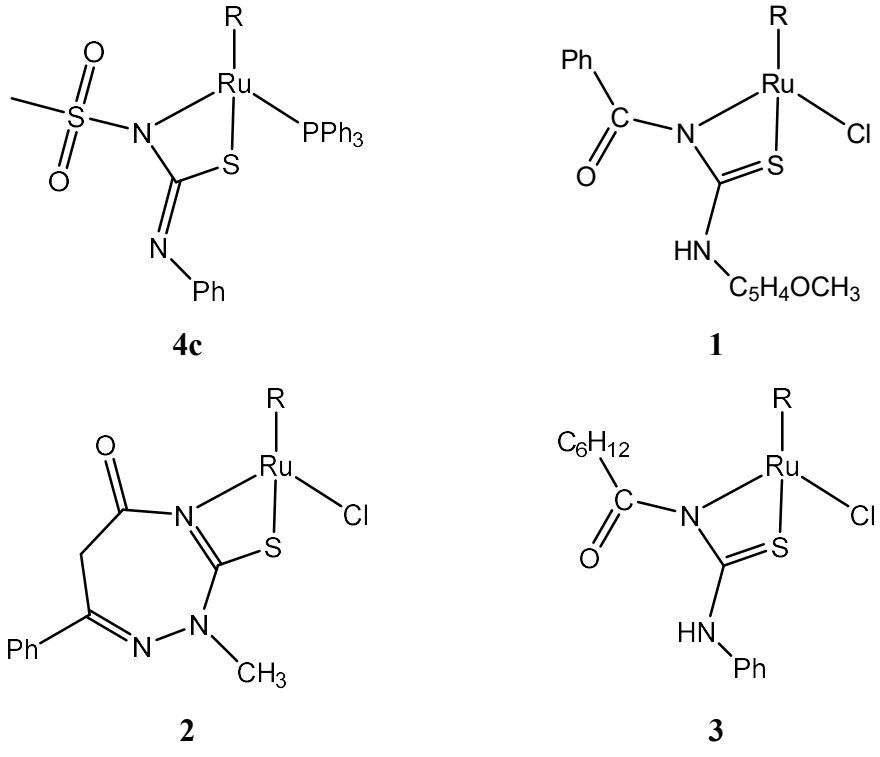

*Figure 4.17: Structure of **4c** and literature reported structures for comparison **1, 2, 3**.*

(R = Benzene or cymene)

This trend was also observed for the C-N bond of the thiourea. However, the S-C and N-Ru bond lengths of all the complexes were comparably close at *ca* 1.75 Å and 2.15 Å, respectively. A possible reason for this observation is the addition of the electron withdrawing sulfonyl group. Moreover, the arene substituent for complex **4c** was a benzene ring while the arene of the remaining bidentate complexes was cymene which may further explain these differences. The bond lengths involved in the bidentate 4 member ring were comparable signalling similar structure and coordination. These bond lengths show a strained four membered ring formed from the core thiourea which has also been observed for complexes **2a** and **3a**.

S1-Ru-N1, S1-Ru-P1 and P1-Ru-N1 bond angles of 67.42(7)°, 89.71(2)° and 89.23(7)° were observed for complex **4c** and C1 bond angles of the thiourea moiety are 104.95° (S1-C1-N1), 130.03° (S1-C1-N2) and 124.93° (N1-C1-N2). These values are comparable with those of the square-planar complex **3a** [107.02, 123.72° and 129.26°] and the literature reported benzyl acylthiourea ruthenium complex[1], which shares similar bidentate S and N coordination in the *proximal* isomer [110.07°, 124.85° and 125.04°][1]. The plane of the core thiourea, defined by the means of S1, C1, N1 and N2 forms a flat plane with an inter-plane angle of 60.73° with the N-Ph substituent. The distance of the ruthenium atom to the centroid of the arene ring was observed to be 1.727 Å which is similar to the centroid to ruthenium distance of similar thioureas ruthenium arene complexes [1.675 Å, 1.658 Å, 2.054 Å, 1.664 Å and 1.777 Å][28].

4.5 Conclusions

In this chapter, (η^6-arene) ruthenium(II) piano-stool complexes derived from *N*-methylsulfonyl-*N'*-phenylthiourea [$CH_3SO_2NHC(S)NHPh$] have been prepared for the purpose of comparing and contrasting the difference between the piano stool structures prepared here with regards to the square-planar structures reported in earlier chapters. Particular interest was made in examining the coordination mode adopted, and isomer thereof, in relation to the structurally similar acylthioureas. Analysis methods, namely single crystal XRD, determined the sulfonylthiourea ligand of these piano-stool complexes to coordinate in a bidentate fashion through both S and N atoms. Moreover, single crystal XRD analysis revealed the benzene ruthenium(II) triphenylphosphine complex, **4c** to be in the unexpected *proximal* isomer which is in contrast to the *distal* isomers reported for the complexes in both Chapters 2 and 3. This observation indicates that the piano stool complexes of sulfonylthiourea ligands more closely resemble the coordination chemistry of the closely related S and N bidentate coordination mode of ruthenium acylthiourea and thiourea complexes. ESI mass spectrum analysis of the triphenylphosphine complexes **4a** and **4c** show strong $[M+H]^+$ ions with $[(M+H)\text{-}PPh_3]^+$ ions increasing relative to the increase in capillary exit voltage. Complex **4b** also showed similar observations of both $[M+H]^+$ and $[(M+H)\text{-TCEP}]^+$ however more predominantly formed $[M+Cl]^-$ and $[2M+Cl]^-$ with complex **4d** only showing these negative mode ions. Interestingly, this unprecedented negative ionisation of complexes **4b** and **4d** correlate to the literature reported [$RuCl_2${TCEP}(η^6-cymene)] and lone TCEP phosphine ligand which also exhibit $[M+Cl]^-$ and $[2M+Cl]^-$ ions, most likely due to interactions between a chloride ion and TCEP alkyl protons. Moreover, the benzene analogue, [$RuCl_2${TCEP}(η^6-benzene)] was prepared by a bridge splitting reaction between TCEP and the benzene ruthenium dimer and showed similar $[M+Cl]^-$ and $[2M+Cl]^-$ peaks and was then used for the preparation of complex **4d**.

4.6 References

1. R. Gandhaveeti, R. Konakanchi, P. Jyothi, N. S. Bhuvanesh and S. Anandaram, *Applied Organometallic Chemistry*, 2019, **33**, e4899.
2. M. M. Sheeba, M. M. Tamizh, L. J. Farrugia, A. Endo and R. Karvembu, *Organometallics*, 2014, **33**, 540-550.
3. C. S. Allardyce, A. Dorcier, C. Scolaro and P. J. Dyson, *Applied Organometallic Chemistry*, 2005, **19**, 1-10.
4. B. Kar, N. Roy, P. Sudhindra, P. Moharana and P. Paira, *Inorganica Chimica Acta*, 2020, 119858.
5. A. K. Singh, D. S. Pandey, Q. Xu and P. Braunstein, *Coordination Chemistry Reviews*, 2014, **270**, 31-56.
6. A. Weiss, R. H. Berndsen, M. Dubois, C. Müller, R. Schibli, A. W. Griffioen, P. J. Dyson and P. Nowak-Sliwinska, *Chemical Science*, 2014, **5**, 4742-4748.
7. B. Feldhaeusser, S. R. Platt, S. Marrache, N. Kolishetti, R. K. Pathak, D. J. Montgomery, L. R. Reno, E. Howerth and S. Dhar, *Nanoscale*, 2015, **7**, 13822-13830.
8. P. Borst, S. Rottenberg and J. Jonkers, *Cell cycle*, 2008, **7**, 1353-1359.
9. W. H. Ang, I. Khalaila, C. S. Allardyce, L. Juillerat-Jeanneret and P. J. Dyson, *Journal of the American Chemical Society*, 2005, **127**, 1382-1383.
10. W. Henderson, A. G. Nair, N. R. Halcovich and E. R. T. Tiekink, *Molbank*, 2018, **2018**, M1025.
11. W. Vullo, *Industrial & Engineering Chemistry Product Research and Development*, 1966, **5**, 346-349.
12. M. A. Bennett and A. K. Smith, *Journal of the Chemical Society, Dalton Transactions*, 1974, 233-241.
13. S. B. Jensen, S. J. Rodger and M. D. Spicer, *Journal of Organometallic Chemistry*, 1998, **556**, 151-158.
14. T. D. Fridgen, J. L. Burkell, A. N. Wilsily, V. Braun, J. Wasylycia and T. B. McMahon, *The Journal of Physical Chemistry A*, 2005, **109**, 7519-7526.
15. K. Jeyalakshmi, J. Haribabu, N. S. Bhuvanesh and R. Karvembu, *Dalton Transactions*, 2016, **45**, 12518-12531.
16. M. K. Rauf, A. Badshah, M. Gielen, M. Ebihara, D. de Vos and S. Ahmed, *Journal of inorganic biochemistry*, 2009, **103**, 1135-1144.
17. P. N. Sathishkumar, N. Raveendran, N. S. Bhuvanesh and R. Karvembu, *Journal of Organometallic Chemistry*, 2018, **876**, 57-65.
18. A. M. Plutín, R. Mocelo, A. Alvarez, R. Ramos, E. E. Castellano, M. R. Cominetti, A. E. Graminha, A. G. Ferreira and A. A. Batista, *Journal of inorganic biochemistry*, 2014, **134**, 76-82.
19. R. S. Correa, K. M. de Oliveira, F. G. Delolo, A. Alvarez, R. Mocelo, A. M. Plutin, M. R. Cominetti, E. E. Castellano and A. A. Batista, *Journal of inorganic biochemistry*, 2015, **150**, 63-71.
20. A. M. Plutín, A. Alvarez, R. Mocelo, R. Ramos, E. E. Castellano, M. M. Da Silva, L. Colina-Vegas, F. R. Pavan and A. A. Batista, *Inorganic Chemistry Communications*, 2016, **63**, 74-80.
21. B. N. Cunha, L. Colina-Vegas, A. M. Plutín, R. G. Silveira, J. Honorato, K. M. Oliveira, M. R. Cominetti, A. G. Ferreira, E. E. Castellano and A. A. Batista, *Journal of inorganic biochemistry*, 2018, **186**, 147-156.
22. W. Henderson, B. K. Nicholson, M. B. Dinger and R. L. Bennett, *Inorganica Chimica Acta*, 2002, **338**, 210-218.
23. W. Su, Z. Tang, Q. Xiao, P. Li, Q. Qian, X. Lei, S. Huang, B. Peng, J. Cui and C. Huang, *Journal of Organometallic Chemistry*, 2015, **783**, 10-16.
24. J. Haribabu, G. Sabapathi, M. M. Tamizh, C. Balachandran, N. S. Bhuvanesh, P. Venuvanalingam and R. Karvembu, *Organometallics*, 2018, **37**, 1242-1257.

25. S. Dutta, F. Basuli, A. Castineiras, S. M. Peng, G. H. Lee and S. Bhattacharya, *European Journal of Inorganic Chemistry*, 2008, **2008**, 4538-4546.
26. D. Obradović, S. Nikolić, I. Milenković, M. Milenković, P. Jovanović, V. Savić, A. Roller, M. Đ. Crnogorac, T. Stanojković and S. Grgurić-Šipka, *Journal of Inorganic Biochemistry*, 2020, **210**, 111164.
27. M. Aitali, M. Y. A. Itto, A. Hasnaoui, A. Riahi, A. Karim, S. Garcia-Granda and A. Gutierrez-Rodriguez, *CCDC 150372: Experimental Crystal Structure Determination*, 2000.
28. I. L. Mawnai, S. Adhikari, W. Kaminsky and M. R. Kollipara, *Journal of Organometallic Chemistry*, 2018, **869**, 26-36.